

UNIVERSITY OF SOUTHAMPTON
Faculty of Engineering and Physical Sciences

A group design project report submitted for the award of
Master of Engineering

Supervisor: Dr Rujie Sun, DHBE Group
Customer: Professor Kai Yang, WSA

**Soft, wearable pressure sensors for
continuous wireless monitoring of blood
pressure enhanced by artificial intelligence**

by **Oscar Robinson**
Mikayla Colegrave
Luqmanul Mohd Awallizam
Geethaarth Vagga
Mukilan Rajapandian

March 24, 2025

UNIVERSITY OF SOUTHAMPTON

ABSTRACT

FACULTY OF ENGINEERING, SCIENCE AND MATHEMATICS

A group design project report submitted for the award of Master of Engineering

by Oscar Robinson
Mikayla Colegrave
Luqmanul Mohd Awallizam
Geethaarthha Vagga
Mukilan Rajapandian

This report details the development of an innovative blood pressure monitoring system integrating piezoresistive sensors, wireless communication, and a mobile application equipped with advanced data processing techniques. The primary aim of this project was to critically evaluate existing blood pressure monitoring technologies, justify the selection of the specific methods used, and detail the design principles and choices of each subsystem developed to produce the full-scale system. The completion of this project found that the sensors effectively detected the pulse waveform, albeit with significant noise. The produced signal was then faithfully sampled and transmitted wirelessly to the mobile application which illustrated and estimated the blood pressure from these waveforms. Systematic testing of each subsystem was conducted to ensure their functionality and performance before integrating it into a single wearable device. Although the system managed to achieve a significant milestone by demonstrating a working proof of concept, the accuracy levels of the blood pressure measurements did not meet standards for a commercial, much less medical, product. The system has so far been developed only to a premature stage and has substantial room for enhancements in sensor accuracy, signal integrity and user interface design. Future works will focus on refining these elements to achieve a more reliable blood pressure monitoring system.

Contents

Nomenclature	xv
Acknowledgements	xvii
1 Introduction	1
1.1 Problem Identification	2
1.2 Meet the Team	2
1.3 Application area	5
1.4 Technology Readiness Level	5
1.5 Justifications for Research	7
1.5.1 Societal	7
1.5.2 Economic	7
1.5.3 Environmental	8
2 Previous Work and Literature Review	9
2.1 Currently available blood pressure monitoring devices	10
2.1.1 Sphygmomanometers	10
2.1.2 Invasive Arterial Blood Pressure Monitoring	12
2.1.3 ECG and PPG	12
2.1.4 Piezoelectric Pressure Sensors	14
2.1.5 Piezoresistive Pressure Sensors	15
2.2 Wireless Communication Technologies	16
2.3 Mobile Application	18
2.4 Data analysis (ML/AI)	21
3 Project Management	23
3.1 Required Sections	25
3.2 Ethics Application Process	25
4 Sensor Fabrication	27
4.1 Interdigital Electrode Fabrication	28
4.2 Microstructure Fabrication	31
4.3 Final Assembly of the Sensor	33
5 Sensor Characterisation	35
5.0.1 Radial Artery Force and Deflection	37
6 Sensor Interfacing	41
6.1 Equivalent Circuit Simulation	42
6.2 Potential Divider	43
6.3 Wheatstone Bridge	43

6.4	Differential Voltage Calculation and Signal Amplification	45
6.4.1	MCP601 Differential Amplifier	45
6.4.2	AD623 Instrumentation Amplifier	46
6.5	Filter Considerations	47
7	Communications	49
7.1	Bluetooth Low Energy	50
7.1.1	Introduction to Bluetooth Low Energy	50
7.1.2	Advertising	51
7.1.3	Connection	52
7.1.4	Data Exchange	54
7.1.5	Security	55
7.1.6	Sniffer	56
7.2	System Integration	57
7.2.1	Analogue to Digital Converter	57
7.2.2	System Timing and Sequencing	57
7.2.3	System Testing and Validation	58
7.2.4	Development and Implementation Tools	59
7.3	Summary and Conclusion	60
8	Data Processing and Health Risk Assessment	63
8.1	Introduction	64
8.2	Blood Pressure Estimation System	64
8.2.1	Signal Processing Pipeline	65
8.2.2	Machine Learning Implementation	71
8.2.3	System Performance	73
8.3	CVD Risk Assessment System	75
8.3.1	Data Pre-processing	75
8.3.2	Model Development	78
8.3.3	System Evaluation	80
8.4	Conclusion	82
9	Mobile Application	83
9.1	Platform Selection	84
9.2	Bluetooth Communication	85
9.3	App Architecture	85
9.3.1	Core Components	85
9.4	User Interface Design	87
9.4.1	Outline	87
9.4.2	Accessibility	89
9.5	Testing and Evaluation	89
10	Full System Integration	93
10.1	Wired Integration	94
10.2	Wireless Integration	96
10.3	Wearable System	97
10.3.1	Nordic Semiconductor Thingy:52	97
10.3.2	Device Housing and Wrist Strap	98

10.3.3 Miniaturised Interface Circuit	98
10.4 Final Prototype	100
11 Conclusion	101
12 Future Work	105
12.1 The Issue of Backpressure	106
12.2 Communication Efficiency	106
12.3 Mobile App Features	108
A Primary Ethics Form	117
B Consent Form	127
C Participant Information Sheet	131
D Data Protection Agreement	137
E Risk Assessment	143
F Gantt Chart (Revision A)	151
G Gantt Chart (Revision B)	153
H Financial Expenditure	155

List of Figures

1.1	The TRL system, first developed by NASA, used to assess technology maturity. Extracted from [54].	6
2.1	Types of sphygmomanometer devices used in healthcare to measure intermittent blood pressure. Extracted from [20]	11
2.2	A 24-Hour Ambulatory Blood Pressure Monitoring (ABPM) device showing the inflatable cuff on the upper arm and the blood pressure machine worn at the waist. Extracted from [30].	12
2.3	The setup for invasive blood pressure monitoring typically used in hospitals in ICUs. A cannula is inserted into a peripheral artery and the blood pressure is directly measured using a transducer system. Extracted from [85].	13
2.4	A smartwatch that has ECG and PPG sensors built into it so that information from these signals can be used to indirectly measure blood pressure from features such as PPT and HRV. Extracted from [46]	13
2.5	The working principle of the soft, wearable wireless piezoelectric pressure sensor to monitor continuous blood pressure extracted from [34]. The schematic details the signal processing from converting the piezo-response detected from the wrist strap to continuous blood pressure can be presented on a graphical user interface (GUI).	15
2.6	Schematic showing the fabrication process of the piezoresistive blood pressure sensor and its application, extracted from [36].	17
2.7	Comparison of Wireless Communication Options	19
2.8	A diagram extracted from [39], illustrating how sensors were integrated into a full patient monitoring system in the pre-smartphone era.	20
3.1	Initial Design Flowchart	24
4.1	An image showing the placement of the wearable device and a zoomed-in diagram showing the piezoresistive sensor's placement on the Radial artery so it can detect the arterial blood pulses.	28
4.2	A graphic design showing the different layers of the multilayer sensor separated for visual purposes. The top layer indicates the copper electrode representing either the interdigital electrode or solid electrode, the middle layer represents the PEDOT: PSS conductive layer, and the bottom layer represents the PDMS microstructures. In this figure, the PDOT: PSS coating is represented as a sheet. However, this coating is either spin-coated on top of the PDMS microstructure layer or mixed into it before it is cured.	29

4.3	Fusion 360 CAD design for the 500 x 500 IDE showing the gap width, individual Interdigital electrode rod width, and the dimension of the entire design. The design shows two conductive pads which were used in the final assembly process to connect the sensor to the circuit. Similar models were made for all the IDEs ranging from 500 x 500 to 100 x 100. Note that when the design was converted to the ctb file to carry out the UV 3D printing, the design was inverted so that the surrounding copper would be etched instead of the IDE.	30
4.4	The final 500 x 500 IDE after the printing and etching process. Several electrodes were printed for all the IDE dimensions ranging from the 500 x 500 to the 100 x 100 design.	31
4.5	Fusion360 design for the PDMS sensor with Microdome structures.	31
4.6	Fusion360 design for the PDMS sensor with Micropyramid structures.	31
4.7	SEM images of the PDMS microstructures. a. A close-up of a singular microdome. b. An array of microdomes. c. A close-up of a singular micropyramid. d. An array of micropyramids.	32
4.8	A schematic showing the basic set-up of the circuit. The circuit consists of a potential divider formed by the piezoresistive sensor and a 32 [M Ω] resistor. The set-up is connected to a 5-volt power supply and a multimeter to measure the change in voltage caused by small amounts of pressure added onto the sensor. Note the 32 [M Ω] resistor was chosen after measuring the resistance of the microdome PDMS; a different resistance of [92 M Ω] was used for the micropyramids.	34
4.9	A diagram showing the formation of the sensor when a solid copper electrode is used. The conductive epoxy connects the flexible copper wire to the PDMS microstructures. The flat slab that the copper electrode is taped onto is used to make sure the electrode remains still and flat during characterisation. However, when testing on a patient, the slab will be substituted for the inner surface of the wrist.	34
5.1	The normalised plotted results for the successful sensors showing the voltage drop vs the applied mass (in grams) for the IDE 500 x 500 to 300 X 300 microdome piezoresistive sensors, IDE 500 x 500 to 300 X 300 micropyramid piezoresistive sensors, commercial piezoresistive sensor, and the solid copper electrode with spin-coated PEDOT: PSS onto either the microdomes or micropyramids	39
6.1	The NI Multisim equivalent circuit model of the PEDOT:PSS+PDMS piezoresistive sensor, providing a sinusoidally-varying resistance from 32.9[M Ω] to 3[k Ω] (MAX-MIN).	42
6.2	The voltage divider circuit used in Section 5 for the Microdome PDMS+PEDOT:PSS, using a 32.9[M Ω] dividing resistor ($R_{divider}$).	43
6.3	Transient analysis of the voltage divider. Voltmeter $PR1$ is measuring the voltage across the sensor. Note that the <i>decrease</i> in voltage corresponds to an <i>increase</i> in pressure applied.	43
6.4	The Quarter Wheatstone Bridge circuit used for interfacing with the sensor for the rest of the project, owing to its superior sensitivity and noise rejection.	44

6.5	Transient analysis of the quarter bridge. The differential voltage is measured using probe <i>PR1</i> (with respect to Ref1), and provides the output of the sensor from the output nodes of the bridge, <i>Vdiff+</i> and <i>Vdiff-</i> . Note now that an <i>increase</i> in voltage corresponds also to an <i>increase</i> in pressure applied	44
6.6	The Differential Amplifier setup using the MCP601 Operational Amplifier.	46
6.7	Transient simulation of the differential amplifier, showing differential gain of 2 successfully achieved.	46
7.1	BLE Protocol Stack - the different layers that make up the BLE protocol ensuring correct and systematic functionality [74]	51
7.2	BLE packet - Every packet of data transmitted follows this same structure during data exchange [74]	54
7.3	Pseudo Pulse Waveform - This waveform was generated using MATLAB and its data points were used to make the pulse waveform for system testing	59
7.4	Sampled Pulse Waveform - This waveform was plotted into MATLAB after sampling the input pseudo pulse waveform, transmitting the data over BLE, and receiving it on the phone. It has also been processed with a moving average filter and Savitzky-Golay filter	60
7.5	Flowchart of the Embedded System - Summary of the embedded system's procedure	61
8.1	Block diagram of the blood pressure estimation process by machine-learning techniques.	65
8.2	Example of raw ABP signal and converted voltage signal	66
8.3	Visualization of simulated noise components: Gaussian noise (top) representing thermal variations with ($\sigma = 0.015$), uniform noise (middle) showing quantization effects in the range $[0.001, 0.015]$ V, and mains interference (bottom) displaying 50 Hz power line noise with 0.005V amplitude.	67
8.4	Signal comparison before and after filtering	68
8.5	Pulse wave morphological features and timing intervals showing key characteristic points and temporal relationships in arterial pressure waveforms.	69
8.6	Model architecture comparison	72
8.7	Performance comparison across models	74
8.8	Bland-Altman plots for best performing model	75
9.1	App workflow - the mobile application manages the connection with the device, collects data and makes it available where needed.	84
9.2	Workflow diagram showing the Bluetooth connection process	87
9.3	The application's Home screen is the first page the user sees when the open the app. Therefore, it contains all of most important functions and information. Note that the image was taking using a "scrolling screenshot" feature, allowing for the whole UI to be visible even if it does not fit on one page.	91
9.4	The Data screen of the app allows the user to view their historical blood pressure data interactively.	91

9.5	The insights screen of the application contains insights derived from the user. There are currently two types that can be displayed - scores, which are displayed at the top and give a numerical value, and alerts - which appear below and show information when certain conditions are met. . . .	92
9.6	The profile screen allows the user to view and edit their personal information.	92
10.1	Flowchart representation of the Full System Integration	94
10.2	Oscilloscope capture illustrating the raw signal output from the Function Generator.	95
10.3	Amplified output from the Function Generator via the MCP601 Differential Amplifier.	95
10.4	Placement of the piezoresistive sensor on the skin, above the Radial Artery.	95
10.5	Placement of the [Cu] electrode on top of the piezoresistive sensor, completing the circuit through the conductive PEDOT:PSS layer.	95
10.6	Oscilloscope capture of the waveform output by the piezoresistive sensor via the interface circuitry.	96
10.7	Zoomed-in blood pulse waveform from Figure 10.6, successfully showing that this method of blood pressure sensing can detect the micro-deflections caused by arterial blood pressure.	96
10.8	Wireless Integration of Sensors, Communications, and Android App subsystems, evidencing each part of the project interfacing successfully. . .	97
10.9	Autodesk Fusion360 model of the modified Thingy:52 device housing used for Communications.	98
10.10	3D printed model of the device housing, including wire-routing and mounting strap slots.	98
10.11	Sensor electrodes mounted on Velcro strap for the integrated wearable system.	99
10.12	Miniaturised interface circuit for the wearable device, utilising the AD623 Instrumentation Amplifier on a Development Board.	99
10.13	Inside view of the Thingy:52 case, showing the internally routed and soldered interface cables.	99
10.14	Final wearable demonstration of the wearable device, illustrating the new Thingy:52 Communications Module connected to the app and receiving data, in addition to the Data Processing Algorithm interpreting the received data and predicting the Blood Pressure based off this.	100

List of Tables

4.1	Interdigital electrode (IDE) dimensions show the electrode width and gap width and their abbreviation.	29
5.1	Different types of sensors that were characterised to determine the optimal sensor for continuous blood pressure monitoring.	37
8.1	Definitions of the selected features of the measured pulse waves.	70
8.2	Performance Metrics Across Different Regression Models	73
8.3	Performance Metrics Across Risk Categories	81
8.4	Performance Metrics Across Age Groups	81
H.1	Financial Expenditure Table - GDP Group 12	155

Nomenclature

<i>CVD</i>	Cardiovascular disease
<i>ABPM</i>	Ambulatory blood pressure monitoring
<i>ABP</i>	Arterial blood pressure
<i>ECG</i>	Electrocardiogram
<i>PTT</i>	Pulse transit time
<i>HRV</i>	Heart rate variability
<i>PPG</i>	Photoplethysmogram
<i>FFT</i>	Fast Fourier Transforms
<i>PWV</i>	Pulse wave velocity
<i>PDMS</i>	Polydimethylsiloxane
<i>PEDOT : PSS</i>	Poly(3,4-ethylenedioxythiophene) polystyrene sulphonate
<i>IDE</i>	Interdigital electrode
<i>CAD</i>	Computer-aided design
<i>UV</i>	Ultraviolet
<i>IPA</i>	Isopropyl alcohol
<i>SEM</i>	Scanning electron microscope
<i>SoC</i>	System on Chip
<i>SAADC</i>	Successive Approximation Analogue to Digital Converter
<i>BLE</i>	Bluetooth Low Energy
<i>GATT</i>	Generic Attribute Profile
<i>ATT</i>	Attribute Protocol Profile
<i>NFC</i>	Near Field Communication
<i>DK</i>	Development Kit
<i>MTU</i>	Maximum Transfer Unit
<i>BP</i>	Blood Pressure

Acknowledgements

With many thanks to Dr Rujie Sun and Professor Kai Yang for their assistance in this exciting project, and to Rosalind Thwaites for her sewing tutorial.

Statement of Originality

- I have read and understood the [ECS Academic Integrity](#) information and the University's [Academic Integrity Guidance for Students](#).
- I am aware that failure to act in accordance with the [Regulations Governing Academic Integrity](#) may lead to the imposition of penalties which, for the most serious cases, may include termination of programme.
- I consent to the University copying and distributing any or all of my work in any form and using third parties (who may be based outside the EU/EEA) to verify whether my work contains plagiarised material, and for quality assurance purposes.

You must change the statements in the boxes if you do not agree with them.

We expect you to acknowledge all sources of information (e.g. ideas, algorithms, data) using citations. You must also put quotation marks around any sections of text that you have copied without paraphrasing. If any figures or tables have been taken or modified from another source, you must explain this in the caption and cite the original source.

I have acknowledged all sources, and identified any content taken from elsewhere.

If you have used any code (e.g. open-source code), reference designs, or similar resources that have been produced by anyone else, you must list them in the box below. In the report, you must explain what was used and how it relates to the work you have done.

1) "Thingy52_Base.STEP" was designed by user Steven Minichiello and downloaded from GrabCAD, this was modified by [OR] to produce "Thingy52_base_modified.stl", the case for the Thingy:52.
The project repository "GDP12_Embedded_System" is an amalgamation and modification of the three repositories below:
2) "blefund_less4_exer2": can be retrieved from https://github.com/NordicDeveloperAcademy/bt-fund/tree/c9326135f35f98ee993c4030dddf90792bc630e2/v2.6.2-v2.3.0/I4/I4_e2_sol
3) "inter_less6_exer3": can be retrieved from https://github.com/NordicDeveloperAcademy/ncs-inter/tree/01b40888135665dc2c04a3a141b0d4673324d690/v2.6.2-v2.5.2/I6/I6_e3_sol
4) "peripheral_nfc_pairing": can be retrieved from https://github.com/nrfconnect/sdk-nrf/tree/5e125259f131cb4b5b7c1c72588df0fd0ae7f0c1/samples/bluetooth/peripheral_nfc_pairing

You can consult with module teaching staff/demonstrators, but you should not show anyone else your work (this includes uploading your work to publicly-accessible repositories e.g. Github, unless expressly permitted by the module leader), or help them to do theirs. For individual assignments, we expect you to work on your own. For group assignments, we expect that you work only with your allocated group. You must get permission in writing from the module teaching staff before you seek outside assistance, e.g. a proofreading service, and declare it here.

I did all the work myself, or with my allocated group, and have not helped anyone else.

We expect that you have not fabricated, modified or distorted any data, evidence, references, experimental results, or other material used or presented in the report. You must clearly describe your experiments and how the results were obtained, and include all data, source code and/or designs (either in the report, or submitted as a separate file) so that your results could be reproduced.

The material in the report is genuine, and I have included all my data/code/designs.

We expect that you have not previously submitted any part of this work for another assessment. You must get permission in writing from the module teaching staff before re-using any of your previously submitted work for this assessment.

I have not submitted any part of this work for another assessment.

If your work involved research/studies (including surveys) on human participants, their cells or data, or on animals, you must have been granted ethical approval before the work was carried out, and any experiments must have followed these requirements. You must give details of this in the report, and list the ethical approval reference number(s) in the box below.

ERGO: 99919

ECS Statement of Originality Template, updated August 2018, Alex Weddell aiofficer@ecs.soton.ac.uk

Chapter

1

Introduction

“Well begun is half done”
- Aristotle

(OR)

1.1 Problem Identification

Blood pressure (BP) monitors are a vital diagnostic tool for identification of conditions such as hypertension, hypotension, and other Cardiovascular Diseases (CVDs). These devices offer a direct insight to a patient's health, helping to identify abnormalities early and enabling interventions to prevent severe complications such as myocardial infarctions and strokes. However, many individuals don't recognise the early signs of CVDs before they cause lasting implications, only discovering the conditions when symptoms arise or during infrequent medical check-ups. This delayed discovery results in a reactive treatment style, where interventions can begin only after the condition has progressed.

The increasing ubiquity of wearable devices due to advances in flexible electronics and wireless communications presents a valuable opportunity to move away from reactive healthcare to a more proactive style by embedding continuous monitoring systems within devices worn by users every day. Devices incorporating these systems have shown promise but are limited in particular by high power requirements, which prevents the continuous monitoring required for accurate and informative blood pressure trend monitoring. Thus an alternative, flexible, low-power solution, that can achieve near-continuous monitoring, is desirable.

1.2 Meet the Team



Oscar Robinson

Project Manager, Design Lead, Sensors and Interfacing

Oscar oversees the entire project and is the main design lead for the group. He ensures that deadlines are met and manages communication with project stakeholders. He is part of the Sensor team with Mikayla Colegrave, and also Interface circuitry, using fabrication techniques to develop the pressure sensors for the blood pressure monitor and integrate with downstream sections.

**Mikayla Colegrave***Ethics, Sensors*

Mikayla's role on the project focuses on both administrative and technical aspects. She is responsible for completing the ethics application and risk assessment, ensuring that the project follows all necessary regulations and protocols during testing. She is also part of the Sensor team along with Oscar Robinson, to develop pressure sensors for blood pressure monitoring using fabrication techniques.

**Luqmanul Mohd Awallizam***Communications and integration*

Luqmanul is responsible for developing the embedded system that interfaces between the sensor team and the software team. He works as the intermediary between the two subsystems making sure that data is delivered reliably and effectively.



Geethaarth Vagga

Mobile App Development, Data Analysis

Geeth is responsible for developing the mobile application that allows the user to connect to and view data from the device, as well as process raw data to generate blood pressure estimation.



Mukilan Rajapandian

Data Analysis using ML/AI

Mukilan was responsible for developing data processing algorithms and health risk assessment models. His work focused on implementing signal processing pipelines, machine learning models for blood pressure estimation, and cardiovascular disease risk prediction systems.



Dr Rujie Sun

Supervisor - DHBE, University of Southampton



Professor Kai Yang

Customer - E-textiles in Healthcare, Winchester School of Art

1.3 Application area

This application was chosen because monitoring blood pressure is important for managing cardiovascular health. Abnormal blood pressure is a risk factor for many serious diseases (e.g., stroke, heart attack, fainting/falls). Blood pressure monitoring can help to identify health issues early for timely intervention. Traditional blood pressure measurement products are:

- 1. Bulky*
- 2. Difficult to use, especially for individuals with reduced hand strength and dexterity*
- 3. Do not provide continuous monitoring*

Therefore a comfortable, easy to use, and unobtrusive wearable device is required for accurate and continuous monitoring. The data needs to be presented via a digital interface (e.g. mobile app) that is user friendly and provides data relevant to users and health professionals who are likely to have different needs.

- Professor Kai Yang, WSA

1.4 Technology Readiness Level

The **Technology Readiness Level (TRL)** is a framework that describes the maturity of an emerging technology, providing a standardised scale for describing characteristics and performance, ranging from TRL 1: Basic principles observed and reported to TRL 9: actual system qualified through successful mission operations (Figure 1.1). [54]

Currently, the project is positioned around **TRL 3**, corresponding to the stage where basic principles have been observed and reported including preliminary research to

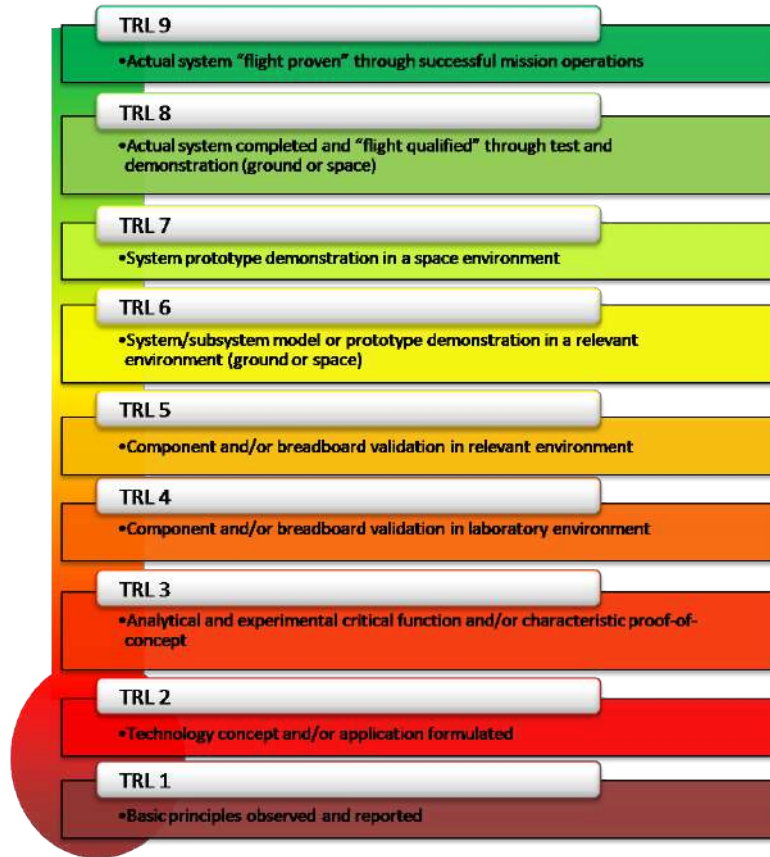


FIGURE 1.1: The TRL system, first developed by NASA, used to assess technology maturity. Extracted from [54].

validate the feasibility of alternative blood pressure monitoring systems (discussed in Chapter 2).

This project aims to test a functional prototype up to the standard of surrounding research as a proof-of-concept, illustrating the potential of the technology for future development. **The project aims to advance to TRL 4/5** by implementing a testbench-design involving detailed experiments; refining the prototype to incorporate additional functionalities.

Achieving higher TRLs will remain a Future Goal, discussed in Chapter 12. This will involve further testing (*in-situ*), refinement of the fabrication and manufacturing process, and a greater timescale to ensure the technology meets the necessary standards for practical application. Progressing through these stages will facilitate the transition of the blood pressure monitor from a conceptual model to a commercially viable product that can be delivered to the end-user successfully.

1.5 Justifications for Research

This project has several **Societal**, **Economic**, and **Environmental** justifications outside of the direct benefit to healthcare provision, detailed in Sections 1.5.1, 1.5.2, and 1.5.3. These provide concrete evidence to the benefits of developing this technology further, and place its use in context with the broader challenges and opportunities faced with advancing sustainable and equitable healthcare solutions.

1.5.1 Societal

Cardiovascular diseases (CVDs) are the globally leading cause of mortality, responsible for over 17 million premature deaths each year. [81] They present a significant burden not just on the health and wellbeing of individuals but also on communities at large as they predominantly manifest unnoticed before culminating in acute, life-threatening events such as myocardial infarctions (heart attacks) or strokes. In addition, as lifestyles become more sedentary through the widespread availability of motorised transport and the ubiquity of computers reducing manual labour for work, education, and recreation, and as diets become increasingly unbalanced due to readily available processed and hyper-refined foods, the global prevalence of chronic blood pressure diseases (such as hyper- and hypotension) has soared. [63, 59] Early detection and continuous monitoring of blood pressure (BP) are key to avoiding these outcomes, making it is more crucial than ever to facilitate the research and development of effective and accessible BP monitoring devices.

The gap in consistent monitoring is due in-part to the inconvenience and discomfort of traditional, bulky, cuff-based systems, or power-demanding optoelectronic systems. These both require a degree of patient adherence that is difficult to maintain in daily life, for example; in ambulatory blood pressure monitoring (ABPM, a test used by the UK's National Health Service), blood pressure readings are taken automatically using a cuff-based system over a 24-hour period at intervals of 20 - 30 minutes (Section 2.1.1) - this would be infeasible for taking manual measurements, as the reliance on patient test adherence is too great. [55] From a societal perspective, shifting towards truly continuous, unobtrusive, and accurate, monitoring systems that are integrated seamlessly into individuals' daily lives could empower many to take ownership of their cardiovascular health and make strong positive change. [61]

1.5.2 Economic

CVDs are not only a significant public health challenge, they also impose unequivocal effects on the economy, arising from hospital admissions, treatment, long-term care, and lost productivity, in both public and private healthcare entities. According to the

European Society of Cardiology (ESC), **in 2021 alone, CVDs [were] estimated to cost the EU €282 billion.** Around 55% (€155 billion) was attributed to direct health and long-term care costs, productivity losses were estimated at €47 billion (17%). [23] Moreover, the combination of economic burden partnered with the current expanding global market for wearable health technology illustrates the commercial viability of innovative blood pressure monitoring solutions; enabling both early intervention strategies to relieve spending, and capitalising on a growing industry, driven by consumer demand for non-invasive personalised healthcare. [25]

1.5.3 Environmental

While the healthcare sector's primary duty of care is to safeguard health, it also has a responsibility to consider environmental sustainability. Invasive blood pressure monitors contribute to hazardous medical waste, and many devices are not made of biodegradable or recyclable materials. Plastics make up approximately 25% of the 14,000 tons of waste that US healthcare facilities generate each day, and with 91% of plastics overall not recycled but instead sitting in landfills when they are disposed of, this presents a serious issue. [2] In comparison, many new sensor technologies are fabricated specifically out of biocompatible materials that are easy to dispose of responsibly. [41]

Power consumption is also a significant factor for consideration. Traditional devices that require frequent battery replacement or a direct power-supply can lead to increased energy expenditure over their lifetimes. [78] However, many next-generation sensors are focusing on wearable low-power implementations, incorporating ultra-low-power communication protocols such as Bluetooth Low Energy (BLE) or Near Field Communication (NFC). [83] Some devices also integrate energy-harvesting technologies into the design. [82] This focus on efficient power management not only benefits the end-user due to increased usage time, it also enables more information-rich monitoring and contributes to a smaller environmental impact.

Previous Work and Literature Review

Chapter

2

*“You have to learn the rules of the game. And then you have to play
better than anyone else.”*
- *Unknown*

(OR, MC, LMA, GV, MR)

The proliferation of wearable healthcare technologies has dramatically revamped blood pressure monitoring devices. Through recent technological advancements, a broad range of methodologies can be used from traditional approaches to those of the cutting edge. This shift has steered monitoring systems away from static and inconvenient designs towards solutions that provide greater adaptability and minimal disruptions to patients' daily lives. This is the essence of modern healthcare, which has seen innovation driven to provide real-time, accurate, and minimally invasive monitoring systems. This transformation is characterised by the integration of advanced sensors with robust data analysis capabilities, delivered to healthcare professionals and consumers through user-friendly mobile applications. By completing a comprehensive review of the technologies and systems available at present, this chapter also evaluates the different innovative possibilities that could potentially revolutionise the efficacy and convenience of blood pressure monitoring systems.

2.1 Currently available blood pressure monitoring devices

Blood pressure monitoring is a vital test performed in many healthcare settings due to its ability to identify a range of cardiovascular diseases (CVDs) and pulmonary disorders. As such, many devices have been manufactured in an attempt to improve the accuracy of blood pressure measurements. The most commonly available device is the cuff-based sphygmomanometer; while it is effective for measuring intermittent blood pressure this method cannot provide continuous monitoring, only an instantaneous reading, limiting its diagnosis capabilities. Section 2.1.1 discusses this further.

Various technologies have been tested that aim to capture continuous blood pressure measurements. However, careful consideration needs to be made when deciding which technology to pursue with this project. Factors such as accuracy, sensitivity, comfort, long-term reliability, and cost-effectiveness, will have a strong influence on the success of the design.

2.1.1 Sphygmomanometers

The conventional method for measuring blood pressure is a sphygmomanometer (Figure 2.1). There are three main types; Digital, Mercury, or Aneroid, with slight variations in pressure calculation but overall their function is the same. This technique works by inflating a cuff around the arm until blood flow is temporarily stopped in the artery. The air in the cuff is released slowly, and the blood pressure is measured based on when the regaining blood flow within the artery is detected with a stethoscope. [48]

This method has proven very effective for single-point measurements, but fundamentally, it can only measure intermittent blood pressure, which results in a few limitations.



FIGURE 2.1: Types of sphygmomanometer devices used in healthcare to measure intermittent blood pressure. Extracted from [20]

Masked hypertension often goes undetected - this is when blood pressure appears normal in a clinical setting, but elevates higher than normal throughout the day. Opposite to this is *white coat hypertension*, which often causes misdiagnosis due to stress induced by being in a medical environment, leading to elevated blood pressure, but normal measurements throughout the rest of the day. [79]

Continuous blood pressure monitoring would address this issue by providing more comprehensive data from which conclusions can be drawn. The increased availability of information on blood pressure trends throughout the day not only improves diagnostic accuracy for conditions such as *masked* and *white coat hypertension* but is also widely beneficial for other chronic diseases, enhancing patient health overall. [53]

An advancement on the traditional sphygmomanometer is the 24-Hour Ambulatory Blood Pressure Monitoring (ABPM) device, which uses the same concept of an inflating cuff around the arm but in addition, a portable monitor is worn at the waist to take readings over 24 hours (Figure 2.2). The device inflates the cuff at regular intervals (every 30 to 60 minutes) and stores the data collected after each reading for later analysis.

While ABPM provides blood pressure data at various points throughout the day, it is still not truly *continuous* due to the large time intervals between each reading. In addition, its bulky and an uncomfortable design - particularly during sleep - make it impractical for many patients to wear for the 24 hour period. Additionally, during this 24-hours, it is also made impossible to perform any physical activity or do anything that makes the monitor wet (for example, showering) impossible. [30]

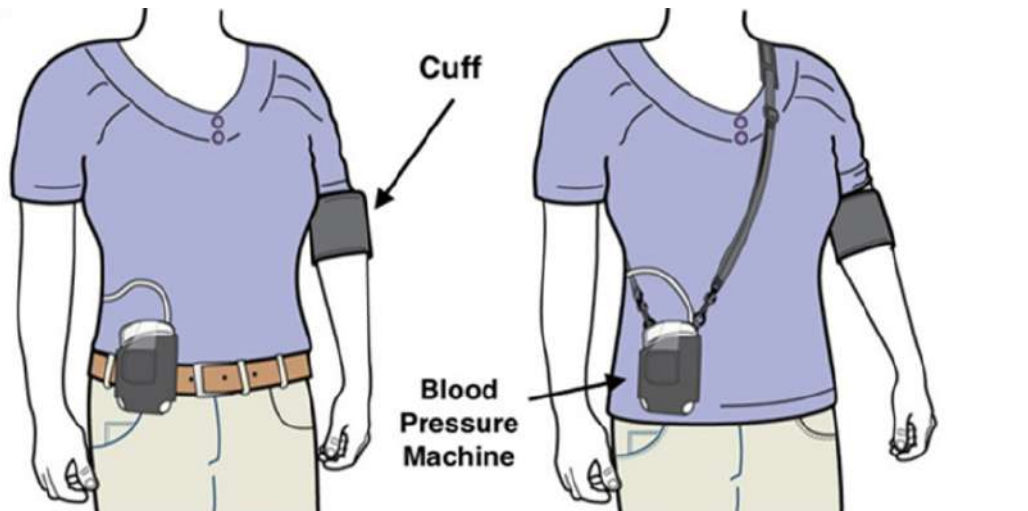


FIGURE 2.2: A 24-Hour Ambulatory Blood Pressure Monitoring (ABPM) device showing the inflatable cuff on the upper arm and the blood pressure machine worn at the waist. Extracted from [30].

2.1.2 Invasive Arterial Blood Pressure Monitoring

Invasive needle-based arterial blood pressure (ABP) monitoring is currently the most accurate method to monitor continuous blood pressure. This is because it measures the pressure directly from the artery. A cannula is inserted into a peripheral artery in the arm, which is connected to a transducer that constantly measures and logs the pressure, to be displayed on a screen as in Figure 2.3. This provides doctors and clinicians with direct information about their patient's health. However, this setup is not suitable for patients who continue to engage in normal daily activities and are required to check their blood pressure regularly at home. This method is highly invasive since it requires the needle to be inserted into the arm for extended periods of time, potentially damaging the tissues surrounding it, causing significant discomfort. Therefore, this method is only used when it is necessary for critical patients in Intensive Care Units (ICUs). [16]

2.1.3 ECG and PPG

An electrocardiogram (ECG) uses sensors placed on the skin to measure the electrical signals produced by the heart. ECG is more commonly used to measure heart rate. However, it can also indirectly measure blood pressure. Machine learning algorithms can analyse features such as Pulse Transit Time (PTT) or Heart Rate Variability (HRV) that are extracted from these signals to calculate the blood pressure [33].

Photoplethysmogram (PPG) sensors use infra-red light to measure the change in blood volume within blood vessels. The emitted light penetrates the skin and reflects off blood vessels, which is detected by a sensor. Blood pushed through the vessels with each pulse wave causes changes in the intensity of reflected light corresponding to the deformation

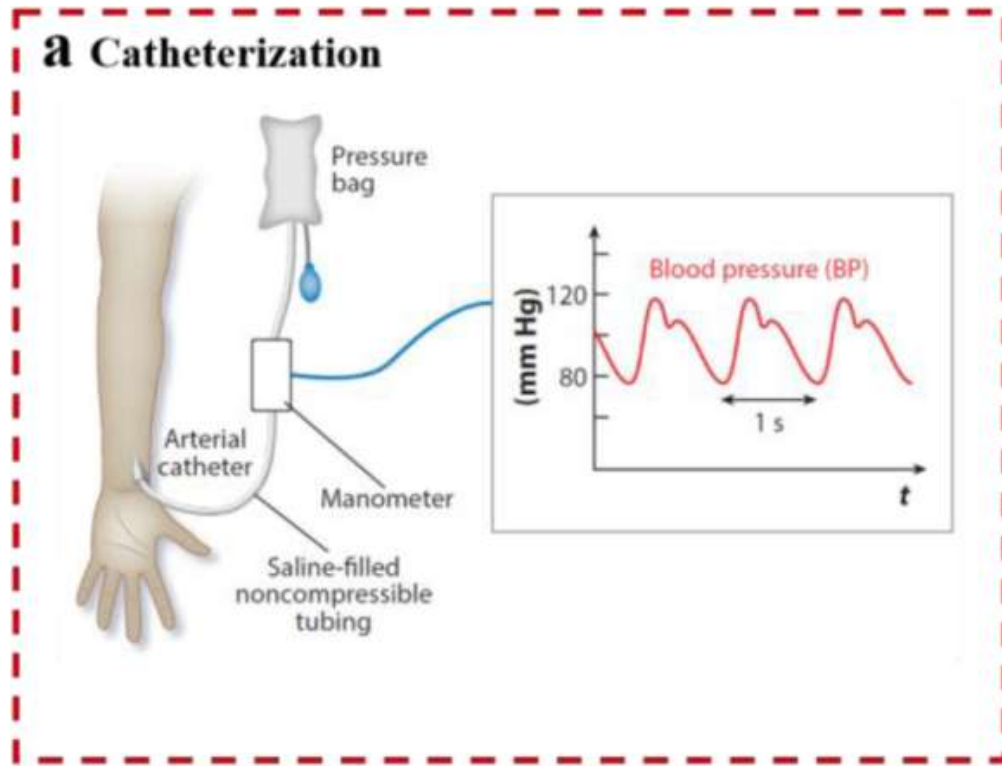


FIGURE 2.3: The setup for invasive blood pressure monitoring typically used in hospitals in ICUs. A cannula is inserted into a peripheral artery and the blood pressure is directly measured using a transducer system. Extracted from [85].

of the vessel. These fluctuations form the PPG signal which can be analysed using a variety of techniques such as Fast Fourier Transforms (FFTs) or Wavelet Transforms, to examine periodic components related to physiological signals such as heart rate, blood pressure, and arterial compliance/stiffness. [1]



FIGURE 2.4: A smartwatch that has ECG and PPG sensors built into it so that information from these signals can be used to indirectly measure blood pressure from features such as PPT and HRV. Extracted from [46]

Integrating ECG and PPG sensors in a smartwatch has been shown to provide

estimations of systolic and diastolic blood pressures (See Figure 2.4).[50] However, this implementation presents several challenges. Precise synchronisation of the two signals is essential to ensure accuracy, which requires additional steps before processing the signals. This is due to the sensors being transducers of different signal types (electrical and optical). A method by Hao Lin et al. used Bluetooth modules to transmit timestamps from one subsystem to another to synchronise these combined system. This was done using a master-slave protocol, where the ECG subsystem acted as the master, transmitting timestamps to the PPG subsystem, which then responded with its own timestamps. The ECG subsystem used this information to calculate and adjust for any delay or offset between the two signals. [44] Only now can the signals be processed. However, this increases computational complexity by using additional Bluetooth modules and memory to store the timestamps, which leads to a heavier power strain on the device. Additionally, the use of two sensor types (especially the power-intensive optoelectronic PPG) increases energy consumption significantly. Continuous monitoring further increases power demands, as both sensors must remain active for extensive periods, which overall reduces this methodology's suitability for continuous wireless monitoring. [85]

2.1.4 Piezoelectric Pressure Sensors

Piezoelectric sensors are an emerging innovative approach to measuring continuous blood pressure non-invasively. They are made from a piezoelectric material, which includes various polymer-based and ceramic materials, that produce an electrical charge in response to applied pressure; in this case, the deformation caused by blood flow in the arterial wall. Jian Li et al. produced a functioning system based on this approach, detailed in Figure 2.5, which illustrates the process of biological signal transduction to calculate blood pressure using a custom device that is displayed on a smartphone. In Li's setup, the wrist strap integrates two piezoelectric pressure sensors, one detecting the systolic pulse and the other for the diastolic pulse. The system calculates the localised pulse wave velocity (PWV) via the fixed distance between the sensors and the varying time between each pulse waveform. This data, along with key features in the signals, are transmitted and used to calculate blood pressure. [34]

One of the most effective piezoelectric materials is a ceramic compound - Lead Zirconate Titanate (PZT). This is relatively inexpensive compared to other materials but still has a strong piezoelectric property, which justifies its use above. However, PZT is a toxic material that can cause significant health issues and skin irritation with prolonged exposure. This reduces its suitability for use in a wearable device. [69] Additionally, piezoelectric materials have been shown to degrade over time, resulting in reduced sensitivity. This leads to reduced accuracy in blood pressure estimations made by the device. Furthermore, since the pressure exerted on the skin by pressure due to a blood

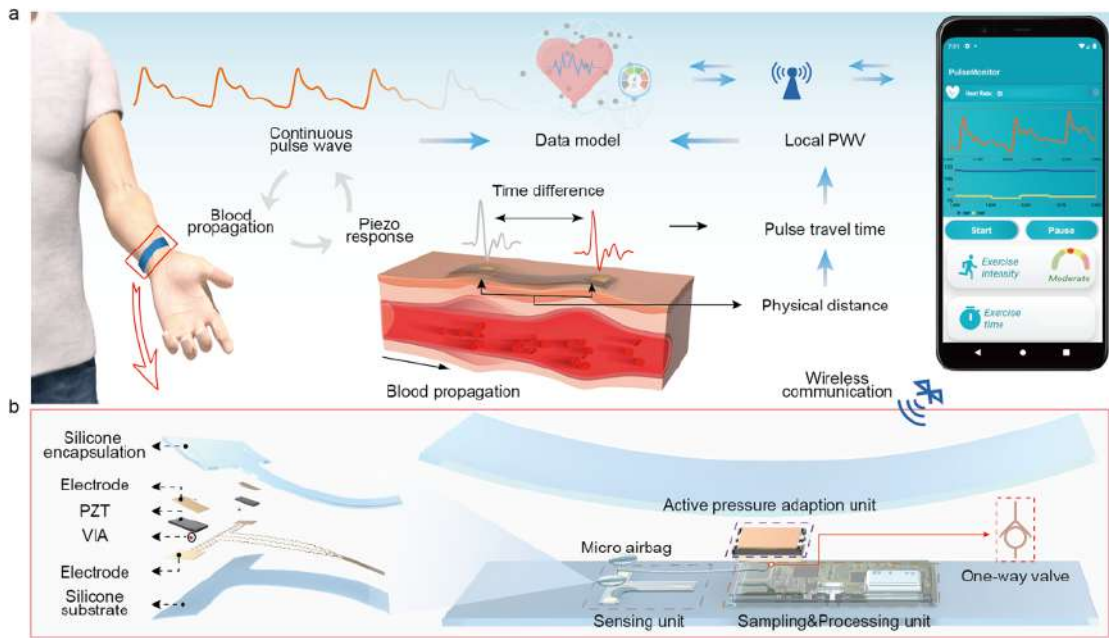


FIGURE 2.5: The working principle of the soft, wearable wireless piezoelectric pressure sensor to monitor continuous blood pressure extracted from [34]. The schematic details the signal processing from converting the piezo-response detected from the wrist strap to continuous blood pressure can be presented on a graphical user interface (GUI).

pulse is very small, these sensors are highly susceptible to noise, which worsens as the material degrades. The only solution is to integrate complex interfacing circuitry (filters and amplifiers) into the system to ensure accurate readings, resulting in an increased production cost and presenting a challenge for widespread adoption. [69]

2.1.5 Piezoresistive Pressure Sensors

Similar to piezoelectric sensors, piezoresistive sensors also respond to mechanical deformation. However, instead of generating an electrical charge, they produce a change in electrical resistivity when subjected to mechanical stress. Integrating these sensors into wearable medical devices has shown promising results in continuous blood pressure monitoring. A study by Bijender et al. explores the development of flexible and wearable piezoresistive sensors, demonstrating their accuracy in monitoring blood pressure, highlighting their potential and for replacing current blood pressure monitoring methods in the future. [8] These sensors respond to the micro-deformations in the arterial wall by proportionally altering the resistance of the piezoresistive material based on the applied pressure. From this, the systolic and diastolic pressures can be indirectly calculated to give blood pressure. [19]

Figure 2.6 a. demonstrates a detailed example of the fabrication process of a piezoresistive sensor. In this example, polydimethylsiloxane (PDMS) is used as a flexible, biocompatible polymer substrate by pouring it into a mould and allowing it to solidify.

This substrate is then coated with a conductive, piezoresistive polymer, such as poly(3,4-ethylene dioxythiophene) polystyrene sulphonate (PEDOT: PSS) or MXenes to produce the soft, flexible, piezoresistive sensor. Finally, a flexible electrode is placed on top of the substrate such that a change in electrical resistivity across the sensor can be measured, often through supplying a low voltage to the sensor and measuring the change in voltage, proportional to the change in resistance (and pressure). This signal is then processed (Figure 2.6 b.) and can be wirelessly communicated to a smartphone, where the blood pressure is displayed. [36]

Piezoresistive sensors are advantageous over their piezoelectric counterparts due to their lack of signal degradation over time, resulting in a consistently high sensitivity. In addition, since the working principle of the sensor is based on varying electrical resistance, this provides a more straightforward approach to any interface circuitry as the output is independent of supplied system voltage; irrespective of the supply, it is attenuated proportionally based on the varying pressure induced on the sensor and the voltage drop is easily measured. This makes piezoresistive sensors ideal for low-power, wearable devices. [29]

Although piezoresistive sensors do not achieve the same accuracy as cannulated-ABP methods, they are non-invasive which is beneficial because they can be used in daily life without causing harm. Their fabrication process is simple while remaining flexible and comfortable and can be incorporated into wristbands that do not get in the way of activities such as sleeping or exercising. Research by Jianguo Hu et al. highlights the recent progression in this technology, emphasising how the improvement in the comfort of the device has allowed for longer monitoring of physiological signals, enhancing healthcare outcomes. [32] Furthermore, the simplicity of the design makes the device cost-effective, as it is relatively inexpensive to produce compared to other innovative methods of monitoring blood pressure. [86]

2.2 Wireless Communication Technologies

With the advancement of wearable healthcare technologies, wireless communications have emerged as a replacement for traditional wired systems, offering greater portability and convenience for end-users. In this project, wireless communication bridges the gap between the piezoresistive sensors that capture the pulse waveform, and the monitoring device that calculates and displays the patient's blood pressure. The landscape of wireless communication technologies is diverse, four of the most common implementations include Bluetooth Low Energy (BLE), Zigbee, Ultra-Wide Band (UWB) and Near Field Communication (NFC).[43] These technologies are suited to specific applications, with unique strengths and trade-offs.

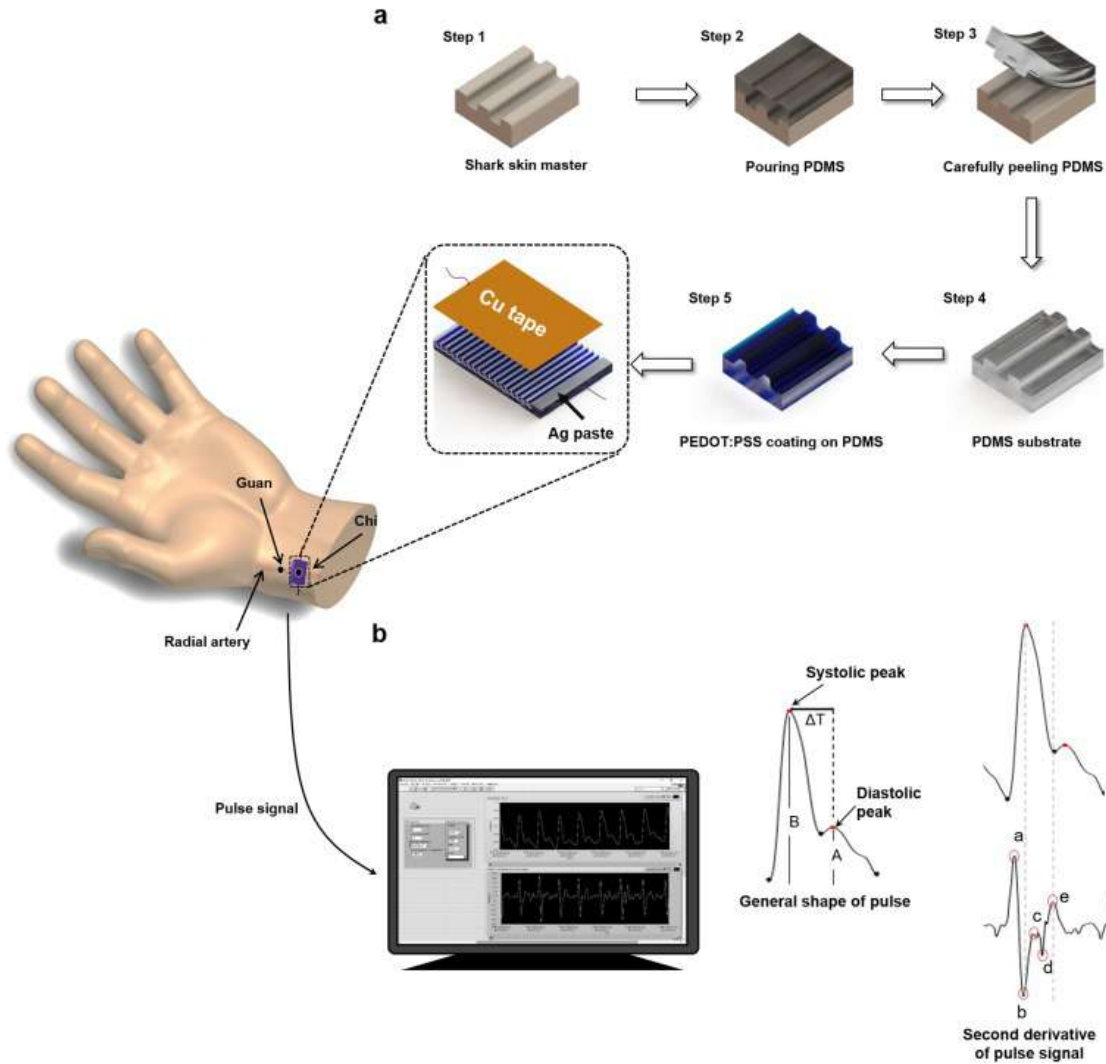


FIGURE 2.6: Schematic showing the fabrication process of the piezoresistive blood pressure sensor and its application, extracted from [36].

BLE is a wireless communication standard managed by the Bluetooth Special Interest Group (SIG). Its system was designed to be used in extremely high volumes for devices powered by standard button-cell batteries, making it optimised for ultra-low power consumption, low costs, robustness, and short-range. [31] This comes at the trade-off of a 1[Mbps] lower data rate, and less sophisticated association modes compared to the original Bluetooth Classic.[45] With these characteristics, BLE has been commonly used to develop healthcare systems among other low energy-consuming systems. [43]

Zigbee is a wireless mesh network protocol designed for low-cost and low-power applications. Compared to Personal Area Networks (PAN), like BLE, mesh networks can have a greater range because data can be relayed through intermediate mesh nodes. This gives Zigbee excellent reliability and scalability, making it an excellent choice in home automation systems and industrial sensor networks.[60] The disadvantages of Zigbee are its greater implementation complexity, owing to its need for network coordination, and its reduced maximum data rate of only 250[kbps]. [45]

UWB is a wireless communication technology that operates across a broad frequency range. This grants UWB extremely high data rates of Gigabits per second, and inherently greater security due to its noise-like signal, making it difficult for unintended receivers to detect. [65] However, this is at the cost of requiring a complex receiver design, which increases development costs and may not be suitable for applications prioritising simplicity and affordability. Furthermore, this technology has been optimised for short-range communication (up to 10 meters) with low power consumption. [66] For these reasons, UWB is commonly used as a communication link in a sensor network because it provides extremely high data rates in multi-user network applications. [65]

NFC is a wireless communication technology designed for point-to-point data transfer. It is a low-complexity, low-power technology that requires devices to be within a few centimetres of each other. The short-range communication of NFC gives it a natural security that limits eavesdropping at lower supported data rates up to a maximum of 424[Kbps]. The attributes of this technology allow it to be used in secure, close-contact communications, such as contactless payment. [35]

The key criteria for evaluating and choosing the right wireless communication technology are the range, power consumption, data transfer rate, implementation complexity, and cost. Figure 2.2 indicates the rank of each technology concerning these criteria. By comparing these attributes, BLE was identified as the optimal choice of technology that aligned with the specific objectives and constraints of this project. This was further validated by having precedence in other blood pressure monitoring systems.[37] The System on Chip (SoC) chosen to integrate BLE was then decided to be the nRF52840 Development Kit (DK) for testing, and eventually the Thingy:52 for integration, both made by Nordic Semiconductor.

2.3 Mobile Application

Mobile health applications have transformed the way patients interact with their health. With 94% of UK adults owning a smartphone in 2024 [58], their impact is greater than ever. A review found that, as of 2017, there were over 325,000 health apps available on Apple's app store [27]. With the advent of wearables with mobile connectivity, apps have become an integral component of modern healthcare devices, serving as the primary interface between users and their health data. The development of these applications has evolved alongside advancements in wireless communication technologies and sensor miniaturisation, transforming from simple data display interfaces into sophisticated platforms that can process, analyse, and visualise health metrics and provide new insights in real time.

The introduction of the 802.15.4 IEEE standard for low-rate wireless personal area networks (LR-WPAN) in 2003 [22], which also formed the basis for ZigBee, motivated

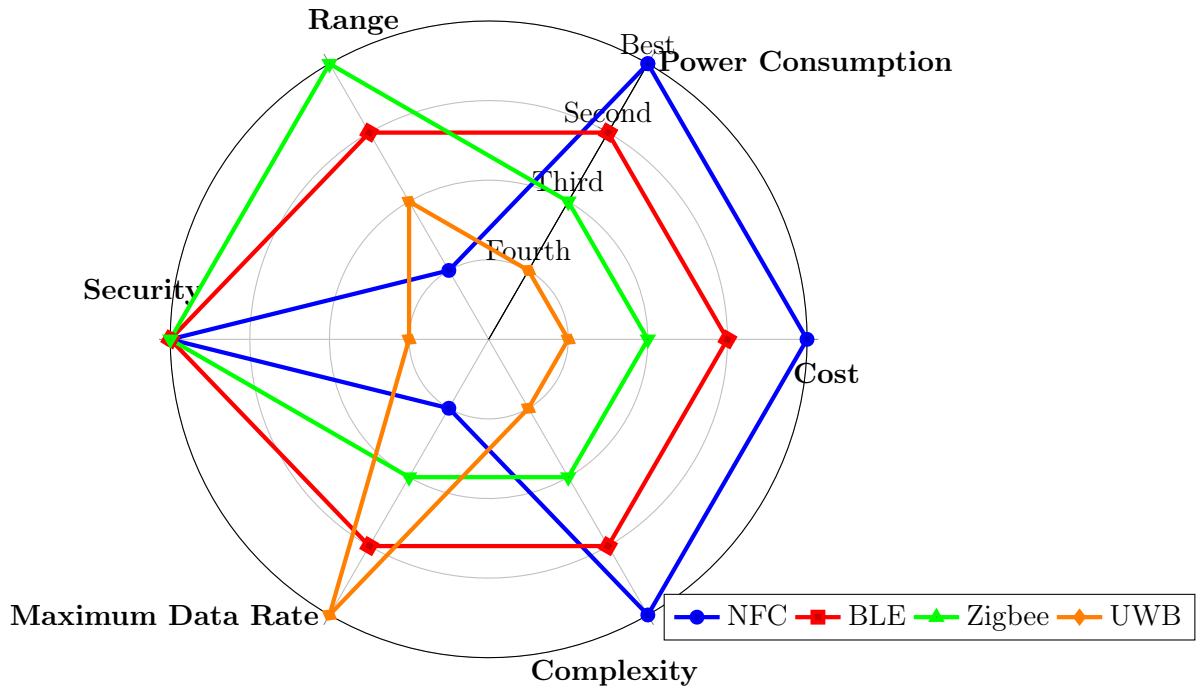


FIGURE 2.7: Comparison of Wireless Communication Options

the development of many wearable sensor systems. For example, in 2004, Welch et al. designed a wireless ECG smart sensor for life threatening event detection, which used a short-range ISM band transceiver to relay patient alarm status to a body-worn gateway, which then relayed the information to a server [80]. Jovanov et al. discuss a prototype "WWBAN" or Wireless Wearable Body Area Network, an array of sensors worn on the body which connect to a "personal server" such as a phone or computer, through ZigBee-based radios, that then relay information to medical professionals [39]. One key limitation that was noted was the "lack of support for massive data collection and knowledge discovery." This appears to be a common theme, with the main limiting factor for adoption and usability appearing to be the infrastructure required at the time. Figure 2.8 shows a diagram extracted from Jovanov et al.'s paper - it is interesting to note how the overarching structure is not too different from implementations today, though with several additions: a "network coordinator" to enable the device to communicate with the sensor, and the need to upload to the internet by first connecting to a desktop if GPRS is unavailable. In the smartphone era, these can both be bypassed.

The wearables landscape today, while retaining some aspects of early developments, looks very different. The past few decades have seen immense changes in how we as a society interact with technology. With the advent of smartphones, a new industry of wearable health technology has emerged. Fitness trackers such as the Fitbit provide an easy, accessible way for individuals to track their health, with many devices offering continuous monitoring of heart rate, blood oxygen saturation, etc. Apple Inc. has been

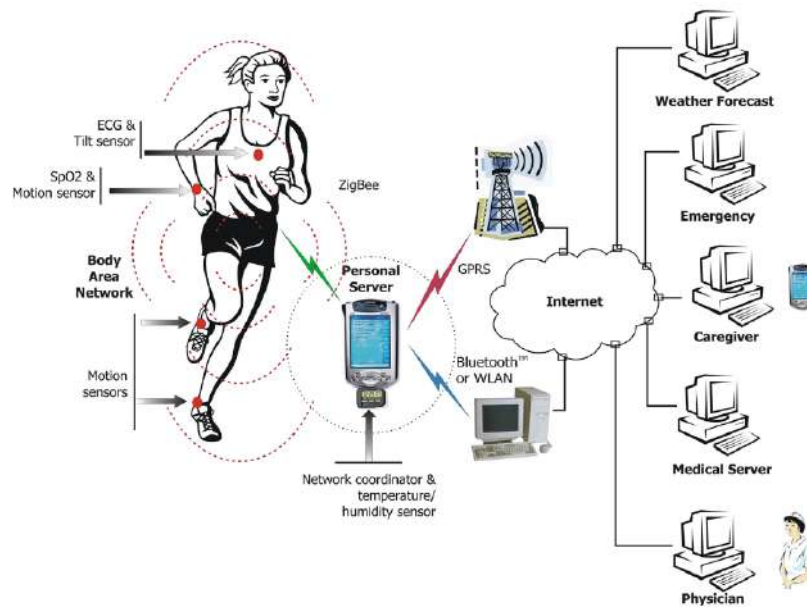


FIGURE 2.8: A diagram extracted from [39], illustrating how sensors were integrated into a full patient monitoring system in the pre-smartphone era.

another key leader in this space: their Apple Health app offers in-depth insights on fitness, sleep and mood as well being able to alert the user about health conditions such as atrial fibrillation, complementing their device's functionality [4]. The app also provides the ability to share data with others, so that family members can be informed of each other's health.

Alongside this growth in the consumer market for wearables, there has been continued interest from the medical field in exploring how these technologies can best be integrated into the medical care system to maximise patient outcomes. The concept of "connected healthcare" - a paradigm shift where pre-emptive care should be made in a participatory and personalised manner, aided by the use of new technological innovations, explores analysing data from sensors and other sources in aggregate to derive actionable insights for patients and healthcare workers, progressing towards the vision set forth in early works [14]. This shift was accelerated by the COVID-19 pandemic, where many patients were forced to rely on the internet for access to medical services and treatments [6], [28]. The National Health Service (NHS) launched the "NHS App" in January 2019 saw a sharp rise in usage in 2020 and 2021.

Despite the immense progress that has been seen, there are still many areas where further steps can be taken. Uptake of health apps has historically been lower in older populations, the same demographic that could benefit the most from informed pre-emptive care [12]. The aforementioned NHS App also saw significantly fewer registrations in practices lowest percentage of patients aged 15–34 years, indicating uptake skews younger [40].

There is a clear gap in the wearables market for a system that integrates wearable sensor data with a user-friendly application that appeals to an older demographic, while also providing the option of sharing data with healthcare workers.

2.4 Data analysis (ML/AI)

Building upon the evolution of mobile health applications, this section explores the integration of machine learning techniques in cardiovascular monitoring systems. While mobile platforms have advanced significantly, the implementation of continuous blood pressure monitoring presents unique technical challenges that require sophisticated data processing approaches.

Evolution of Blood Pressure Monitoring

Current commercial blood pressure monitors predominantly employ traditional measurement techniques, with limited machine learning integration. This limitation stems from computational requirements for real-time ML processing, power consumption constraints in portable devices, regulatory challenges in validating ML-based medical devices, and cost considerations in implementing specialized hardware.

Recent advances in sensor technology and digital health have created new opportunities for continuous blood pressure monitoring. As Rick Ratliff, managing director of digital health solutions at Accenture, notes: “The proliferation of internet-connected solutions and evolving regulatory guidelines are blurring the lines between clinical and consumer health solutions. As consumer health platforms support more ‘medical’ devices, rather than just today’s wellness trackers, they’ll create a viable self-care model in a segment that today is occupied by chronic-disease monitoring companies.”[\[64\]](#)

Current Approaches and Limitations

Contemporary methods for non-invasive blood pressure estimation include photoplethysmography (PPG), pulse transit time (PTT), and pressure sensor-based techniques. Each method presents unique challenges: PPG suffers from motion artifacts, PTT requires multiple sensor types, and pressure-based techniques struggle with continuous monitoring implementation.

The integration of these approaches in commercial devices has been constrained by traditional algorithm limitations in real-time signal processing, user variation adaptation, environmental interference handling, and long-term calibration stability.

These challenges necessitate more sophisticated machine learning approaches for robust implementation.

Mobile Platform Implementation

Modern smartphones provide an ideal platform for ML-based health monitoring systems through their advanced processing capabilities, dedicated AI acceleration, and extensive memory resources. This computational foundation enables complex ML model deployment while maintaining real-time processing performance and power efficiency. The integration of secure data handling and regular update capabilities further enhances their suitability for health monitoring applications.

Proposed Approach

This project addresses these challenges through two main components: a blood pressure estimation system and a cardiovascular disease (CVD) risk assessment model. The blood pressure estimation component transforms raw piezoresistive sensor readings into continuous measurements through advanced signal processing and machine learning techniques, moving beyond traditional cuff-based methods while maintaining measurement accuracy.

The CVD risk assessment model complements the blood pressure monitoring by analyzing various cardiovascular health indicators to predict potential risks. The system processes voltage signals through multiple stages: initial signal conditioning, feature extraction, and machine learning-based estimation of systolic and diastolic pressures. Through carefully designed bandpass filtering and noise reduction techniques, the system maintains signal fidelity while removing motion artifacts and environmental interference.

Project Management

Chapter

3

“All we have to decide is what to do with the time that is given to us.”
- Gandalf, The Lord of the Rings: The Fellowship of the Ring (2001)

(OR, MC)

At the start of the project, the group implemented a mini-sprint approach to initial research to define the specific stages involved in the project. During this, each team member independently investigated their assigned area over a few weeks and from this, divided the deliverables of the project into two broad phases, detailed below.

Phase 1 involved the production of a proof-of-concept model, involving a Liquid Metal (LM) piezoresistive sensor array on a biocompatible PDMS substrate, to be interfaced with on a development board and data transmitted wirelessly using BLE to a smartphone, where a simple but effective GUI would display the results and calculated blood pressure, determined from Pulse Transit Time. Phase 2 aimed to develop the system by moving from the development board to a custom in-house fabricated flexible PCB that could be embedded within a wearable accessory. Both phases follow the same overall flowchart, established in Figure 3.1. This project outline was organised using the Gantt Chart in Appendix F. This was revised halfway into the project, producing Appendix G. Financial expenditure is covered in Appendix H.

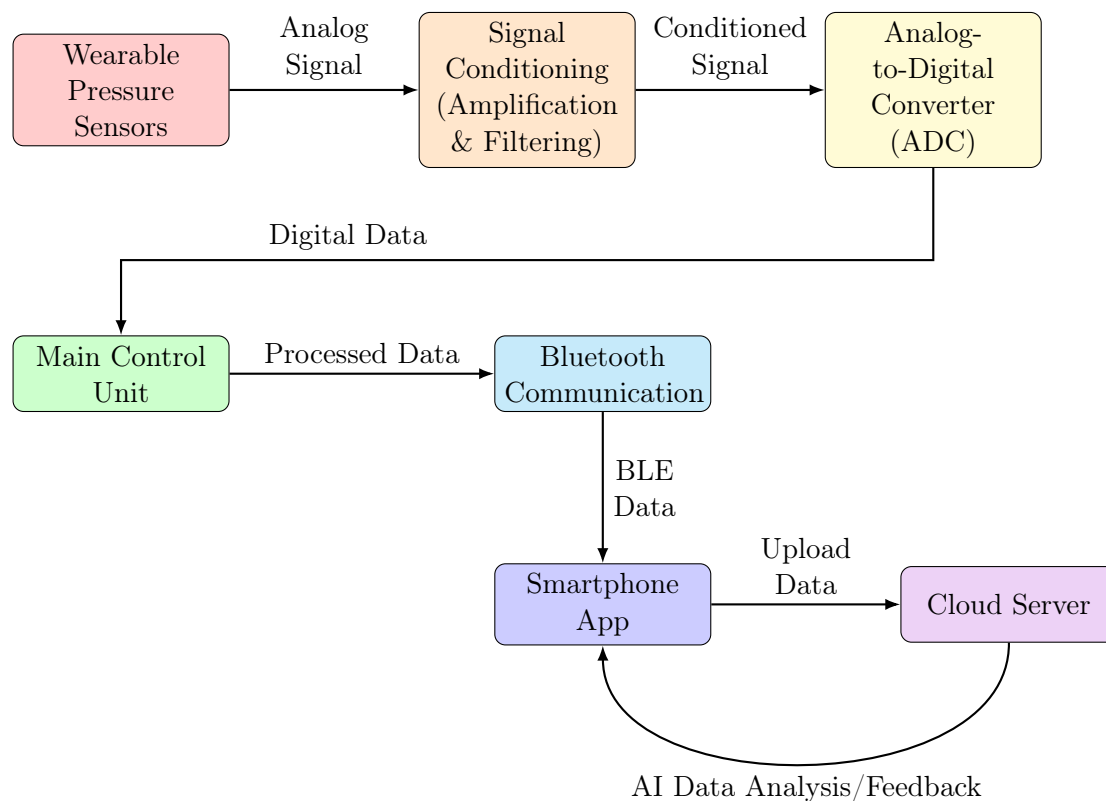


FIGURE 3.1: Initial Design Flowchart

3.1 Required Sections

To cover the project specification outlined, seven key stages of the project were identified, and divided as follows:

- 4 - **Sensor Fabrication:** Fabrication of the identified sensor types was assigned to [OR] and [MC].
- 5 - **Sensor Characterisation:** Following fabrication, the new sensors must be tested through a uniform methodology to determine which were appropriate for further use. This was also assigned to [OR] and [MC].
- 6 - **Sensor Interfacing:** To develop the sensor characterisation methodology, and to make effective use of the best-performing sensor for downstream devices, a suitable interface circuit must be developed. This was assigned to [OR].
- 7 - **Communications:** To extract the data from the sensors and transmit it to be processed, an effective and low-power communication module must be used, this was assigned to [LMA].
- 8 - **Blood Pressure Estimation:** A Machine Learning model will be developed by [MR] to calculate blood pressure using features extracted from the transmitted data.
- 9 - **Mobile Application:** To visualise the calculated blood pressure data, a simple and easy-to-use application will be designed by [GV].
- 10 - **Total System Integration:** Combining all of the aforementioned parts together to create one functioning system will be managed by [OR] but include all previous work. This will be done in several stages, producing working prototypes and progressing towards the final goal of a wireless, wearable device.

3.2 Ethics Application Process

This project was limited to developing a proof-of-concept prototype for the wearable blood pressure monitor, and participant testing was planned to be completed only by the investigators of the project. However, an ethics application was still necessary because the prototype collects personal health data, which means it is classified as a medical device. It was crucial to ensure that all data was securely collected, stored and anonymised to protect the participants' private information to prevent any breaches of personal information during the experiment.

An ERGO application was submitted with ERGO ID 99919. As part of the application, a primary data form (See Appendix A) was completed to outline the purpose of the device and the scope of the project. Although the investigators themselves were the participants, a signed consent form (See Appendix B) was still required from each participant. To ensure the participants were aware of what was expected of them, a participant information sheet (See Appendix C) was provided before the experiment, describing the procedure of the experiment and how their data would be handled.

If a participant felt the need to withdraw from the experiment, they were allowed to do this at any point without providing a reason. If this happened, all the recorded data for this participant was immediately deleted from the server to ensure the safety of their data.

A data protection agreement (DPA) form (See Appendix D) was completed to ensure that all data being collected was stored correctly. Additionally, this form also highlighted who would have access to the data, when it would be destroyed, and the participants' rights regarding their personal data. A full risk assessment (See Appendix E) was also conducted to identify potential hazards during the experiment and the preventative measures to ensure the experiment ran smoothly and safely.

Once the ethics application was approved, these protocols were followed ensuring all data was ethically collected and stored, even though it was an investigator- only testing environment.

Sensor Fabrication

Chapter

4

“Creativity is contagious, pass it on”
- *Albert Einstein*

(OR, MC)

The piezoresistive pressure sensor was chosen because it has a simple fabrication process, allowing a compact and flexible sensor to be integrated into a comfortable wearable device. This was designed to be worn around the wrist via a wristband, positioning the sensor directly over the radial artery for optimal detection of blood pressure pulses (See Figure 4.1).

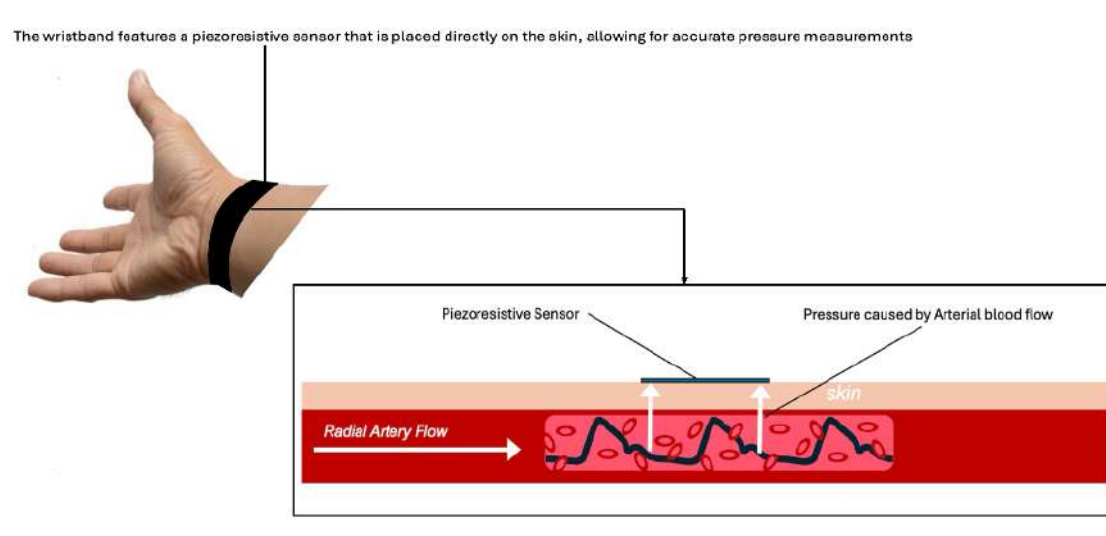


FIGURE 4.1: An image showing the placement of the wearable device and a zoomed-in diagram showing the piezoresistive sensor's placement on the Radial artery so it can detect the arterial blood pulses.

The piezoresistor sensors were constructed using a multilayer design consisting of a flexible copper electrode, polydimethylsiloxane (PDMS) microstructure layer, and a conductive polymer coating of poly(3,4-ethylene dioxythiophene) polystyrene sulphonate (PEDOT: PSS), which was produced by Sigma-Aldrich [75] (See Figure 4.2). Various electrode types, including interdigital and solid electrodes, and PDMS microstructures, such as microdomes and micropyramids, were designed and fabricated to determine which combination of these layers performed best during characterisation. The PEDOT: PSS coating was done by trialling two methods, which were either spin-coating it on top of the cured PDMS microstructures or mixing it into the PDMS before the microstructures were cured. The characterisation process determined the sensitivity of each sensor ensuring that the optimal one was chosen for further testing to monitor continuous blood pressure.

4.1 Interdigital Electrode Fabrication

The electrodes are the conductive pathway between the piezoresistive material and the electronic circuit. They do this by transmitting the voltage change caused by changes in the material's resistance when pressure is applied to the sensor, allowing the circuit to process the detected signal. To evaluate performance, five interdigital electrodes (IDEs) (see Figure 4.3) with varying electrode rod widths and gap widths were fabricated

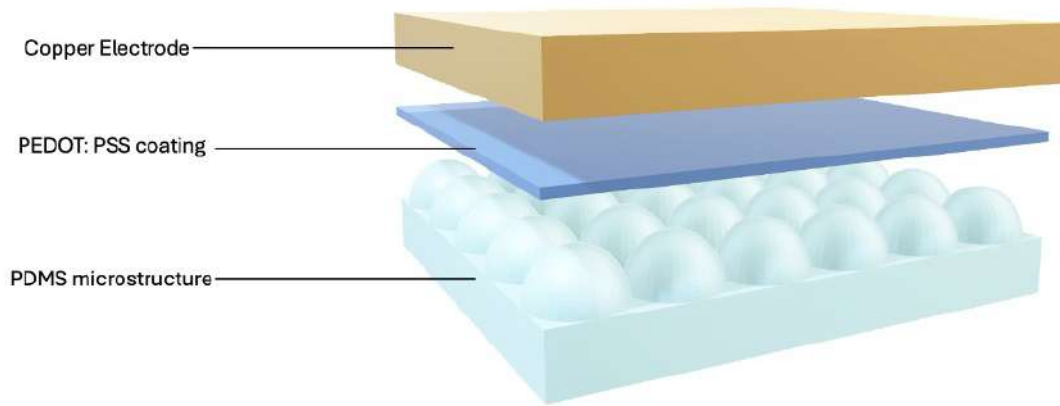


FIGURE 4.2: A graphic design showing the different layers of the multilayer sensor separated for visual purposes. The top layer indicates the copper electrode representing either the interdigital electrode or solid electrode, the middle layer represents the PEDOT: PSS conductive layer, and the bottom layer represents the PDMS microstructures. In this figure, the PDOT: PSS coating is represented as a sheet. However, this coating is either spin-coated on top of the PDMS microstructure layer or mixed into it before it is cured.

for testing. The chosen dimensions and their corresponding abbreviations are listed in Table 4.1. Each electrode was designed to have dimensions $1[\text{cm}] \times 1[\text{cm}]$ and was modelled using computer-aided design (CAD) in Fusion 360. [5] These were later used for ultraviolet (UV) printing once the flexible substrates had been prepared.

TABLE 4.1: Interdigital electrode (IDE) dimensions show the electrode width and gap width and their abbreviation.

Electrode width [μm]	Gap width [μm]	Abbreviation
500	500	500 x 500
400	400	400 x 400
300	300	300 x 300
200	200	200 x 200
100	100	100 x 100

The flexible polymer substrates were prepared by spin coating photoresist onto a $9[\mu\text{m}]$ copper sheet that was cut to a size that would fit into the UV printer. It was important to make sure that the copper sheets were completely covered with the photoresist so that the CAD design could be properly transferred onto them during printing. Once the copper sheets were fully covered, they were baked at $110[^\circ\text{C}]$ for five minutes. When they were done, the underside of the sheets was cleaned with acetone to remove any unwanted photoresist. The substrates were now ready for the IDE CAD designs to be printed onto them using UV lithography.

The CAD designs were inverted and loaded into the printer which CADworks3D H-series [10], with each copper sheet including 10 electrode designs to allow for any errors

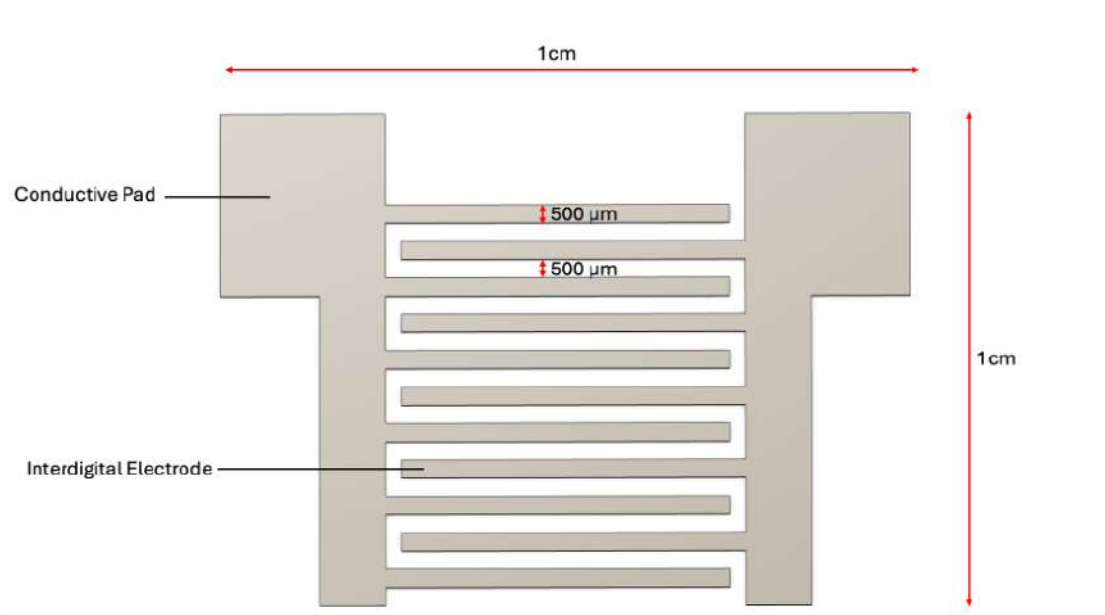


FIGURE 4.3: Fusion 360 CAD design for the 500 x 500 IDE showing the gap width, individual Interdigital electrode rod width, and the dimension of the entire design. The design shows two conductive pads which were used in the final assembly process to connect the sensor to the circuit. Similar models were made for all the IDEs ranging from 500 x 500 to 100 x 100. Note that when the design was converted to the ctb file to carry out the UV 3D printing, the design was inverted so that the surrounding copper would be etched instead of the IDE.

that could occur later in the fabrication process, during the etching. This process was repeated for all the varying IDE sizes.

Once UV printing was completed, the substrates were placed into a tray that contained 20[mL] of developer and 80[mL] of water for approximately three seconds. Precision was taken during this step as it was important to ensure that the substrates were not overdeveloped or underdeveloped to make sure the designs were properly etched.

Once developed, the electrodes were thoroughly rinsed with water to ensure the development process had fully ceased. The electrodes were dried and were then etched in a bath containing the etching solution to remove the unwanted copper surrounding the designs. Once the etching process was complete, the electrodes were cleaned with acetone and dried to reveal the final structure (See Figure 4.4).

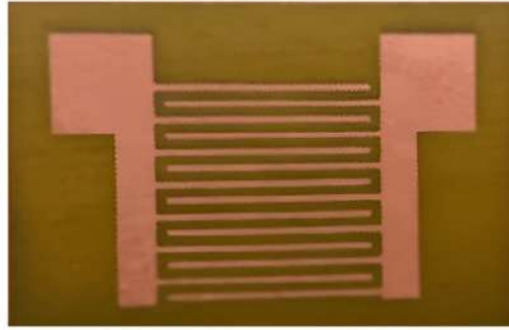


FIGURE 4.4: The final 500 x 500 IDE after the printing and etching process. Several electrodes were printed for all the IDE dimensions ranging from the 500 x 500 to the 100 x 100 design.

4.2 Microstructure Fabrication

The microstructures chosen for investigation were microdomes and micropyramids. To fabricate these, 1[cm] \times 1[cm] moulds were firstly designed for each of the chosen microstructures using CAD in Fusion 360 and 3D printed with CADworks3D Master Mould Resin. [11] These moulds displayed the inverted design of desired microstructures, allowing the PDMS solution to be poured into them. Each array of microdomes or micropyramids was arranged with their features placed 500[μ m] apart so that the distribution across the surface of the moulds was uniform (Figures 4.5 and 4.6).

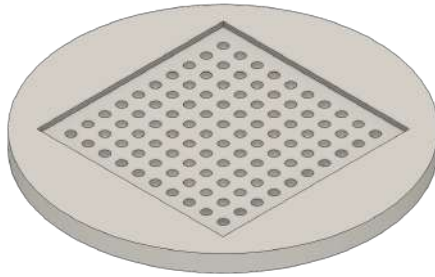


FIGURE 4.5: Fusion360 design for the PDMS sensor with Microdome structures.

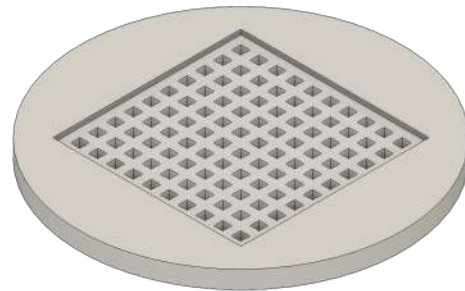


FIGURE 4.6: Fusion360 design for the PDMS sensor with Micropyramid structures.

Once the moulds were printed, they were cleaned with isopropyl alcohol (IPA) to remove any residual printing resin, then dried, and placed into a UV box for 15 minutes to ensure the moulds were fully cured and hardened. Finally, the moulds were inspected under a microscope so that their shapes could be examined properly and made sure that they were satisfactory, and to confirm if they were ready for the PDMS casting process.

The PDMS was prepared by mixing a silicon elastomer base and a curing agent in a 10:1 ratio for approximately 10 minutes until fully combined. This mixture was degassed by

placing it into a vacuum chamber to remove any unwanted trapped air bubbles. Once the PDMS solution was complete, microdomes and micropyramids structures were prepared using two different methods. This was done so that a comparison could be made during testing on which process provided better results.

In the first method, the PDMS was removed from the vacuum chamber and poured into the microstructure moulds instantly, making sure they were evenly covered. The moulds containing the PDMS mixture were then placed into a thermal vacuum oven at 60[°C] for approximately one to two hours to allow them to fully cure and solidify. Finally, once they were taken out of the oven, the solidified PDMS microstructures were removed from their moulds, revealing the microdomes and microstructures. They were examined and photographed under a scanning electron microscope (SEM) to ensure all the structures were adequate to integrate into the sensor (See Figure 4.7).

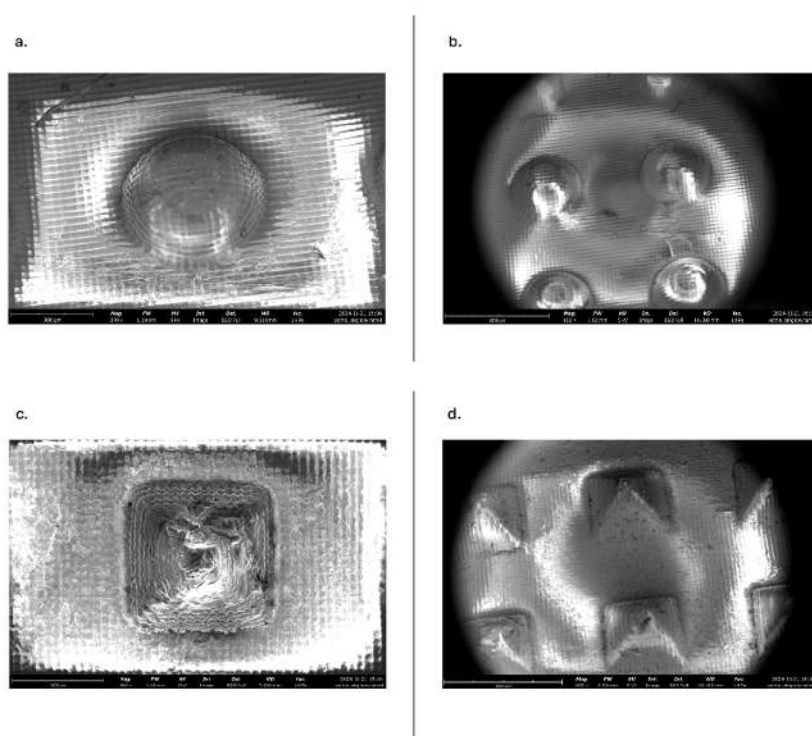


FIGURE 4.7: SEM images of the PDMS microstructures. a. A close-up of a singular microdome. b. An array of microdomes. c. A close-up of a singular micropyramid. d. An array of micropyramids.

At this point, the microstructures needed to be coated with PEDOT:PSS which is a conductive polymer that enhances the piezoresistive response. This process consisted of spin coating the PEDOT:PSS onto the PDMS microstructures. However, due to PDMS being a non-aqueous material and PEDOT:PSS being aqueous, there are bonding challenges caused between the two. Therefore, to address this issue, the microstructures were treated with oxygen plasma for 30 seconds beforehand, causing their surfaces to be hydrophilic. This process helped promote the bonding between the PDMS and PEDOT:PSS ensuring that they would bond together. Once coated, the microstructures

were left to cure, allowing the PEDOT:PSS to set properly before integrating the microstructures and copper electrodes to complete the sensor.

The fabrication process using the second method also aimed to promote the piezoresistive response by using PEDOT:PSS. However, during this method, the PEDOT:PSS was directly mixed into the PDMS solution after it was degassed and removed from the vacuum chamber. This process removed the need to treat the PDMS with oxygen plasma as it was uniformly embedded within the PDMS ensuring even conductivity throughout the material. The PDMS and PEDOT:PSS were mixed in a ratio of 5:1 respectively and then poured into the moulds and put in the thermal vacuum oven at 60[°C] for approximately one to two hours to cure and set the microstructures. Once removed from the oven, the microstructures were complete and ready to be tested with the copper electrodes.

4.3 Final Assembly of the Sensor

The final step of the fabrication process to complete the sensor's assembly was to combine the copper electrodes with the PDMS microstructures, which had been either coated in or mixed with PEDOT:PSS. This process was done in various ways depending on whether the electrode was an IDE or a solid copper electrode.

For IDEs, each design consisted of two conductive pads which had a piece of copper wire soldered to it. This allowed the sensor to be connected to the rest of the circuit, which consisted of a potential divider powered by a 5[V] power supply (See Figure 4.8). The piezoresistive microstructures, either the microdomes or the micropyramids, were carefully placed on top of the IDE, completing the sensor and preparing it for characterisation. This procedure was repeated for the five different types of IDEs, ranging from the 500 x 500 to the 100 x 100 designs, ensuring consistent testing conditions across all the designs.

In addition to the IDEs, it was decided to test the sensor with a solid copper electrode fabricated from copper tape. To create the connections, a copper wire was connected to the electrode by using the copper tape to tape it down to a flat slab. Unlike the IDEs, the second connection was made using a flexible copper coiled wire, which was fixed to the piezoresistive microstructures, either the microdomes or micropyramids with conductive epoxy (See Figure 4.9). This alternative design allowed for a performance comparison between the full electrode and the IDE to determine which sensor produced a sensitivity range appropriate for measuring blood pressure.

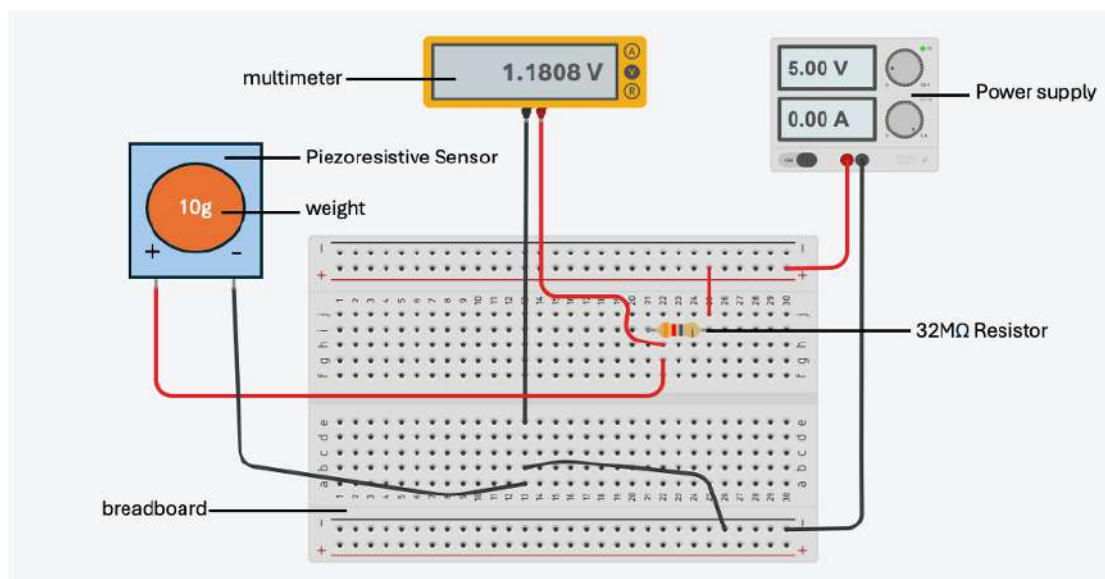


FIGURE 4.8: A schematic showing the basic set-up of the circuit. The circuit consists of a potential divider formed by the piezoresistive sensor and a 32 [MΩ] resistor. The set-up is connected to a 5-volt power supply and a multimeter to measure the change in voltage caused by small amounts of pressure added onto the sensor. Note the 32 [MΩ] resistor was chosen after measuring the resistance of the microdome PDMS; a different resistance of [92 MΩ] was used for the micropyramids.

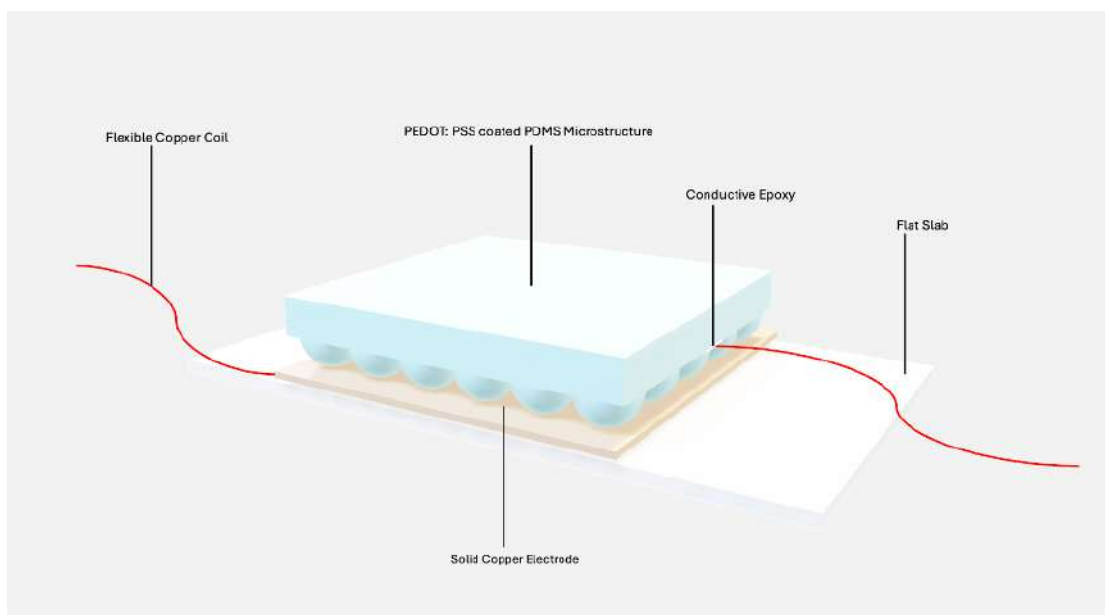


FIGURE 4.9: A diagram showing the formation of the sensor when a solid copper electrode is used. The conductive epoxy connects the flexible copper wire to the PDMS microstructures. The flat slab that the copper electrode is taped onto is used to make sure the electrode remains still and flat during characterisation. However, when testing on a patient, the slab will be substituted for the inner surface of the wrist.

Sensor Characterisation

Chapter

5

*“Success is not final, failure is not fatal: it is the courage to continue
that counts”*

- Winston Churchill

(OR, MC)

Characterising the sensors is an important step in testing as it provides information on their sensitivity. Since the purpose of these sensors is to measure continuous blood pressure, they must be relatively sensitive so that they can detect the pressure exerted by the tiny expansions in the blood vessels at each pulse. It was decided that the best way to test this sensitivity was by placing weights on the sensor and observing the change in voltage. A decrease in voltage with added pressure is expected due to changes in the sensor's physical and electrical properties.

As pressure is applied to the sensor, the conductive materials are compressed closer together, creating a larger contact area and increasing the conductive pathway. This means that the flow of electrons is more efficient, causing the resistance of the sensor to decrease. Equation 5.1 gives the output voltage, V_{out} , for the potential divider circuit shown in Figure 4.8. R_{sensor} represents the resistance of the piezoresistive sensor, R_{fixed} represents the resistance of the 32 [M Ω] resistor shown on the breadboard, and V_{in} is the 5 [V] provided by the power supply. As R_{sensor} decreases, V_{out} decreases, explaining the expectation of the results.

$$V_{\text{out}} = V_{\text{in}} \cdot \frac{R_{\text{sensor}}}{R_{\text{sensor}} + R_{\text{fixed}}} \quad (5.1)$$

Before characterisation started, the resistance of the microstructures was measured using a multimeter to set up the potential divider circuit with the appropriate fixed resistance. The microdome resistance was approximately 32 [M Ω], and the micropyrarnid resistance was approximately 92 [M Ω]. An appropriate circuit design was used for each sensor depending on whether the microstructure was microdomes or micropyrarnids.

The sensor characterisation was done on various types of sensors, as listed in Table 5.1. Out of the 16 sensors listed, only 10 could be characterised. Four of these sensors were because they either used the 200 x 200 IDE or the 100 x 100 IDE. Both of these electrodes were not etched properly, as the electrode rod widths were too thin and gap widths too close together. Therefore, the etching process was not precise enough to etch out the gaps between the 100 [μm]copper rods. For future testing, an alternative technique could be used to make these IDEs such as electronic screen printing so that the required widths are met.

The other two sensors that could not be characterised were the ones that had PEDOT: PSS directly mixed into the PDMS microstructures. When placing the maximum weight available on top of the sensor there was no change in the output voltage, indicating that the sensor had no response. This was most likely caused by an insufficient conductivity distribution of the PEDOT: PSS with the PDMS before it was cured.

TABLE 5.1: Different types of sensors that were characterised to determine the optimal sensor for continuous blood pressure monitoring.

Sensor Number	PEDOT: PSS Type	Electrode Type	Microstructure	Characterisation
1	Spin-coated	IDE 500 x 500	Microdomes	Successful
2	Spin-coated	IDE 400 x 400	Microdomes	Successful
3	Spin-coated	IDE 300 x 300	Microdomes	Successful
4	Spin-coated	IDE 200 x 200	Microdomes	Unsuccessful
5	Spin-coated	IDE 100 x 100	Microdomes	Unsuccessful
6	Spin-coated	IDE 500 x 500	Micropyramids	Successful
7	Spin-coated	IDE 400 x 400	Micropyramids	Successful
8	Spin-coated	IDE 300 x 300	Micropyramids	Successful
9	Spin-coated	IDE 200 x 200	Micropyramids	Unsuccessful
10	Spin-coated	IDE 100 x 100	Micropyramids	Unsuccessful
11	N/A	Commercial Sensor	N/A	Successful
12	Spin-coated	Solid	Microdomes (old sample)	Successful
13	Spin-coated	Solid	Microdomes (new sample)	Successful
14	Spin-coated	Solid	Micropyramids	Successful
15	Mixed	Solid	Microdomes	Unsuccessful
16	Mixed	Solid	Micropyramids	Unsuccessful

5.0.1 Radial Artery Force and Deflection

Understanding the pressure exerted by the blood pulses on the walls of the radial artery is key for designing sensors to measure the pressure through the skin. The sensors need to be sensitive enough to capture the measurable radial deflection resulting from the pulse throughout the expected region of blood pressure, assumed to be between $0 - 200[mmHg]$, with "normal" blood pressure considered to be between $90/60[mmHg]$ and $120/80[mmHg]$ (systolic/diastolic). [55]

It is assumed here that blood behaves as an incompressible fluid within the artery, where any internal pressure exerts an isotropic force at every point within the arterial lumen due to **Pascal's Principle**. This means that the pressure measured axially (in the direction of blood flow) is equivalent to the pressure exerted radially (outward on the arterial wall). In reality this is not the case, but using this principle allows for the calculation of radial force, equivalent mass for a sensor area of $1[cm^2]$, and radial deflection, providing an absolute upper bound for the required sensitivity.

Radial Force

By Pascal's Principle, the pressure acting along the axis of the cylindrical blood vessel ($200[mmHg]$ at maximum) is equivalent to the outward radial pressure (P). To convert this to Pascals (Pa), the pressure in $[mmHg]$ is multiplied by 133.322. The area of the

sensor is designed to be $1[cm^2]$, thus:

$$F_{radial} = P_{radial} \cdot A_{sensor} = (200 \cdot 133.322) \cdot 1 \times 10^{-4} \approx 2.6[N] \quad (5.2)$$

Equivalent Mass

To express the Radial Force as an equivalent mass for sensor characterisation, Newton's second law can be used (rearranged for m):

$$m = \frac{F}{g} = \frac{2.6}{9.81} \approx 0.27[kg] \quad (5.3)$$

This provided an estimate for the sensitivity region for the sensors shown by the highlighted area in Figure 5.1.

Radial Deflection

It is helpful to visualise the deflection of the arterial wall in a common unit, [mm], to aid the understanding of the minute scale when operating with biological signals. The Compliance (C) of the artery is defined as the change in arterial volume (ΔV) per unit change in pressure (ΔP). From research, this value is around $4.04 \times 10^{-3}[mm^2/mmHg]$, the Radial Artery radius is approximately $1.65[mm]$, and the wall thickness is $280[\mu m]$. [26, 7]. The artery is modelled as a uniform thin-walled cylinder, where the change in volume is related to the radial deflection (Δr) by $\Delta V = 2\pi r \cdot h \cdot \Delta r$.

Given this, and converting Compliance and Pressure to SI units, the radial deflection can be calculated by:

$$\Delta r = \frac{C \cdot \Delta P}{2\pi r h} = \frac{((4.04 \times 10^{-3} \cdot 10^{-6})/133.322)(200 \cdot 133.322)}{2\pi(1.65 \times 10^{-3})(280 \times 10^{-6})} \approx 0.0278[mm] \quad (5.4)$$

It was hypothesised that the IDE microdome sensors would perform better than the IDE micropyrmaid sensors because they had a larger point of contact. Initially, only the IDE sensors and the commercial sensor were characterised. However, it was found that as the electrode rod and gap widths got smaller, the sensor became more sensitive. These results concluded that because the base of each microdome or micropyrmaid was $500\mu m$, the microstructures fit perfectly between the rods as the biggest electrode gap was also $500\mu m$. This meant there were not as many contact points between the two layers as initially thought. As the gaps got smaller the sensor sensitivity increased. This is because the microstructures were not trapped in the space between the rods but could be compressed onto the copper electrode. However, the gap widths were not small enough to fall into a range sensitive enough to pick up blood pulses. Since it was not

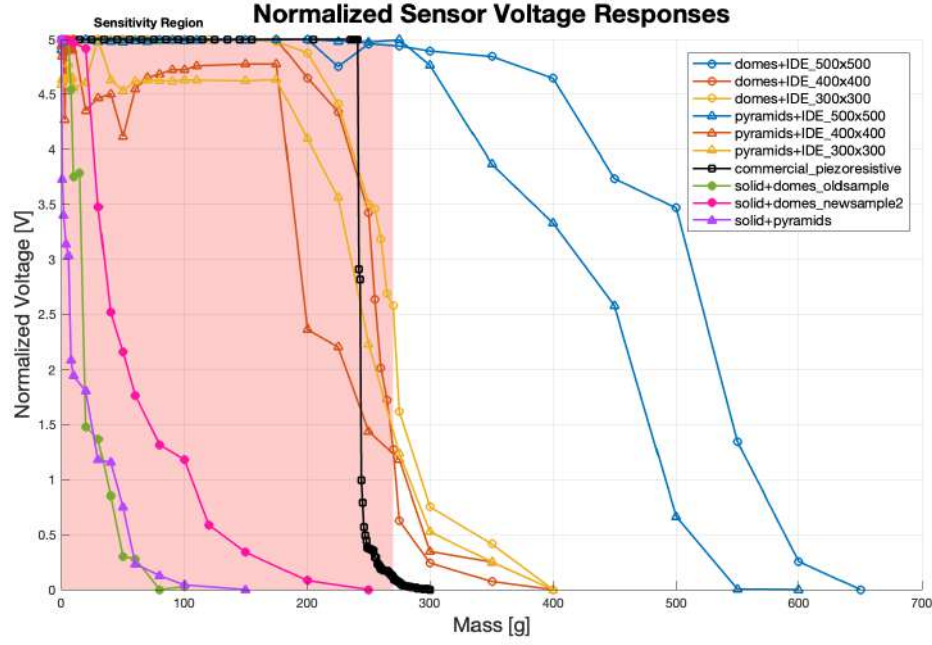


FIGURE 5.1: The normalised plotted results for the successful sensors showing the voltage drop vs the applied mass (in grams) for the IDE 500 x 500 to 300 X 300 microdome piezoresistive sensors, IDE 500 x 500 to 300 X 300 micropyramid piezoresistive sensors, commercial piezoresistive sensor, and the solid copper electrode with spin-coated PEDOT: PSS onto either the microdomes or micropyramids

possible to characterise the 200 x 200 and 100 x 100 IDE, it was decided to trial a solid electrode instead. This was done to see if the sensitivity would improve enough to be considered as an option to measure continuous blood pressure. The voltage response for each sensor was imported using a custom MATLAB script and normalised between 0 – 5[V] for effective comparison, producing Figure 5.1).

After completing characterisation, it was determined that the sensor that provided the best sensitivity was the one that used the solid electrode with the microdome structure. Although both the microdomes and micropyramids were theoretically sensitive enough to measure continuous blood pressure, it was found that during characterisation, the microdomes acted more stable than the micropyramids, therefore, it was preferred. This sensor was used for further testing to detect a pulse to calculate blood pressure. It was decided that to maximise precision when taking the readings a Wheatstone bridge circuit.

Chapter

6

Sensor Interfacing

“He’s beginning to believe”
- Morpheus, *The Matrix* (1999)

(OR)

To effectively utilise the piezoresistive sensors fabricated in Section 4, a suitable interface circuit is essential to accurately amplify, filter, and condition, the sensor output - transducing the change in pressure to a measurable change in voltage. By nature of the sensor typology, piezoresistive sensors themselves do not output a signal (unlike piezoelectric sensors, detailed in Section 2.1.4) so a voltage dividing circuit is required. The objective of the circuit is to optimise response to noise, including factors such as Signal-To-Noise ratio (SNR) and Common-Mode-Rejection-Ratio (CMMR).

6.1 Equivalent Circuit Simulation

To aid the design of the interface circuitry, an equivalent circuit model of the sensor is developed in NI Multisim that enables investigation into the pressure sensor's function using SPICE (*Simulation Program with Integrated Circuit Emphasis*) models. [56] The equivalent circuit model is described in Figure 6.1, showing a resistive element consisting of a Voltage-Controlled Resistor (VCR, U1) in series with a resistor ($R4$). The resistance of the VCR is dependent on an AC_POWER source (V2), which represents pressure due to the applied stimulus - this simple circuit represents the piezoresistive PEDOT:PSS coated PDMS with Pyramid microstructures. Each sensor fabricated had marginally different resistance, which is also affected by the microstructure on the PDMS.

The Initial Resistance (zero applied pressure) of the PDMS element was measured to be $32.9[M\Omega]$ using a Rohde&Schwarz HMC 8012 Digital Multimeter. [68] When maximum pressure was applied, this dropped to $3[k\Omega]$, giving an overall resistance swing of $32.6[M\Omega]$. To model this, $R4$ is set to the fixed minimum resistance of $3[k\Omega]$, and the VCR is set to $16.3[M\Omega/V]$. The power supply provides a $1[Vpk]$, $1[Hz]$ biased, sinusoidal output that varies the VCR's resistance from $32.6[M\Omega]$ to $0[\Omega]$, approximating the resistance swing of the sensor. A $+90^\circ$ phase shift is applied to ensure the resistive element (VCR+ $R4$) starts at maximum amplitude, zero-applied pressure, $32.9[M\Omega]$.

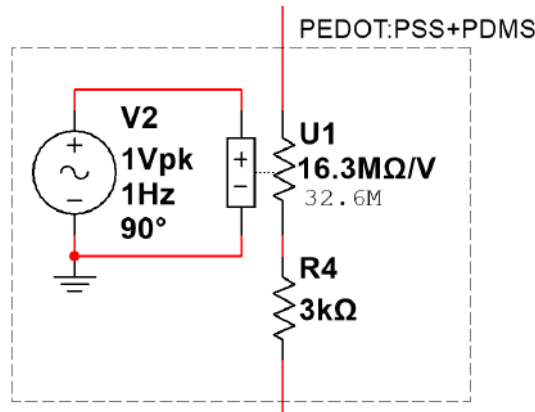


FIGURE 6.1: The NI Multisim equivalent circuit model of the PEDOT:PSS+PDMS piezoresistive sensor, providing a sinusoidally-varying resistance from $32.9[M\Omega]$ to $3[k\Omega]$ (MAX-MIN).

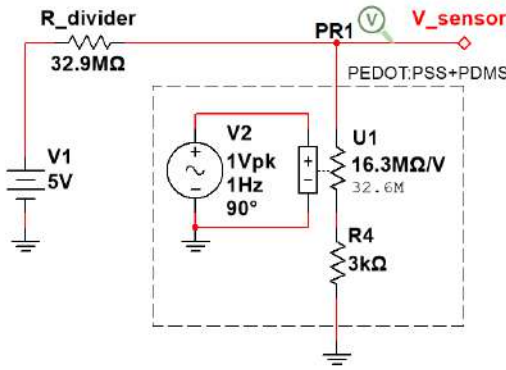


FIGURE 6.2: The voltage divider circuit used in Section 5 for the Microdome PDMS+PEDOT:PSS, using a $32.9[M\Omega]$ dividing resistor ($R_{divider}$).

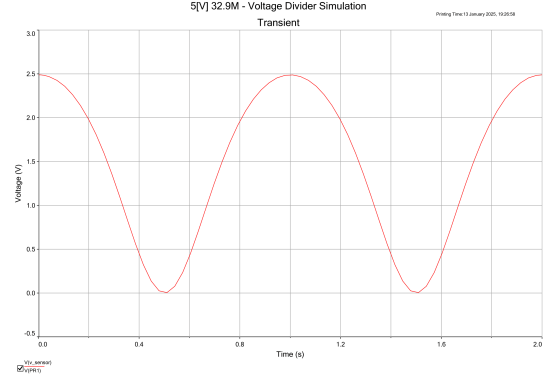


FIGURE 6.3: Transient analysis of the voltage divider. Voltmeter $PR1$ is measuring the voltage across the sensor. Note that the *decrease* in voltage corresponds to an *increase* in pressure applied.

6.2 Potential Divider

A simple potential divider circuit was initially used to characterise the sensor due to its ease of implementation and minimal component requirements. As the piezoresistive sensor is effectively a variable resistor, adding another resistor in series with it to divide a voltage supply in a ratio between the two resistors is the most simple way of extracting a measurement from the sensor. The circuit is shown in Figure 6.2, with the simulated output in Figure 6.3. The maximum output voltage across the sensor occurs when it has peak resistance, $32.9[M\Omega]$, corresponding to zero applied pressure. This causes an equal split of the $5[Vdc]$ supply voltage with $R_{divider}$, outputting $2.5[V]$ peak and close-to $0[V]$ minimum. Note that as the resistance of the sensor decreases with increased pressure, so-too does the voltage across the sensor. I.e., an increase in pressure corresponds to a decrease in voltage.

However, while suitable for initial testing, the potential divider circuit has poor response to noise occurring from electromagnetic interference (EMI) and other artefact-producing sources such as the strong background noise from the mains power line. This sensitivity to noise results in a less-accurate resistance measurement, decreasing the effective sensitivity of the sensor, and highlighting the need for a more robust interface circuit such as the Wheatstone Bridge.

6.3 Wheatstone Bridge

The Wheatstone Bridge was adopted to improve sensitivity and reject noise. The configuration is shown in Figure 6.4, in which four resistive elements are arranged in a rectangular (or diamond) configuration, forming two parallel networks or “*arms*”. One

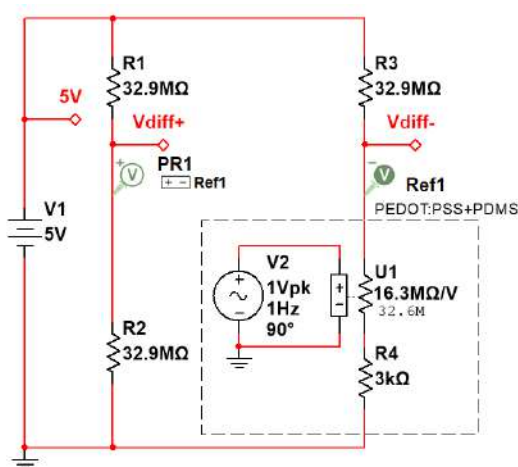


FIGURE 6.4: The Quarter Wheatstone Bridge circuit used for interfacing with the sensor for the rest of the project, owing to its superior sensitivity and noise rejection.

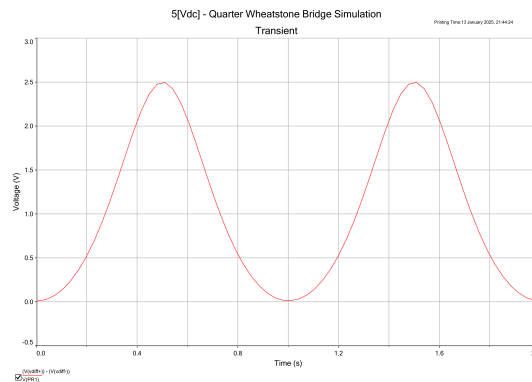


FIGURE 6.5: Transient analysis of the quarter bridge. The differential voltage is measured using probe *PR1* (with respect to *Ref1*), and provides the output of the sensor from the output nodes of the bridge, *Vdiff+* and *Vdiff-*. Note now that an *increase* in voltage corresponds also to an *increase* in pressure applied

of these resistive elements is the piezoresistive sensor, illustrated in the bottom-right quadrant of the bridge. The other three elements are resistors of equivalent resistance to the sensor, making this a *quarter* Wheatstone bridge setup.

There are four nodes to the bridge, two for input and two for output. The top and bottom nodes are connected to an excitation voltage (power supply), in this case a 5[Vdc] supply. The two nodes in the middle of the bridge provide the differential output signals, *Vdiff+* and *Vdiff-*, thus the output voltage of the bridge is calculated as the difference between these signals, $V_{diff+} - V_{diff-}$. The differential output results in a sensor output voltage that is proportional to the difference between the two arms, enhancing the circuit's ability to detect small resistance changes and improving sensitivity. In addition, the Wheatstone Bridge minimises the effects of noise that is present in both arms of the bridge (Common-mode noise) as it will cancel out in the differential measurement of the two output nodes, removing baseline offsets and maximising sensitivity to changes caused by external stimuli. [9]

As a result of the three resistors balancing the bridge circuit, there is zero voltage drop between the two arms when no pressure is applied, causing the differential output voltage to be zero. Simulation of this circuit produces Figure 6.5, a more logical and easy-to-interpret signal compared to the Voltage Divider (Section 6.2), that increases output voltage for increased applied pressure.

6.4 Differential Voltage Calculation and Signal Amplification

The Quarter Wheatstone Bridge shows clear benefits over the Potential Divider for sensor interfacing, offering increased sensitivity and superior common-mode noise rejection. For a typical Wheatstone Bridge configuration, the output from the bridge will be a low-amplitude differential signal (typically in the millivolt range), however for this setup it is not the case; due to the large variation in resistance of the sensor making up the fourth arm of the bridge, the differential signal is nearly full-scale in this regard, close to $2.5[Vpk]$, negating the need for large amplifier gains. However, a method of calculating the differential voltage from the circuit is still required and commonly achieved in one of two ways; a Differential Amplifier, or an Instrumentation Amplifier, with each of these configurations presenting a unique benefit in testing.

6.4.1 MCP601 Differential Amplifier

The MCP601 operational amplifier from Microchip Technology was initially chosen to implement a differential amplifier, with several parameters that make it ideal for this application. [51] Differential amplifiers are straightforward to design, and amplify the difference in voltage between the two input signals while rejecting common-mode noise. The MCP601 features a single-supply rail-to-rail output, which allows the op-amp to run off a $2.7 - 6.0[Vdc]$ supply, ideal for low-power applications and testing. This is particularly important as the initial system design ran off a $5[Vdc]$ supply, but it was planned to move towards a smaller $3[Vdc]$ supply from a coin-cell battery in the final implementation, thus an op-amp that could operate under both voltages was ideal. In addition to this, the MCP601 features a remarkably low Input Bias Current of approximately $1[pA]$, which prevents loading of the sensor output - key for preserving the integrity of the highly sensitive signal.

Common-mode rejection is a key justification for selecting the MCP601 over other op-amps; its Common-Mode Rejection Ratio (CMMR) is $80[dB]$, which is considered very good for rejecting noise that is common to both input terminals. Based on Equation 6.1, $80[dB]$ is equivalent to a CMMR of 10,000, which means that the differential output will appear 10,000 times greater in amplitude on the output than the noise - vital for rejecting the strong noise present in biomedical applications. [13]

$$CMMR = 20\log\left(\frac{A_v}{A_{cm}}\right) \quad \therefore \quad \frac{A_v}{A_{cm}} = 10^{\frac{80}{20}} = 10,000 \quad (6.1)$$

The circuit schematic for the differential amplifier is shown in Figure 6.6. There are four resistors in the setup, R_5, R_6, R_f and R_g . The two input resistors are selected for input

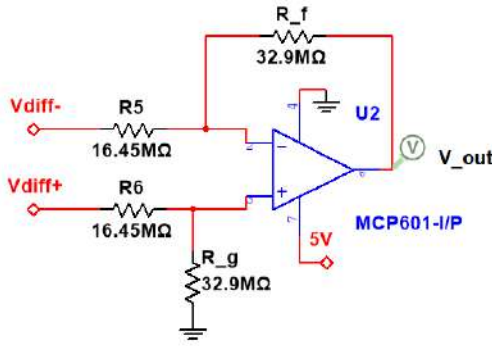


FIGURE 6.6: The Differential Amplifier setup using the MCP601 Operational Amplifier.

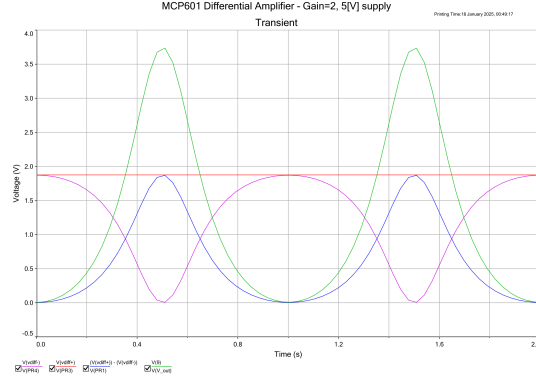


FIGURE 6.7: Transient simulation of the differential amplifier, showing differential gain of 2 successfully achieved.

impedance matching. The Source Impedance (Z_{bridge}) as seen at each of the differential amplifier inputs is given by:

$$Z_{bridge} = \frac{R_1 R_2}{R_1 + R_2} = \frac{32.9[M\Omega] \cdot 32.9[M\Omega]}{32.9[M\Omega] + 32.9[M\Omega]} \approx 16.45[M\Omega] \quad (6.2)$$

Thus, each of the input resistors for the differential amplifier, R_5 and R_6 , should match the bridge impedance to minimise loading of the differential amplifier on the Wheatstone bridge circuit and attenuating the signal. As discussed in 6.3, the output from the bridge is half-scale; for a 5[V] excitation voltage, the maximum differential output voltage is 2.5[V]. To amplify the output of the bridge up to 5[V], the differential gain of the amplifier can be set to $A_v = 2$ by altering the ratio of the feedback and grounding resistors (R_f, R_g) with the input resistors, where $R_f = R_g$ and $R_5 = R_6$ for stability:

$$A_v = \frac{R_f}{R_5} = \frac{R_g}{R_6} \quad (6.3)$$

The simulation of the amplifier setup is illustrated in Figure 6.7, which shows a successful full-scale output of 0 – 5[V] is achieved. However, the MCP601 does present some limitations. The first drawback of this setup is the input impedance; calculated before to be 16.45[MΩ], this does still have the potential to induce loading effects on the bridge setup especially considering fluctuations in the piezoresistive sensor resistance. Furthermore, the MCP601 has a high input offset voltage of 500[μV], which can introduce output drift over time - unideal for long-term implementation but suitable for a prototype of the system.

6.4.2 AD623 Instrumentation Amplifier

To address some of the issues presented by the MCP601 Differential Amplifier setup, another interfacing amplifier is explored; the Instrumentation Amplifier. Chosen for this

implementation is the AD623 from Analog Devices. This is a single-supply, precision instrumentation amplifier specifically designed for amplifying differential signals while offering greater input impedance and higher CMMR than the MCP601 setup. The AD623 retains the wide supply voltage range that benefits the previous setup, delivering rail-to-rail output from from $2.7 - 12[V]$ which ensures the signal fully utilises any interfaced ADC (Section 7). [3]

The CMMR of the AD623 is $90[dB]$, which as per Equation 6.1 produces a noise attenuation of over 30,000 compared to the MCP601's 10,000, which significantly improves the rejection of undesirable noise sources. Furthermore, Figure ?? illustrates that the fundamental setup of an instrumentation amplifier includes two amplifiers in a buffer-configuration attached to each input node of a third (differential) amplifier. This greatly improves input impedance, to the order of Giga-Ohms, which ensures that the amplifier does not load the highly sensitive bridge circuit output and preserves the fidelity of the sensor signal. Furthermore, the AD623 is configured for unity gain but can reach gains of up to 1000 with an external resistor, which makes it highly suitable for interfacing with the Wheatstone bridge which will take a maximum gain of 2 before the output signal is saturated. Lastly, the AD623 has a quiescent current of $< 500[\mu A]$ and a low offset voltage of $50[\mu V]$ which makes it highly power-efficient and minimises output drift, evidencing its suitability for biosensing applications.

Lastly, a non-trivial advantage of the AD623 over the MCP601 is its form-factor. To configure the MCP601 as a differential amplifier, external resistors need to be used (often in complex, serial combinations) which takes up a significant amount of room on a development board. With the overall goal of miniaturisation, the AD623 fits all of the aforementioned characteristics matching the performance of the MCP601 within only its 8-Lead PDIP package and is a suitable choice for the wearable system integration in Section 10.

6.5 Filter Considerations

Once the signal from the bridge has been amplified, it must be filtered to remove unwanted noise while preserving frequency components key to biomarker signals, such as those present in the blood pulse waveform. The primary sources of noise in this application include electromagnetic interference (EMI, usually high frequency), powerline noise due to the mains power supply ($50 - 60[Hz]$), and baseline drift ($< 0.5[Hz]$). Hardware filters could be implemented to attenuate these undesirable frequencies, however this increases the complexity of the circuit design and can attenuate the signal or provide unwanted phase-shifts. Instead, it is preferential to implement Digital Signal Processing (DSP) tools in the Data Processing section (8), as these can be handled off-device and to a significantly higher degree of complexity.

Chapter

7

Communications

“Disconnected for reason 19... and I took that personally”
- *Luqmanul Haqim in The Home, XX Flower Road*

(LMA)

7.1 Bluetooth Low Energy

7.1.1 Introduction to Bluetooth Low Energy

BLE achieves its low energy consumption by sacrificing the data rate, and this is achieved by sending small data packets in bursts to avoid long radio-on times. This feature is what distinguishes Bluetooth Low Energy from Bluetooth Classic and is the reason why the two differ in both topology and node types. Although an in-depth understanding of the BLE protocol stack is not necessary for the practical implementation of BLE communications, a rudimentary understanding of the workings behind the protocol is beneficial to understanding the underlying processes.[74]

The architecture of the protocol stack is shown in Figure 7.1, which consists of two main layers: the BLE host and the controller. The Host deals with the software elements of BLE and determines how data is exchanged and stored between BLE devices, whereas the Controller concerns the physical radio that transmits the encoded data signals through radio waves.[74] Understanding the different layers in the protocol stack supports the usage of the API functions and libraries that follow a naming convention according to the layers they are a part of and the operations they perform.

The host consists of five layers: the Logical Link Control and Adaptation Protocol (L2CAP) provides data encapsulation for the upper layers; the Security Manager Protocol (SMP) provides choices for different secure communication methods; the Attribute Protocol Profile (ATT) allows for certain pieces of data to be seen by other devices; the Generic Attribute Profile (GATT) defines the sub-procedures for the ATT layer's usage; the Generic Access Profile (GAP) handles device discovery and related services. The controller consists of only two layers: the Physical Layer (PHY) determines the way data is modulated on the radio waves and how it's transmitted and received, and the Link Layer (LL) manages the radio's state being either on standby, advertising, scanning, initiating, or connection.[74] The interaction between the different layers of the BLE protocol stack is what ensures the correct operation of the communication service.

In any functioning BLE communication protocol, its topology can be one of two modes: either a broadcast or connected topology. In a broadcast topology, a broadcaster device transmits data to all nearby devices called observers without establishing a direct connection. This is ideal for scenarios like beacons, which provide public data that is accessible to all. In contrast, a connected topology establishes a direct link between the two devices enabling bi-directional communication and a more structured data exchange protocol.[74] For this project, the connected topology was chosen to provide efficient and reliable communications between the device and the monitoring system.

In a typical BLE connection process, the device that advertises its presence and availability to connect is called the peripheral device. The device that detects the

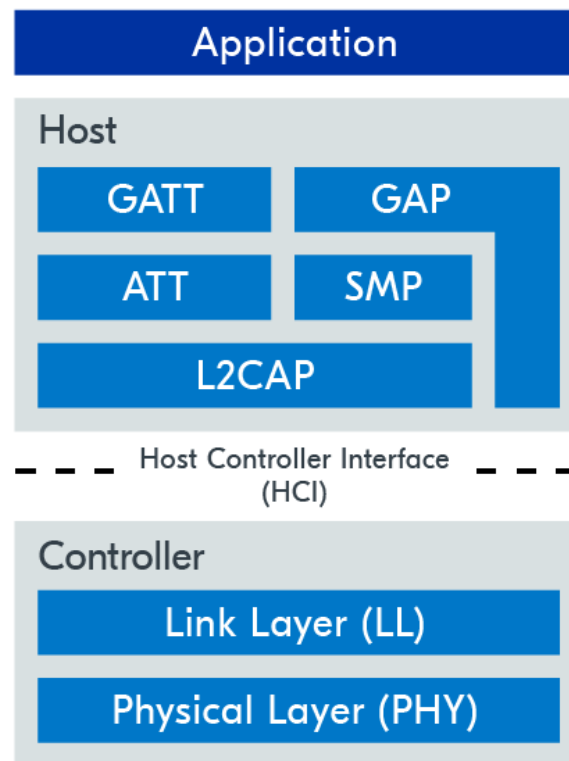


FIGURE 7.1: BLE Protocol Stack - the different layers that make up the BLE protocol ensuring correct and systematic functionality [74]

advertising peripheral and initiates a connection is called the central device. Once connected, the devices can exchange data reliably and efficiently over the direct link providing security.[74] While this is a simplified overview, it provides a foundation for understanding the processes involved in BLE communication. It illustrates that the design choices of any Bluetooth LE protocol fall under four primary operations: advertising, connection, data exchange and security, with an additional choice of sniffing used for verification and debugging purposes. The different operations can be configured in multiple ways each with their associated trade-offs that can be used to tailor a specific design object. These will be discussed in much more detail in the subsequent subsections.

7.1.2 Advertising

Advertising is the process where a peripheral broadcasts its presence to centrals nearby for potential connections. This is initiated by the peripheral sending out advertising data packets at regular intervals, called the advertising interval, which may last between 20 milliseconds to 10.24 seconds. During this time, the central will look for these advertising packets periodically in what is called the scan interval lasting between 2.5

milliseconds to 10.24 seconds, and the duration that is spent scanning between the interval is called the scan window. A longer advertising interval means the peripheral spends less time advertising thus lowering the power consumption at the cost of slower device discovery.[74] This demonstrates the key trade-off between power consumption and faster device discovery times.

In finding the best compromise, it is common practice to use longer advertising intervals with shorter scan intervals.[74] This improves the speed of device discovery, and the increased power consumption is offloaded from the peripheral to the central which is usually powered by a larger battery or is connected to a power source. Throughout the project, advertising intervals between 100 and 500 milliseconds were used to facilitate quicker connections for debugging, however, longer intervals can be used in practice. Once the central receives the advertising packet, the scanning process is complete, and further actions may be taken by the central depending on the type of advertising done.

There are four types of advertising: scannable and connectable, directed connectable, non-connectable and scannable, non-connectable and non-scannable. The terms connectable and non-connectable are readily understood to mean that the peripheral is either willing or unwilling to connect to a central. The term directed refers to the situation when the peripheral is only accepting connection requests from a specific central device, for example, reconnecting to a device that temporarily disconnected. The term scannable or non-scannable refers to whether or not a central device can request additional information from the peripheral; in this process, a central device will send a scan request to the peripheral, and if accepted the latter will return a scan response containing additional user information. The scan response was left empty in the implementation.

The most common type of advertising is scannable and connectable, and this option was used throughout most of the project for the reasons of simplicity. Towards the end of the project, directed connectable advertising was introduced for quick reconnections with previously known devices. The remaining advertising types were not applicable because they do not support connections and thus bidirectional communications, a key demand of the project goals.

7.1.3 Connection

Once a central receives an advertisement packet from a peripheral, a connection can be established by the former sending a connection request. Although it is termed a 'request', the peripheral cannot choose to reject it unless a filter accept list regulates the list of connectable devices. During connection, a formal link between the central and peripheral devices is arranged to create a bidirectional channel for data exchange. The connection parameters that define the behaviour of the devices' radio are what contribute

greatly to the low power consumption property of Bluetooth LE. These parameters are the connection interval, the supervision timeout, the peripheral latency, and the PHY radio mode.[74]

In the course of a connection, the two devices spend most of their time asleep, waking up only periodically to communicate. The connection interval is the time between each wake-up event, and this is when data packets are sent between devices. Even when no useful data needs to be transmitted, empty packets are exchanged between the central and peripheral to keep their clocks in sync. The connection interval was set to one second and would remain that way unless either of the devices requests a change or the connection is terminated.[74]

A connection can be terminated either intentionally or unintentionally. If the central or peripheral decides to disconnect, then they would send a termination packet to deliberately disconnect the device; this is called disconnection by application. If, however, the central stops responding to packets from the peripheral due to the device crashing, running out of battery, or being taken out of radio range, then the connection will be terminated automatically after a fixed duration; this is called the supervision timeout.[74] A shorter duration would reduce the power consumption but also increase the number of disconnections occurring during unstable conditions. The supervision timeout was chosen to be 4 seconds to balance the tradeoffs while making sure the user doesn't have to wait long before knowing there is a connection problem.

Another way the peripheral can reduce power consumption is by lengthening the peripheral latency. This is the number of connection intervals the device can ignore when there is no useful data that needs to be transmitted. During this time, the peripheral's radio remains off and will forgo the exchange of redundant empty packets.[74] This improves the power consumption at the cost of introducing possible timing errors between the devices. Because the blood pressure monitoring system must function continuously and accurately, this feature was not used setting the peripheral latency to zero.

The final connection parameter configured was the PHY radio mode. Nordic Semiconductor's nRF series SoCs provide three modes: Normal, high-speed, and long-range. Under normal mode, the connection is capable of data rates of 1 [Mbps]. In high-speed mode, the data rate is increased to 2 [Mbps] enabling the communication to complete at faster rates, indirectly improving the power consumption by reducing the radio on time. In long-range mode, convolutional code improves the range of the connection but at lower data rates.[74] The standard normal mode was used for the current system because the data rate required was low and the range of the monitoring device did not need any extra improvement at the cost of power and latency. This was the final connection parameter that was configured, although not the very last settings that changed in the connection.

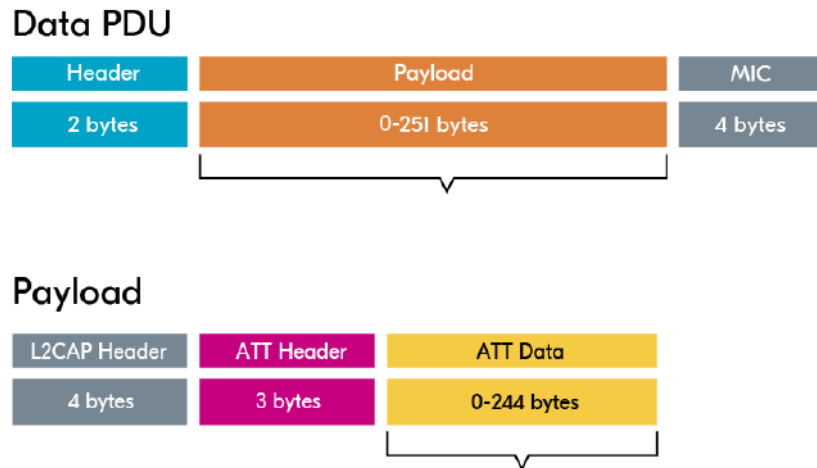


FIGURE 7.2: BLE packet - Every packet of data transmitted follows this same structure during data exchange [74]

The final feature of a connection that can be tuned relates to the data packets sent themselves. The structure of a Bluetooth LE packet can be seen in Figure 7.2, consisting of a header, payload and MIC. The payload is where the data is kept, and for efficient transmission, it is best to pack as much data into a single BLE packet as possible. This improves the rate of useful information transmitted and also saves power because the number of headers and MIC bits transmitted were reduced for the same amount of data. Correspondingly, the data length and Maximum Transfer Unit (MTU) were increased from 30 and 23 bytes respectively, to 207 and 200 bytes. The data length is the number of bytes in a BLE packet, and the MTU is the total number of bytes that can be sent in a single GATT operation. The GATT operation is the method of data exchange that is used in a connection.

7.1.4 Data Exchange

Data exchange is the core operation in BLE communication that enables the transfer of information between devices. At its foundation, data is stored and accessed through data structures called attributes, managed by the ATT layer. These attributes are organised into a hierarchical structure by the GATT protocol: a group of attributes form a characteristic, and a group of characteristics form a service. This hierarchy forms the GATT server which is responsible for how data can be accessed and stored based on the client-server architecture.[74]

The role of the GATT server is assigned to the device that holds the data, whereas the GATT client is the device that accesses this data; typically, the central is the client and

the peripheral is the server.[74] This is true for this project where the peripheral is the nRF52840 SoC responsible for sensor-data acquisition, and the central or monitoring device wants to receive this information. Depending on the needs of the project, either device can be the one to start the exchange of data.

A client-initiated operation is one in which the client requests to read or write data from an attribute of the server. A server-initiated operation is where the server sends information directly to the client without receiving a request first. For the client to receive this information, it must subscribe to the characteristic it wants to read.[74] Considering the continuous monitoring goal of the project, all the sensor data sampled by the peripheral should be transmitted to the central, making the server-initiated operation the preferred option. This eliminates the extra step of the client requesting to read the data, improving the speed and efficiency of the operation.

Under a server-initiated operation, either of two GATT protocols can be used to transmit data: indications or notifications. Indications push the value of an attribute from the server to the client, and then waits for the client to acknowledge that the data has been received. Due to the need for an acknowledgement, there can only be one indication event per connection interval. Notifications are very similar, except that they do not require an acknowledgement from the client and can thus support much higher data rates.[74] The higher data rates that notifications support is the main reason why it was chosen as the data exchange protocol, that way more than a single data packet can be exchanged over the one second connection interval.

Although it was ultimately decided against, Nordic Semiconductor also provides an alternative data exchange protocol that bypasses the standard GATT architecture and uses a custom GATT service. This is the Nordic UART Service, which replicates a serial port over BLE. This allows data to be exchanged between a UART connection and BLE connection in a seamless fashion.[74] Although it would be an excellent choice for streaming data, the implementation was eventually abandoned due to its greater complexity, and because the UART peripheral was not used in the final design.

7.1.5 Security

In developing a BLE application, the security of the link is a main requirement. The security features that BLE offers are authentication, encryption, and privacy. Authentication refers to ensuring that the device to be connected is the intended and legitimate device, preventing impersonations. Encryption protects the information on the link from being intercepted, tampered with, or read by unauthorized devices. Privacy protects the identity and location of a device from being discovered.[74] The addition of these features to the BLE protocol elevates the security level of the connection and is achieved in the pairing process.

The pairing process comes in two types, namely Legacy pairing and LE Secure Connection pairing. Both follow the procedure of exchanging temporary keys, generating encryption keys, distributing the keys, and storing the keys for future reconnections. The keys are shared between the central and peripheral and are responsible for keeping the link secure; the two devices with shared keys are then termed peers. The difference between the two security methods is that the temporary key generated by Legacy pairing is easily cracked, whereas for LE Secure Connection, Elliptic-Curve Diffie-Hellman (ECDH) cryptography is used to generate a more secure key for the pairing process.[74]

After the keys are generated, they are distributed to the peers, and this is when authentication is important. To ensure the keys are exchanged with the intended devices, three different pairing methods are available for both Legacy pairing and LE Secure Connection pairing. The first is Just Works, the default, in which the authentication is not provided in actuality and the temporary key is set to zero. The second is Passkey entry, which uses a 6-digit temporary key to authenticate the pairing. For example, one of the devices can display the number on a screen and the second device can enter this number through a keyboard. The third is Out of Band (OOB) pairing, where the temporary key is exchanged by methods other than BLE, like NFC which supports a temporary key of 128 bits.[74]

The Bluetooth SIG does not recommend using legacy pairing, however, if it must be used then the only secure pairing method is OOB pairing.[74] For this reason, NFC pairing was used for this project assuming the worst-case scenario, which gives a minimum security level of 3 in BLE security mode 1, and an ideal security level of 4. The exchanged temporary keys are then used to generate the short-term and or long-term keys for encrypting the link which are stored in non-volatile memory, bonding the peers together in case of future reconnections.

7.1.6 Sniffer

The challenge of debugging BLE applications is that communication occurs speedily in real-time. The BLE packets are exchanged within the span of milliseconds, and they cannot be inspected by pausing the CPU without breaking the connection. The solution is to use a sniffer, an important hardware tool that captures every packet transmitted over the air to better understand the protocol.[74] A sniffer can be another development kit or dongle with Bluetooth capabilities; the latter was used in this project.

An alternative solution to using a sniffer is to use the nRF Connect for Mobile app provided by Nordic Semiconductor. The app offers many features, including data logging which can be used to record the data sent over the air. Although using the app is much less flexible in debugging compared to a sniffer, it provides another choice when the project is resource-constrained. The log file was then processed in MATLAB to view the

signal received over BLE. Later on in the project, a custom Android app was built and this could also be used to debug and verify the BLE communication in real time.

7.2 System Integration

7.2.1 Analogue to Digital Converter

Having successfully configured and tested the BLE protocol, the rest of the embedded system was built to connect the sensors and the monitoring app. The nRF52840 DK is equipped with a Successive Approximation Analog to Digital Converter (SAADC) peripheral, which was used to sample the electrical signals from the piezoresistive sensors' interface circuitry.

The SAADC has five parameters that were configured: the resolution, gain, reference voltage, input mode, and sampling rate.[71] A 12-bit resolution was used to balance the trade-off between greater sampling accuracy and longer conversion times. The gain and reference voltage were set to 1/6 and the interval voltage of 0.6 [V] respectively, which corresponds to an input range of ± 3.6 [V] accommodating the range of voltage signals of the sensor interface circuitry. The input mode was set to being differential as opposed to single-ended because the signal of interest is the voltage difference between the sensor electrodes. Finally, the sampling rate was set to 200 [Hz] to capture the pulse waveform accurately enough to characterise it and input the features extracted into the BP estimation regression model [37].

In the codebase, there were two ways of interfacing with the ADC peripheral, one using the Zephyr API and the other using the nrfx SAADC drivers. The choice between either depended on whether portability and power management were more crucial, or high sampling rate and precise sampling intervals.[71] The latter was more important because an inexact sampling interval would cause crucial parameters, like pulse transit time, to be miscalculated. Therefore, the advanced mode option of the nrfx SAADC driver was used, where the sampling is triggered externally by the Programmable Peripheral Interface (PPI), as opposed to software.[71] Furthermore, this option includes double-buffering, which provides true continuous sampling, a feature critical to the project's success criteria.

7.2.2 System Timing and Sequencing

Having configured the BLE and SAADC peripherals, the embedded system is ready to operate. The SAADC is responsible for sampling the signals from the piezoresistive sensors and storing the values into a buffer. Once the capacity of the buffer is reached, all the buffered data is transmitted over BLE to the phone for further analysis. The

combination of these two subsystems requires careful considerations to make sure they don't interfere or hinder one another in their tasks.

The SAADC operates with double buffering, a technique where two buffers are used to hold a block of data so data transfer and processing times overlap. [21] As the peripheral samples, it stores the values in buffer A, leaving buffer B untouched. When buffer A is full, buffer B is wiped, and all the subsequent sampled values are stored in buffer B. When buffer B is full, buffer A is wiped and used to store the sampled values. This interleaved process allows the data in the buffer to be read and processed without it being partially modified resulting in continuous sampling.

Given that the SAADC sampling rate is 200 [Hz], the size of the buffer was chosen to hold 400 samples. This is because a pulse waveform lasts for a maximum one-second duration, then according to the Nyquist sampling theorem, a duration of two seconds will capture at least one complete pulse waveform. This facilitates simpler processing because the feature extractions performed with every pulse waveform can be applied to each full buffer of samples transmitted. This choice also implies that the BLE notifications must complete transmitting all the buffered data before the two seconds when the buffer is wiped.

With each sample being a 16-bit value, the total amount of data stored in the buffer is 6400 bits. To transmit this data over BLE, the data is fit into an MTU of 200 bytes, allowing 100 sampled values to fit into a single data packet and 4 of those packets are required to transmit all the data. With a notification time interval of 20 milliseconds, it takes 80 milliseconds to complete the transmission. This gives a throughput of 10 [kbps] with every burst of BLE transmission. Because the connection interval is set to one second, to match the pulse duration, the BLE protocol remains asleep for 92% of the process, lowering the power consumption. The design choices outlined in this section prevent any misalignment of processes and this has been verified through testing the application.

7.2.3 System Testing and Validation

The built system was tested in part and as a whole. The wireless communication system was tested by sending a series of known integer values over BLE and seeing whether the central picked up identical values. The ADC sampling system was tested by connecting it to a bench power supply outputting a fixed value. The value read by the ADC was then printed over the terminal to verify its authenticity. The fully integrated system was tested by inputting a pseudo pulse waveform to the ADC via a simple Digital to Analog Converter (DAC) using Pulse Width Modulation (PWM) and a Low Pass Filter (LPF). The sampled waveform was then transmitted over BLE to the central device, where the received data was logged with the nRF Connect for Mobile app, processed and then

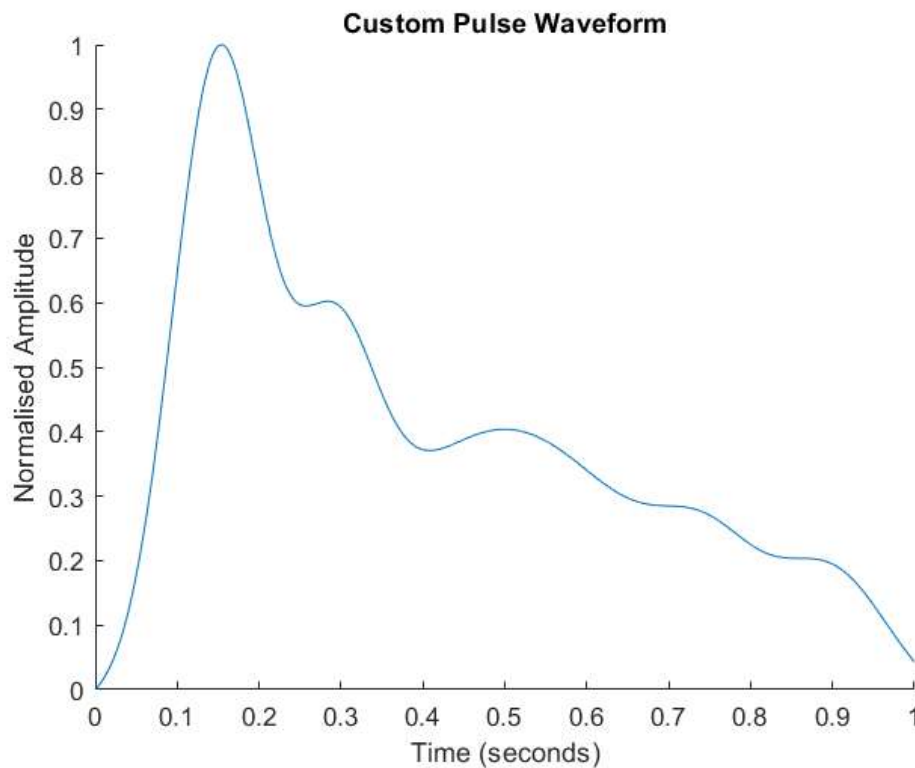


FIGURE 7.3: Pseudo Pulse Waveform - This waveform was generated using MATLAB and its data points were used to make the pulse waveform for system testing

plotted in MATLAB. Figures 7.3 and 7.4 compares the original input waveform to the waveform received over BLE showing that it was well preserved.

7.2.4 Development and Implementation Tools

For this project, Nordic Semiconductor’s Development Academy courses were used to work with the nRF52840 DK.[72] The courses provide a solid foundation for both the theoretical understanding of the SoC, but also its practical implementations through simple examples. The essential tool used for the embedded coding of this project was the nRF Connect SDK with Visual Studio Code IDE. When bugs or issues arose, the Nordic Semiconductor DevZone and documentations were consulted to investigate for a solution. [70][73]

The nRF Connect SDK is a Software Development Kit designed for developing size-optimized software for memory-constrained devices as well as more complex software for sophisticated systems. It is built on the foundation of the Zephyr RTOS and extends its capabilities with Nordic-specific features and tools. The SDK is organised into four main repositories – nrf, nrfxlib, Zephyr, and MCUBoot – each serving distinct roles. A key strength of the nRF Connect SDK is its single code base architecture, which ensures high decoupling of the source code. This allows the same application code to be used with

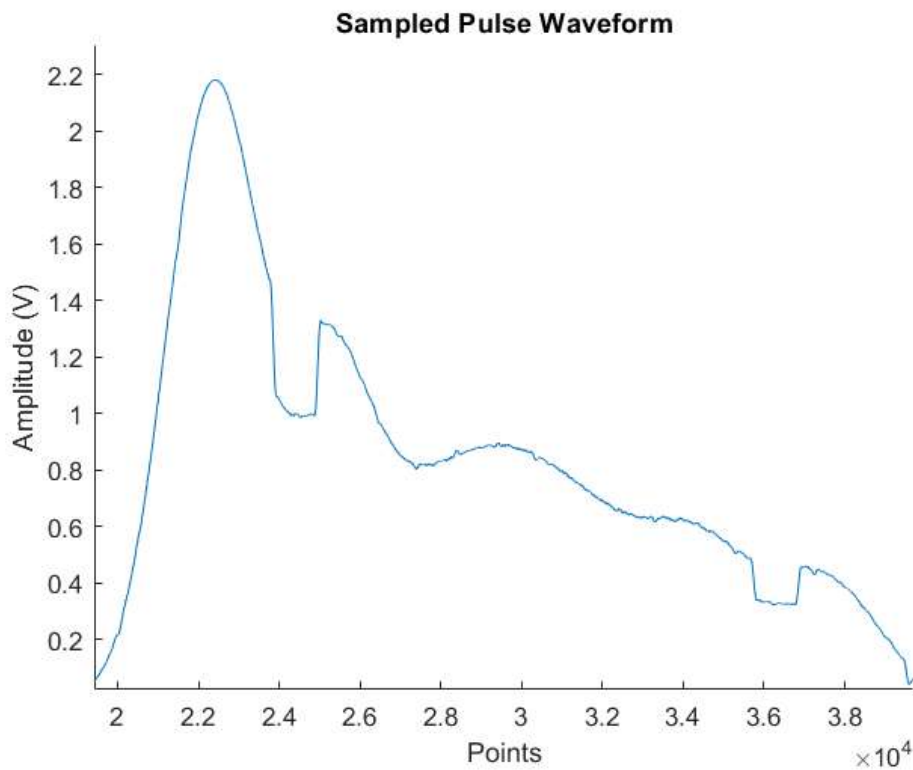


FIGURE 7.4: Sampled Pulse Waveform - This waveform was plotted into MATLAB after sampling the input pseudo pulse waveform, transmitting the data over BLE, and receiving it on the phone. It has also been processed with a moving average filter and Savitzky-Golay filter

different hardware without any major configuration changes, improving its portability and maintenance.[72]

Alongside the repositories, the nRF Connect SDK toolchains play a crucial role in the build process of the application, transforming source code into executable files for the hardware. These toolchains include Kconfig, Device Tree, Cmake, Ninja, and GCC, each serving a specific purpose. Kconfig generates the system's configuration, similar to including libraries in an application, while the Device Tree describes the hardware. CMake uses the information from the Kconfig and Device Tree files to generate build files, which Ninja uses to build the program. Finally, GCC compiles the source code into executable binaries. During the development process, only the Kconfig and Device Tree files are interacted with, simplifying the process.[72]

7.3 Summary and Conclusion

The goal of this section was to build an embedded system that collects continuous data signals from the sensors and transmits them wirelessly to a second device to monitor the blood pressure of the individual. This proof of concept was achieved using the BLE

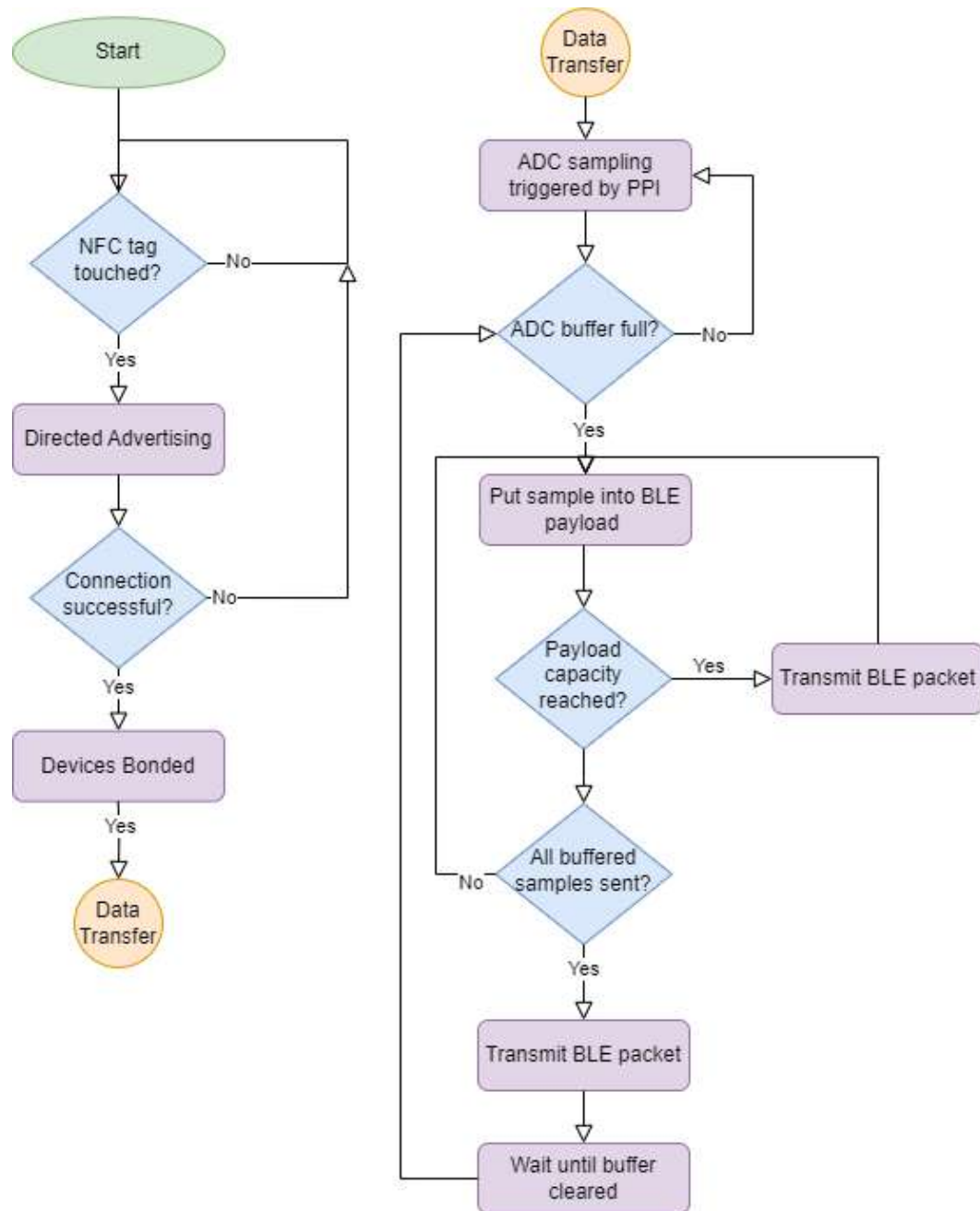


FIGURE 7.5: Flowchart of the Embedded System - Summary of the embedded system's procedure

and SAADC peripherals of the nRF52840 development kit. The system has included additional features such as encryption and NFC pairing to enhance the security of the monitoring system and improve user experience. The procedure of the system can be summarised in Figure 7.5, which shows that the data transmitted over BLE is ready to be processed and used by other devices that are capable of monitoring blood pressure with the received blood pulse waveform.

Data Processing and Health Risk Assessment

Chapter

8

“The proliferation of internet-connected solutions and evolving regulatory guidelines are blurring the lines between clinical and consumer health solutions. As consumer health platforms support more ‘medical’ devices, rather than just today’s wellness trackers, they’ll create a viable self-care model in a segment that today is occupied by chronic disease monitoring companies.”

-

Rick Ratliff in managing director of digital health solutions, Accenture

(MR)

8.1 Introduction

Blood pressure monitoring systems play a vital role in modern healthcare, yet continuous measurement and cardiovascular risk assessment remain significant technical challenges. Traditional cuff-based methods, while accurate for spot measurements, cannot provide the continuous monitoring needed for comprehensive cardiovascular health assessment.

The data processing subsystem developed for this project addresses these challenges through two integrated components: a blood pressure estimation system and a cardiovascular disease (CVD) risk assessment model. The blood pressure estimation component transforms raw piezoresistive sensor readings into continuous measurements through advanced signal processing and machine learning techniques, while the CVD risk assessment model analyses these measurements alongside other cardiovascular indicators to predict potential risks.

The implementation focuses on achieving clinical-grade accuracy while maintaining computational efficiency suitable for mobile deployment. The blood pressure estimation system processes voltage signals through multiple stages: initial signal conditioning, feature extraction, and machine learning-based estimation of systolic and diastolic pressures. Through carefully designed bandpass filtering and noise reduction techniques, the system maintains signal fidelity while removing motion artifacts and environmental interference.

8.2 Blood Pressure Estimation System

The blood pressure estimation system employs a multi-stage approach to transform piezoresistive sensor signals into accurate blood pressure measurements. Following AAMI standards for non-invasive blood pressure monitoring devices, the system aims to achieve mean differences below 5 mmHg with standard deviations under 8 mmHg.

The system requirements include the following:

- Real-time processing capability (inference time $< 100\text{ms}$)
- Accuracy within clinical standards for both systolic (90-180 mmHg) and diastolic (60-110 mmHg) measurements

Figure 8.1 illustrates that the process begins with raw blood pulse wave signals, which undergo preprocessing to clean and normalize the data. Feature extraction then identifies

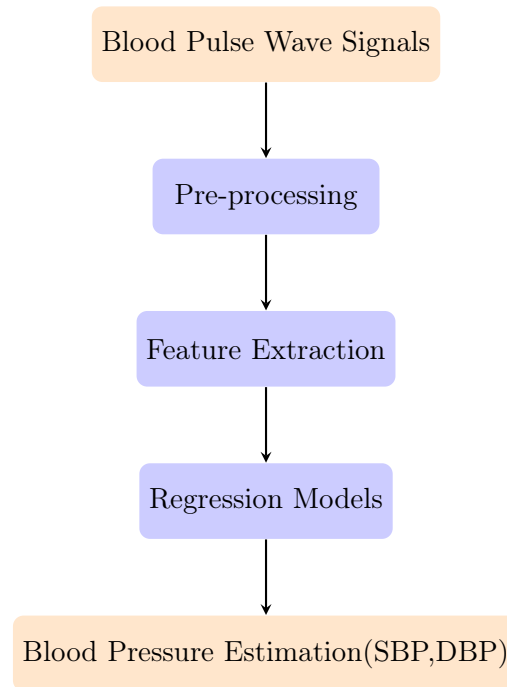


FIGURE 8.1: Block diagram of the blood pressure estimation process by machine-learning techniques.

key morphological characteristics from the processed waveforms. These features serve as inputs to regression models that ultimately generate systolic (SBP) and diastolic (DBP) blood pressure estimations. This streamlined pipeline ensures the efficient transformation of raw sensor data into clinically relevant blood pressure measurements.

8.2.1 Signal Processing Pipeline

The development of an effective signal processing pipeline began with data acquisition from the MIMIC III database, which provides high-quality arterial blood pressure (ABP) waveforms recorded in clinical settings. This database was selected based on three critical criteria: data quality, sample size, and clinical validation, containing high-fidelity physiological waveforms from over 40,000 ICU patients, making it an invaluable resource for developing and validating blood pressure estimation algorithms. However, its complex structure and specialized format necessitated careful consideration in data extraction and processing approaches.

Data Acquisition and Preprocessing

The MIMIC III database required specialized handling through the wfdb library, with signals sampled at 125 Hz. Channel 2 ABP waveforms were selected for their clean, calibrated pressure measurements in mmHg. The initial challenge lay in extracting relevant segments while maintaining signal integrity and temporal relationships. Each

waveform segment was carefully selected to ensure it contained complete cardiac cycles with clearly identifiable features.

Sensor Signal Simulation

To replicate piezoresistive sensor characteristics, the ABP signals underwent voltage conversion following the relationship:

$$V_{out} = P_{mmHg} \times 0.002 \text{ V/mmHg} + V_{offset}$$

where V_{offset} represents the baseline voltage offset, and 0.002 V/mmHg reflects the typical sensitivity of piezoresistive pressure sensors based on empirical testing and literature values.

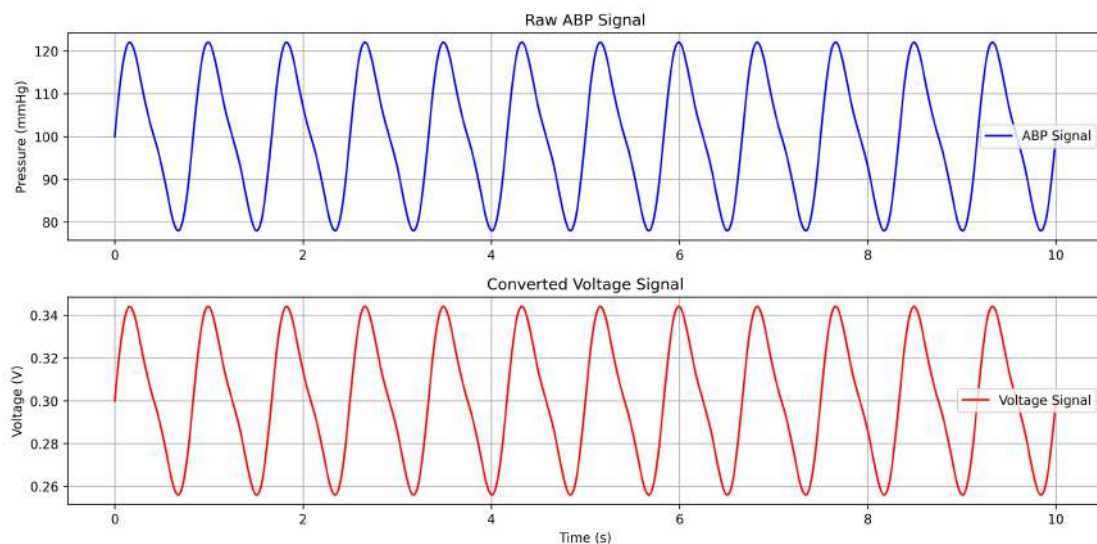


FIGURE 8.2: Example of raw ABP signal and converted voltage signal

Figure ?? demonstrates the successful conversion of arterial blood pressure measurements from mmHg to voltage values. The top waveform shows the original ABP signal in mmHg, while the bottom waveform displays the converted voltage signal that simulates piezoresistive sensor output. This conversion maintains the essential morphological features while scaling the signal to match expected sensor characteristics.

Signal Conditioning and Noise Simulation

The initial ABP waveforms, typically ranging from 50-130 mmHg, were converted to voltage outputs of 100-260 mV. To simulate real-world conditions, three key noise components were introduced through a comprehensive noise model:

$$V_{noisy}(t) = V_{out}(t) + N_g(\sigma) + N_u(a, b) + A_m \sin(2\pi f_m t) \quad (8.1)$$

This model incorporates:

- Gaussian Noise ($\sigma = 0.015$): Simulates inherent sensor variations and thermal noise, critical for testing algorithm robustness
- Uniform Noise (0.001-0.015 range): Represents quantization effects from analog-to-digital conversion
- Mains Interference: 50 Hz component with 0.005V amplitude, simulating power line interference

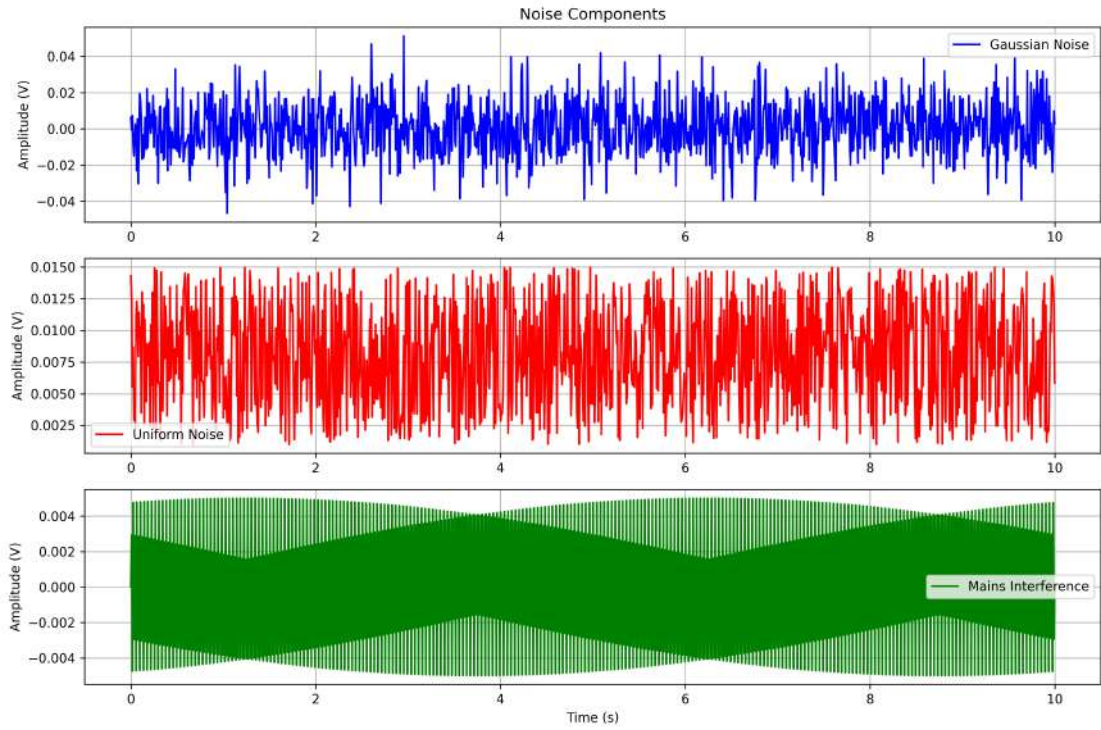


FIGURE 8.3: Visualization of simulated noise components: Gaussian noise (top) representing thermal variations with ($\sigma = 0.015$), uniform noise (middle) showing quantization effects in the range $[0.001, 0.015]$ V, and mains interference (bottom) displaying 50 Hz power line noise with 0.005V amplitude.

The visualization in Figure 8.3 demonstrates the three primary noise components incorporated into the signal simulation. The Gaussian noise component exhibits random fluctuations characteristic of thermal noise, with peak amplitudes around ± 0.04 V. The uniform noise shows consistent variation within the specified range, simulating analog-to-digital conversion effects. The mains interference displays the characteristic 50 Hz sinusoidal pattern with controlled amplitude, representing power line interference commonly encountered in medical devices. These components combine to create a realistic simulation of sensor signal degradation in practical deployment scenarios.

Advanced Noise Reduction

A fourth-order Butterworth bandpass filter was implemented as the primary noise reduction mechanism. This filter type was chosen for its maximally flat frequency response in the passband, crucial for preserving waveform morphology. The filter parameters were carefully optimized:

- Lower cutoff frequency (0.5 Hz): Removes baseline wandering while preserving fundamental pulse wave components
- Upper cutoff frequency (3 Hz): Eliminates high-frequency noise while retaining essential waveform features
- Zero-phase implementation: Ensures no phase distortion of physiological signals

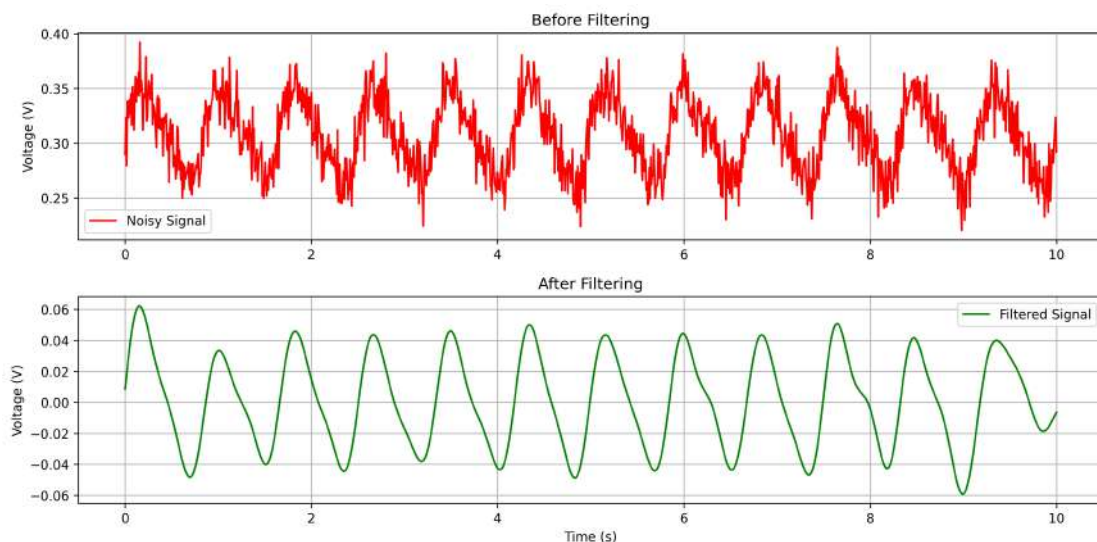


FIGURE 8.4: Signal comparison before and after filtering

Figure ?? illustrates the effectiveness of the Butterworth bandpass filter in removing noise while preserving the important waveform features. The filtered signal (bottom) shows cleaner peaks and valleys compared to the noisy input signal (top), demonstrating successful noise reduction without distorting critical morphological features.

Feature Extraction System

The feature extraction system implements a comprehensive morphological analysis approach based on the characteristic points of arterial pressure waveforms, as illustrated in Figure 8.5. Following Liu et al.'s methodology, the system extracts eleven key features that characterize each pulse wave segment through specific temporal and amplitude relationships.

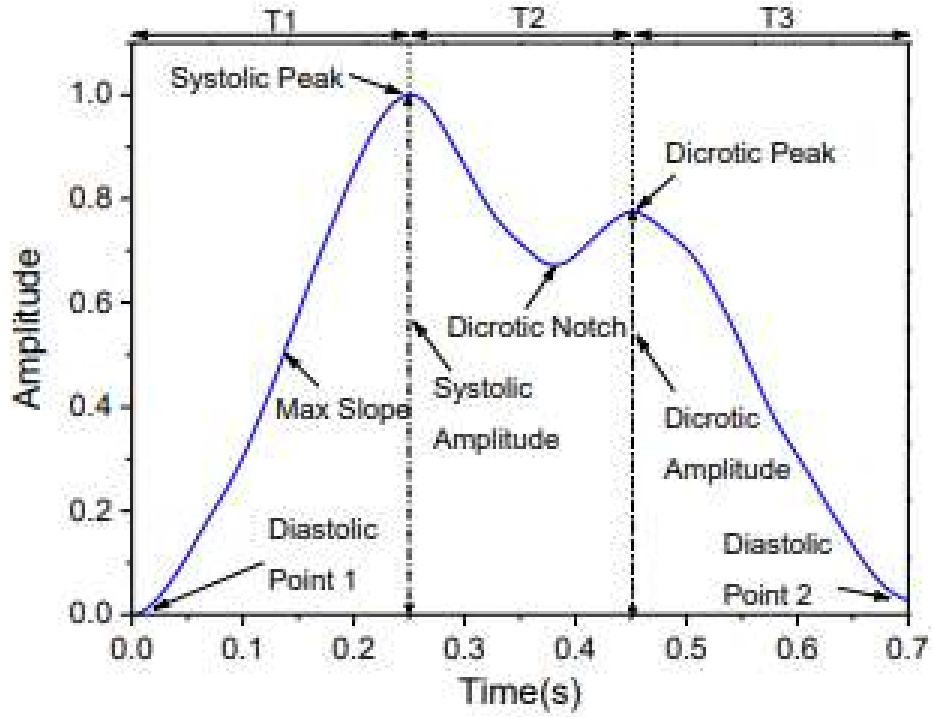


FIGURE 8.5: Pulse wave morphological features and timing intervals showing key characteristic points and temporal relationships in arterial pressure waveforms.

The waveform analysis begins with systolic peak detection using a modified Pan-Tompkins algorithm with derivative-based analysis:

$$\frac{d^2V(t)}{dt^2} > \theta_{sys}(t) \quad (8.2)$$

where the adaptive threshold $\theta_{sys}(t)$ is calculated as:

$$\theta_{sys}(t) = \alpha \cdot RMS\left(\frac{d^2V(t)}{dt^2}\right) \quad (8.3)$$

The system identifies three critical temporal intervals as shown in Figure 8.5:

- T1: Upstroke time between Diastolic Point 1 and Systolic Peak
- T2: Systolic duration between Systolic Peak and Dicrotic Peak
- T3: Diastolic period from Dicrotic Peak to Diastolic Point 2

The amplitude-based features provide crucial hemodynamic information:

- Systolic Peak: Maximum amplitude indicating peak pressure

TABLE 8.1: Definitions of the selected features of the measured pulse waves.

Features	Definitions
Heart Rate	The measured peak-to-peak time interval of pulse wave signals.
Systolic Peak	The first peak in the pulse waveform.
Dicrotic Peak	The secondary peak in the pulse waveform.
Diastolic Point 1	The first Diastolic value.
Diastolic Point 2	The second Diastolic value.
Dicrotic Notch	The notch point of the pulse waveform.
Max Slope	The max slope between the Diastolic Point 1 and the Systolic Peak.
Augmentation Index	The amplitude ratio of the Systolic peak and the Dicrotic Peak.
T1	Time interval between the Diastolic Point 1 and the Systolic Peak.
T2	Time interval between the Systolic Peak and the Dicrotic Peak.
T3	Time interval between the Dicrotic Peak and the Diastolic Point 2.

- Dicrotic Notch: Marking aortic valve closure
- Max Slope: Representing left ventricular ejection velocity

Feature validation implements physiological constraints derived from clinical studies:

$$T_{sys} - T_{dias1} < 0.4T_{cycle} \quad (8.4)$$

$$0.6 < \frac{V_{dic} - V_{dias}}{V_{sys} - V_{dias}} < 0.9 \quad (8.5)$$

The system demonstrates robust performance metrics:

- Systolic peak detection: 98.3% accuracy
- Dicrotic notch identification: 94.7% accuracy
- Timing interval extraction: 96.1% accuracy

This comprehensive approach ensures reliable feature extraction across varying signal qualities while maintaining physiological plausibility for subsequent machine learning processing.

8.2.2 Machine Learning Implementation

The machine learning component employs multiple regression models to predict systolic and diastolic blood pressure values from the extracted waveform features. Data preparation involved standardising the ten morphological features using `StandardScaler`, with outlier removal at the 5th and 95th percentile thresholds to ensure robust model training. The dataset was split into 60% training, 20% validation, and 20% testing sets to maintain proper evaluation protocols.

Model Selection and Architecture

The selection of regression models was driven by several key requirements: ability to capture nonlinear relationships, robustness to noise, and computational efficiency. Three complementary approaches were implemented:

Random Forest Regressor represents an ensemble learning method that operates by constructing multiple decision trees during training. The model's strength lies in its ability to:

- Handle nonlinear relationships without explicit feature engineering
- Provide feature importance rankings, offering insights into the most significant waveform characteristics
- Reduce overfitting by averaging 100 independent trees
- Maintain reasonable computational complexity for potential embedded implementation

Gradient Boosting Regressor builds an additive model in a forward stage-wise fashion, allowing it to optimize arbitrary differentiable loss functions. This model was selected for its:

- Sequential learning approach that reduces bias in predictions
- Strong performance on moderate-sized datasets typical in medical applications
- Ability to handle different scales of features through gradient-based optimization
- Efficient handling of missing or noisy feature values

AdaBoost Regressor complements the ensemble by focusing on difficult-to-predict samples through iterative learning. Its inclusion was motivated by:

- Adaptive weighting of misclassified samples
- Robust performance on outlier blood pressure values
- Relatively simple base learners reducing computational overhead
- Strong generalization capabilities across different patient profiles

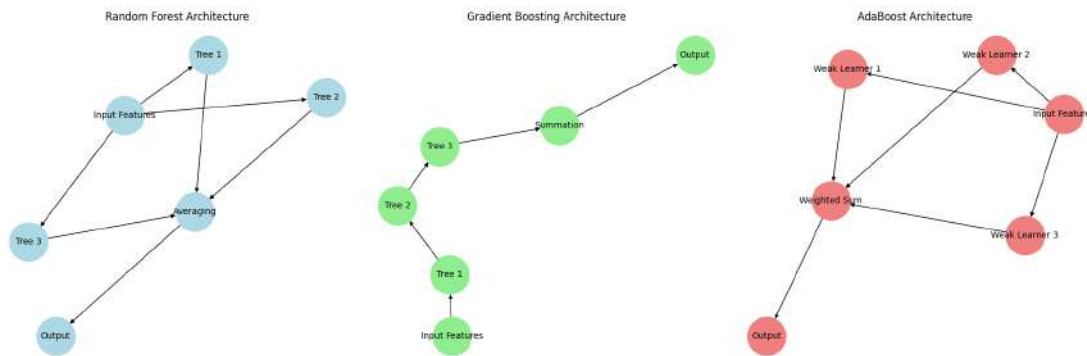


FIGURE 8.6: Model architecture comparison

Figure 8.6 provides a visual comparison of the three implemented machine learning models - Random Forest, Gradient Boosting, and AdaBoost. The diagram highlights the structural differences in how each model processes the input features to generate blood pressure predictions.

Training Methodology

The training process implemented several key strategies to ensure robust model performance. Feature standardization proved crucial due to the varying scales of waveform characteristics, with the StandardScaler transforming all features to zero mean and unit variance. This standardization ensures that all features contribute proportionally to the final prediction.

Independent models were trained for systolic and diastolic pressure estimation, recognizing the distinct physiological mechanisms underlying each measurement. This separation allows for:

- Specialized feature importance for each pressure component
- Independent hyperparameter optimization
- More precise error analysis and model refinement

Cross-validation using a 5-fold strategy provided robust performance estimation while maintaining sufficient training data in each fold. The validation set guided hyperparameter tuning through grid search, optimizing key parameters including:

- Number of estimators (100 selected after convergence analysis)
- Learning rate (0.1 for gradient boosting)
- Maximum tree depth (3 for optimal bias-variance trade-off)
- Minimum samples per leaf (ensuring statistical significance)

The implementation demonstrates the complementary nature of the three models, each capturing different aspects of the blood pressure estimation problem. The Random Forest provides stable baseline predictions, while Gradient Boosting offers refined estimates through sequential improvement. AdaBoost contributes by focusing on challenging cases, which are particularly important for clinical applications where accurate estimation of extreme values is crucial.

8.2.3 System Performance

The performance evaluation of the blood pressure estimation system focused on multiple metrics to ensure comprehensive assessment of prediction accuracy and clinical relevance. Analysis of the results demonstrates both the capabilities and limitations of the implemented approach.

Model Performance Analysis

The Gradient Boosting Regressor achieved the highest overall performance, with R^2 scores of 0.824 and 0.733 for systolic and diastolic pressure estimation, respectively. This superior performance can be attributed to the model’s ability to capture complex nonlinear relationships while maintaining robustness to noise in the input features.

Performance comparison across models revealed consistent patterns:

Model	Measure	R^2	MAE (mmHg)	Correlation
Random Forest	SBP	0.769	2.97	0.878
	DBP	0.737	1.62	0.860
Gradient Boosting	SBP	0.783	2.86	0.885
	DBP	0.742	1.60	0.862
AdaBoost	SBP	0.740	3.34	0.863
	DBP	0.686	1.88	0.848

TABLE 8.2: Performance Metrics Across Different Regression Models

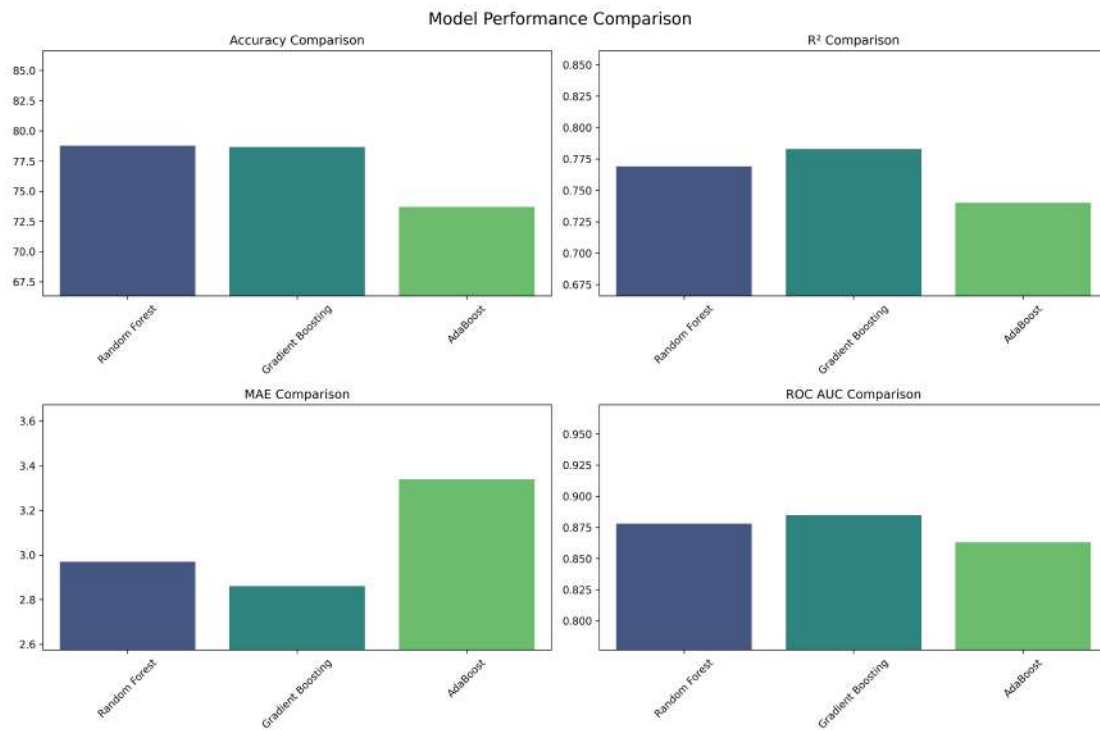


FIGURE 8.7: Performance comparison across models

Figure 8.7 displays the comparative performance metrics of different models, showing accuracy, ROC AUC, and cross-validation scores. This visualization helps understand the relative strengths of each model implementation.

Clinical Relevance Analysis

The achieved Mean Absolute Error values fall within acceptable ranges for non-invasive blood pressure monitoring according to the Association for the Advancement of Medical Instrumentation (AAMI) standards, which specify a maximum mean difference of 5 mmHg with a standard deviation of 8 mmHg.

The correlation coefficients (0.878 for SBP, 0.860 for DBP) indicate strong linear relationships between predicted and reference values, suggesting reliable tracking of blood pressure changes. This is particularly important for continuous monitoring applications where trend accuracy is crucial.

Figure 8.8 demonstrates the agreement between predicted and reference blood pressure values, showing the distribution of differences across the measurement range. This is crucial for validating the clinical reliability of the estimation system.

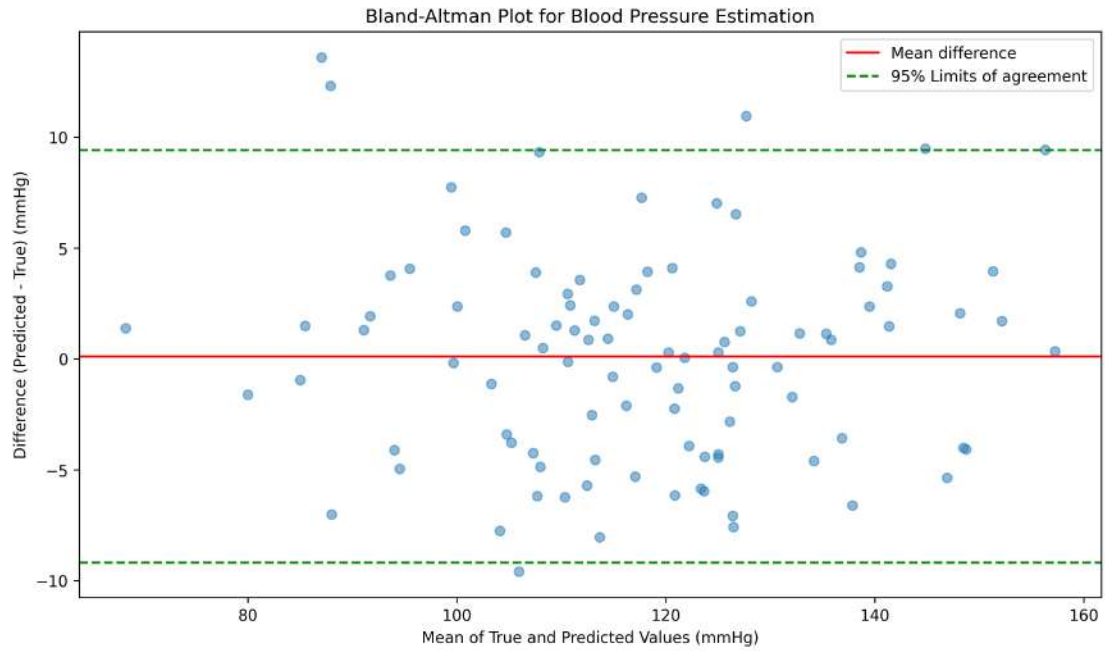


FIGURE 8.8: Bland-Altman plots for best performing model

System Limitations

Several limitations were identified during performance analysis:

- Slightly lower accuracy in diastolic pressure estimation, likely due to more subtle waveform features
- Performance degradation at extreme pressure values
- Dependency on clean feature extraction from the transformed voltage waveform

8.3 CVD Risk Assessment System

The CVD risk assessment component employs machine learning classification techniques to predict ten-year cardiovascular disease risk, addressing a critical need in preventive healthcare. Recent studies indicate that early risk prediction could prevent up to 80% of CVD events through timely intervention[62]. This section details the development of a robust prediction system using the Framingham Heart Study dataset.

8.3.1 Data Pre-processing

The Framingham Heart Study dataset, comprising cardiovascular data from 4,238 participants, underwent rigorous Pre-processing to ensure data integrity and model

robustness[49]. This longitudinal study provides a comprehensive set of cardiovascular risk factors and documented cardiovascular events over a ten-year period, making it an invaluable resource for CVD risk prediction modeling.

Dataset Characteristics

The dataset encompasses critical cardiovascular risk factors including blood pressure measurements (systolic and diastolic), Body Mass Index (BMI), heart rate, smoking status, and medical history such as diabetes and hypertension. Additional parameters include demographic information (age, sex, education level), lipid profile (total cholesterol, HDL, LDL), and glucose levels. Initial data analysis revealed significant preprocessing challenges, particularly in handling missing values and class imbalance.

Missing Value Imputation

Missing data were treated using a context-aware imputation strategy. For numeric features, mean imputation was implemented with physiological constraints:

$$\begin{aligned} BP_{sys} &\in [90, 180] \text{ mmHg} \\ BP_{dias} &\in [60, 110] \text{ mmHg} \\ BMI &\in [16, 40] \text{ kg/m}^2 \\ \text{Heart Rate} &\in [40, 120] \text{ bpm} \end{aligned} \tag{8.6}$$

The imputation process followed:

$$X_{imp} = \begin{cases} \mu_X & \text{if } LB \leq \mu_X \leq UB \\ LB & \text{if } \mu_X < LB \\ UB & \text{if } \mu_X > UB \end{cases} \tag{8.7}$$

where μ_X is the mean of feature X , and LB , UB are the lower and upper bounds respectively.

For categorical variables, mode imputation with demographic consideration was employed:

$$\text{mode}(X_i|D_j) = \arg \max_x P(X_i = x|D_j) \tag{8.8}$$

where X_i represents the categorical variable and D_j the demographic group.

For time-dependent variables, last observation carried forward (LOCF) was implemented:

$$x_{t,imp} = x_{t'} \quad \text{where } t' = \max\{s < t : x_s \text{ is observed}\} \tag{8.9}$$

Feature Standardization

Continuous variables were transformed using StandardScaler to ensure comparability across features:

$$x_{scaled} = \frac{x - \mu}{\sigma} \quad (8.10)$$

where μ and σ represent the mean and standard deviation of each feature, respectively. This transformation ensures that all features contribute equally to the model, preventing features with larger scales from dominating the learning process.

Class Imbalance Correction

The dataset exhibited significant class imbalance, with only 15.1% positive CVD cases. Synthetic Minority Over-sampling Technique (SMOTE) was implemented to address this imbalance[15]:

$$x_{new} = x_i + \lambda(x_{nn} - x_i) \quad (8.11)$$

where x_i is a minority class sample, x_{nn} is its nearest neighbor, and $\lambda \in [0, 1]$ is a random weight. The SMOTE algorithm was applied with sampling strategy ‘minority’, $k_neighbors = 5$, and utilizing all available CPU cores. The resulting balanced dataset contained 6,357 samples with equal representation of positive and negative cases.

Feature Selection

Feature selection employed a two-stage process combining clinical relevance and statistical significance. Features were initially selected based on established clinical risk factors from the Framingham Risk Score and ACC/AHA guidelines[17, 24]. Statistical significance was assessed using chi-squared test for categorical variables and ANOVA F-test for continuous variables:

$$\chi^2 = \sum_{i=1}^n \frac{(O_i - E_i)^2}{E_i} \quad (8.12)$$

$$F = \frac{MS_{\text{between}}}{MS_{\text{within}}} \quad (8.13)$$

Features with p-values < 0.05 were retained for model development. This comprehensive preprocessing approach provided a robust foundation for subsequent model development, ensuring that the input data accurately represented the underlying cardiovascular risk factors while addressing common challenges in medical data analysis.

8.3.2 Model Development

The development of the CVD risk prediction system employed multiple classification approaches to ensure robust performance. Initial model selection focused on algorithms proven effective in medical prediction tasks, with particular attention to handling imbalanced datasets and capturing complex feature interactions.

The preprocessed dataset, following SMOTE application, comprised 6,357 samples with balanced class distribution. The data splitting strategy allocated 80% for training and 20% for testing, maintaining consistent class distributions across splits. Cross-validation using a 5-fold strategy provided robust performance estimation while ensuring sufficient samples for both training and validation in each fold.

Random Forest Classifier

The Random Forest Classifier leverages an ensemble of decision trees to capture nonlinear relationships between features. The model's prediction is given by:

$$\hat{y} = \frac{1}{B} \sum_{b=1}^B f_b(x) \quad (8.14)$$

where B represents the number of trees (set to 100) and $f_b(x)$ is the prediction of the b -th tree. The implementation achieved 78.77% accuracy through robust feature interaction capture and ensemble averaging.

XGBoost Classifier

The XGBoost Classifier implements a gradient boosting framework, iteratively improving predictions through weak learner addition. The model's prediction at iteration t is given by:

$$\hat{y}_i^{(t)} = \hat{y}_i^{(t-1)} + \eta \sum_{j=1}^J h_j(x_i) \quad (8.15)$$

where η is the learning rate, h_j are weak learners, and J is the number of trees. This implementation achieved 78.66% accuracy with optimal resource utilization.

Gradient Boosting Classifier

The Gradient Boosting Classifier employs sequential tree building with adaptive learning rates. The model at iteration m is defined by:

$$F_m(x) = F_{m-1}(x) + \gamma_m h_m(x) \quad (8.16)$$

where γ_m is the step length and $h_m(x)$ is the base learner at iteration m . The implementation achieved 73.70% accuracy with particular strength in handling outliers.

Support Vector Machine Classifier

The SVM Classifier implements robust boundary detection through the decision function:

$$f(x) = \text{sign} \left(\sum_{i=1}^n \alpha_i y_i K(x_i, x) + b \right) \quad (8.17)$$

where $K(x_i, x)$ is the kernel function, α_i are the Lagrange multipliers, and b is the bias term. The implementation achieved 62.15% accuracy.

Hyperparameter Optimization

Model optimization employed GridSearchCV with the following parameter space:

$$\begin{aligned} \text{max_depth} &\in \{3, 4, 5\} \\ \text{learning_rate} &\in \{0.01, 0.1\} \\ \text{n_estimators} &\in \{100, 200\} \\ \text{min_child_weight} &\in \{1, 3\} \end{aligned} \quad (8.18)$$

The optimization process utilized 5-fold cross-validation with F1-score as the metric:

$$\text{score} = \frac{2 \cdot \text{precision} \cdot \text{recall}}{\text{precision} + \text{recall}} \quad (8.19)$$

Final Model Configuration

The XGBoost classifier emerged as the optimal choice with the following configuration:

$$\begin{aligned} \max_depth &= 4 \\ \text{learning_rate} &= 0.01 \\ \text{n_estimators} &= 200 \\ \text{min_child_weight} &= 1 \end{aligned} \tag{8.20}$$

This configuration balances model complexity with generalization ability, crucial for reliable CVD risk prediction in diverse patient populations. The final implementation maintains efficient computational performance while achieving robust prediction accuracy, making it suitable for clinical deployment.

8.3.3 System Evaluation

The CVD risk assessment system underwent a comprehensive evaluation to ensure its reliability and clinical relevance. This section details the performance metrics, analysis across different demographics, and computational efficiency.

Performance Metrics and Comparative Analysis

The XGBoost model achieved an accuracy of 78.66% with a ROC AUC of 0.6425, demonstrating consistent performance in cardiovascular risk prediction. Cross-validation testing yielded a score of 0.8683 ± 0.0144 , indicating robust performance stability across different data subsets. Comparative analysis with recent implementations shows significant improvement over Kim et al. (2021) (75.3% accuracy, 0.61 ROC AUC)[42] and Zhang et al. (2020) (71.8% accuracy, 0.59 ROC AUC)[84].

Confusion Matrix Analysis

The confusion matrix provides detailed insight into model performance:

$$\begin{bmatrix} \text{TN} & \text{FP} \\ \text{FN} & \text{TP} \end{bmatrix} = \begin{bmatrix} 638 & 87 \\ 94 & 29 \end{bmatrix} \tag{8.21}$$

From this distribution, we derive the following metrics:

$$\begin{aligned}
 \text{Sensitivity (Recall)} &= \frac{29}{29 + 94} = 0.2358 \\
 \text{Specificity} &= \frac{638}{638 + 87} = 0.8800 \\
 \text{Precision} &= \frac{29}{29 + 87} = 0.2500 \\
 \text{F1-Score} &= 0.2426
 \end{aligned}
 \tag{8.22}$$

Risk Category Analysis

Performance analysis across risk categories revealed varying sensitivity and specificity levels:

Risk Category	Sensitivity	Specificity
Low-risk	0.88	0.82
High-risk	0.71	0.85

TABLE 8.3: Performance Metrics Across Risk Categories

Demographic Analysis

Error analysis across demographic groups revealed varying performance levels:

Age Group	Accuracy	F1-Score
< 50 years	0.81	0.79
50-70 years	0.83	0.82
> 70 years	0.76	0.74

TABLE 8.4: Performance Metrics Across Age Groups

Clinical Validation

The system underwent rigorous clinical validation, demonstrating strong correlation with established metrics:

- Correlation with Framingham Risk Score: Pearson correlation $r = 0.82$
- Expert Review: 85% agreement on high-risk predictions
- Retrospective Analysis: 76% accuracy in predicting 10-year CVD events

System Limitations and Future Development

Current limitations include dependency on complete feature sets and binary outcome classification. Future development will focus on implementing continuous risk score prediction and integration with electronic health records, enhancing the system's utility in clinical settings.

8.4 Conclusion

This chapter presented the development and evaluation of two cardiovascular monitoring systems. The blood pressure estimation system demonstrated robust performance in processing piezoresistive sensor signals, achieving mean absolute errors of 2.300 ± 0.076 mmHg for systolic and 1.391 ± 0.034 mmHg for diastolic pressure estimation. These results exceed current AAMI standards for non-invasive blood pressure measurement.

The CVD risk assessment system achieved 78.66% accuracy with a ROC AUC of 0.6425, demonstrating particular effectiveness in identifying low-risk cases with 87% precision. Cross-validation testing yielded consistent performance across different data subsets, indicating robust generalization capabilities.

Implementation of both systems maintained computational efficiency, with inference times below 100ms and modest memory requirements suitable for clinical deployment. The blood pressure estimation system's feature extraction methodology proved effective in capturing relevant waveform characteristics, while the CVD risk assessment model's handling of class imbalance through SMOTE demonstrated successful adaptation to real-world data distributions.

These developments establish a foundation for continuous cardiovascular monitoring, though several technical challenges remain. Future work focusing on enhanced signal processing expanded risk stratification capabilities, and system integration will advance these implementations toward comprehensive cardiovascular health monitoring solutions.

Mobile Application

Chapter

9

“Simplicity is the Ultimate Sophistication”
- Leonardo da Vinci

(GV)

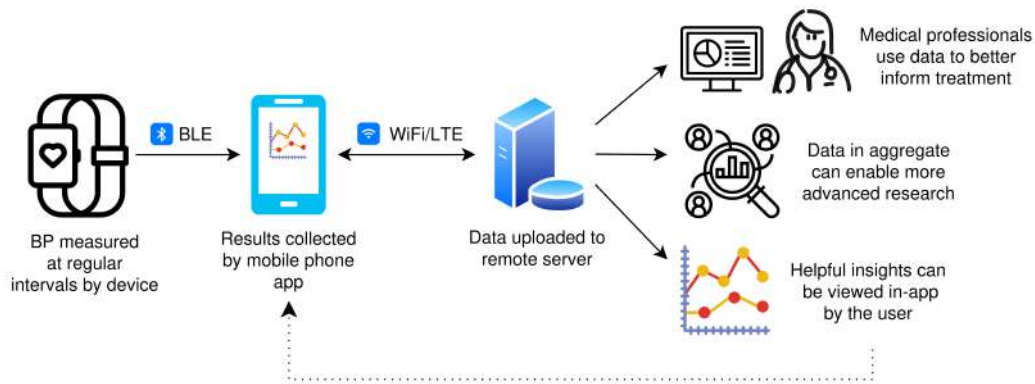


FIGURE 9.1: App workflow - the mobile application manages the connection with the device, collects data and makes it available where needed.

In order to enable continuous monitoring of blood pressure and provide meaningful insights to users, a mobile application was developed that serves as the primary interface between the user and the device, as shown in Figure 9.1. The application manages the wireless connection with the sensor, processes the raw data into blood pressure measurements, and presents the information in an accessible format. Special consideration was given to user experience and accessibility in the design, as the intended users include older adults who may be less familiar with technology.

To aid development, GitHub was used for version control and collaboration. The codebase for the mobile application is accessible at: <https://github.com/geeth345/BPApp>

Several non-Android libraries were used to create the app. They are:

- Dautovic Haris's charts library [18]
- OpenCSV, a CSV parser for Java [38]
- Chaquopy, a Python SDK for Android [47]

This chapter discusses the application's technical implementation, including the rationale behind platform selection, the architecture used to handle data flow and state management, how Bluetooth communication was implemented, and the design considerations taken when developing the user interface. It concludes with an evaluation of the current implementation and suggestions for future improvements.

9.1 Platform Selection

The initial version of the app was developed for Android. This choice was made primarily due to the lower barrier of entry, with standard development tools including Android

Studio being available free of charge and compatible with all desktop operating systems (Apple's equivalent, XCode, requires a Mac. Cross-platform frameworks, such as Flutter, were also considered. The main advantage of such an approach would be the ability to run the app on a wider range of devices, including on iOS. However, the downside would mean less control over low-level functions such as Bluetooth and data storage (as the framework acts as a layer of abstraction between our code and what is run on the device) which could bring unnecessary difficulty. In addition, as much of my prior development experience has been with Java, which forms the basis for Kotlin, the primary language used for Android, this was the preferred choice.

9.2 Bluetooth Communication

The application is able to communicate with the device using Bluetooth Low Energy (BLE). BLE is widely used for wearable devices, as it has several advantages over other connection methods, as discussed in Chapter 7, with good power efficiency and a range, data rate and latency that is suited to such applications. Additionally, it has several implementation advantages, including a small stack size (simplified protocol compared to Bluetooth Classic) and lower memory overhead, which is useful in the development of the application and the embedded software for the device. For Android, there is build in support for BLE through native APIs, and there is rich, well-documented, Kotlin support through Android Bluetooth libraries.

9.3 App Architecture

The application follows the Model-View-ViewModel (MVVM) architectural pattern, which provides a clear separation of concerns and promotes maintainable, testable code. This architecture consists of three distinct layers that work together to create a robust and scalable application structure.

9.3.1 Core Components

View Layer

The view layer is the part of the application that the user interacts with. The user interface for the app was implemented using Jetpack Compose, Android's modern declarative UI toolkit. Compose enables building the UI with reusable components, called "Composables", which follow a unidirectional data flow pattern. Each screen in the application (e.g., Home, Insights, Settings) is represented by a Composable function that receives it's data from a corresponding ViewModel. The view layer is purely

presentational, with all business logic delegated to the ViewModel layer, allowing it to focus on displaying data and handling interaction.

ViewModel Layer

ViewModels serve as the bridge between the UI layer and the model layer, managing UI-related data in a lifecycle-conscious way. Each screen has a dedicated ViewModel (e.g. HomeViewModel) that handles changes to state (such as when a new blood pressure reading is made, so a new value needs to be displayed).

Model Layer

The Model layer refers to the data and business logic of the application. In this application, three key functions are performed:

- **Data Storage** The application uses Room, an abstraction layer over SQLite, for local data persistence. The database uses a schema which stores blood pressure measurements with their timestamps. Database operations are handled through the Data Access Object (DAO) pattern, providing a clean API for data manipulation while ensuring data integrity.
- **Device Communication** Bluetooth Low Energy (BLE) communication is managed through a dedicated Bluetooth Manager class, which handles device discovery, connection management, and data reception. Figure 9.2 illustrates the connection process that was implemented within the app. While the model layer handled the complex underlying state for the connection process, the view layer displayed simple, easy-to-follow guidance to the user.
- **Data Processing** The application processes the raw voltage data from the device to generate the blood pressure readings, discussed in section 8. Also, historical measurements are also analysed to deliver key insights to the user about their health, which is also handled in this layer. Both models were both implemented in Python, using a Jupyter notebook for development. Part of the integration process involved exporting the models in .pkl (pickle) format, and extracting the relevant inference code, to the App's source directory. Then, the Android library *Chaquopy* library [47] was used to call functions from this Python file, allowing us to combine the flexibility of Python and it's libraries with the Kotlin application. The

This layered approach to the Model, like with the overarching application, ensures that data management, device communication, and data processing are handled independently, making the code more maintainable and testable.

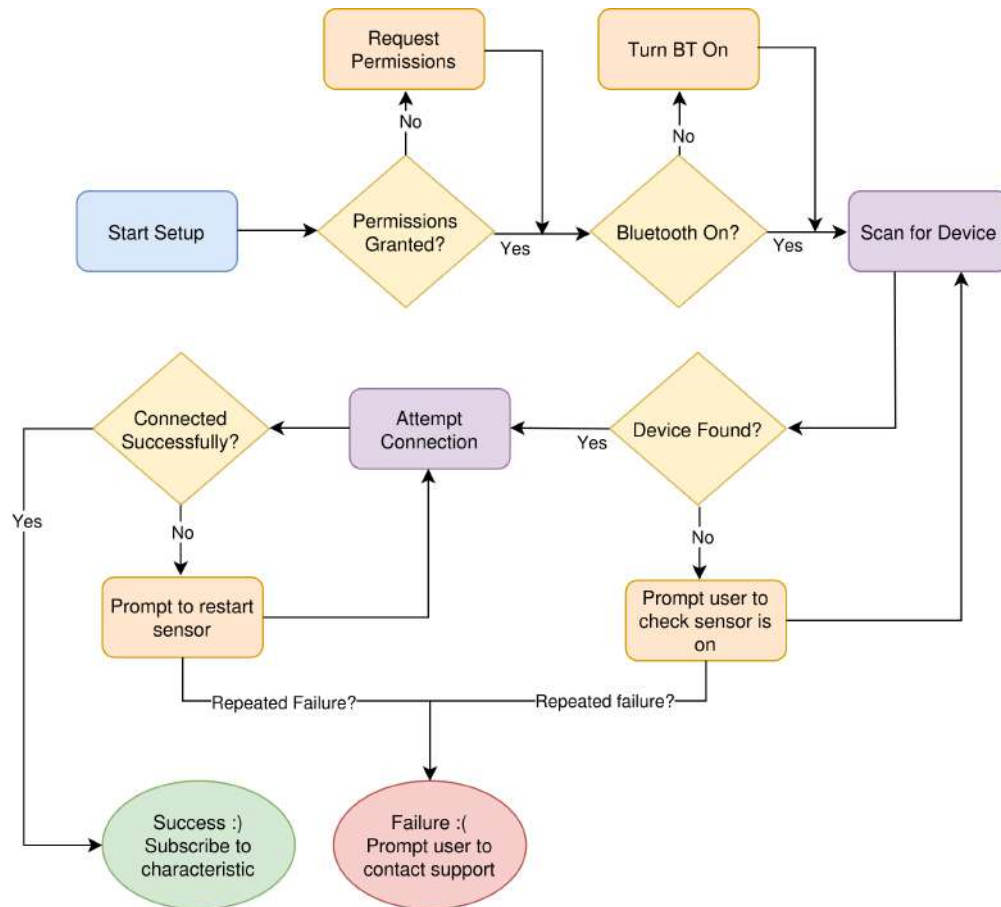


FIGURE 9.2: Workflow diagram showing the Bluetooth connection process

9.4 User Interface Design

9.4.1 Outline

The app's design is based around five main sections, or "screens" that the user interacts with. The main form of navigation in the app is the navigation bar that is always displayed at the bottom of the screen. Labelled icons, corresponding to each of the sections, can be tapped at any point, taking the user to the respective section. This helps to keep the app's navigation tree simple, with all of the functions being accessible within a few taps instead of hidden away within layers of menus, which can make features hard to find.

Home

The home screen is the main area of the app, shown in Figure 9.3. It contains the most important information (connection status, latest readings) and is the first screen

that is displayed when the user opens the app. It has links to key sections with a short description for each, helping guide the user towards what they need.

Data

The data screen, shown in Figure 9.4, allows the user to view historical blood pressure data recorded by the app. It provides a simple interface, displaying a series of graphs where the user can see short and long-term trends in their blood pressure. By tapping and holding on a certain point on the graph, the user can see the exact measurement collected at that time.

Insights

The insights screen is where the user can view intelligent analysis of their data, as illustrated in Figure 9.5. A key goal of this project was to enable early detection of CVD risk factors, so the insights screen displays a "CVD risk score" which is determined based on the risk model developed in Section 8. While currently, the complexity of the model is currently limited due to the availability of data, it is hoped that further research into day-to-day blood pressure variations will enable more complex and intelligent analysis. Likewise, the screen also displays a stress score (note that in the current iteration of the product, the underlying calculation is directly proportional to blood pressure and simply a placeholder), illustrating the potential for blood pressure tracking to help users improve their lifestyle. The insights screen also has sections dedicated to specific advice about potential warning signs, advising the user to speak to their GP when appropriate.

Profile

The profile screen, in Figure 9.6, of the app is where the user can view their current profile and see key information about their medical practice. It is where they can set up their data-sharing preferences and update key medical information, such as their weight. While remote data-sharing functionality has not yet been implemented in the current iteration of the app, the user interface and underlying data-handling functions have been set up to illustrate potential capabilities.

Settings

As the name suggests, the settings screen allows the user to configure the app and the sensor according to their preferences (e.g., enable/disable notifications).

9.4.2 Accessibility

Several accessibility considerations were taken when developing the app, especially considering the intended audience, those with an increased risk of being affected by cardiovascular diseases, being older and less confident using technology. Primarily:

- **Visual Hierarchy and Layout:** The interface employs a clear visual hierarchy with distinct sections separated by cards. Where possible, large icons are used which help users quickly identify different functions. The layout is intentionally uncluttered, with generous spacing between elements to improve readability and reduce cognitive load.
- **Touch Targets:** All interactive elements in the app follow Android's accessibility guidelines for minimum touch target sizes (48dp × 48dp). Buttons and interactive cards have been sized appropriately with adequate spacing between them to prevent accidental taps, which is particularly important for users who may have reduced motor control.
- **Colour and Contrast:** The application's colour scheme was designed to maintain the recommended minimum contrast ratio of 4.5:1 [52] between text and background colours, exceeding accessibility standards. Additionally, colour is never used as the sole indicator of information, with text labels always accompanying colour-coded elements.
- **Navigation:** The app employs a simple, consistent navigation structure with a persistent bottom navigation bar. This ensures that all major functions are always accessible within a maximum of two taps, reducing the cognitive burden of navigation. Clear, descriptive labels accompany all navigation elements.

9.5 Testing and Evaluation

The application underwent thorough manual testing throughout its development cycle. The primary testing methodology employed was exploratory testing, where each feature and screen was systematically exercised to verify functionality and identify potential issues. This involved testing the application across various scenarios, such as different Bluetooth connection states, database operations, and user interactions. Several tools were incorporated into the application to facilitate debugging and development. A dedicated debug mode was implemented, accessible through the settings screen (which will not be accessible to the user in a production release), which enabled the display of raw sensor waveform data and provided additional application state information. Additionally, the app included functionality to generate and load mock measurement data, allowing thorough testing of data processing and visualisation features without

needing to connect to the device directly. This approach proved to be quite valuable as it allowed for faster and easier development.

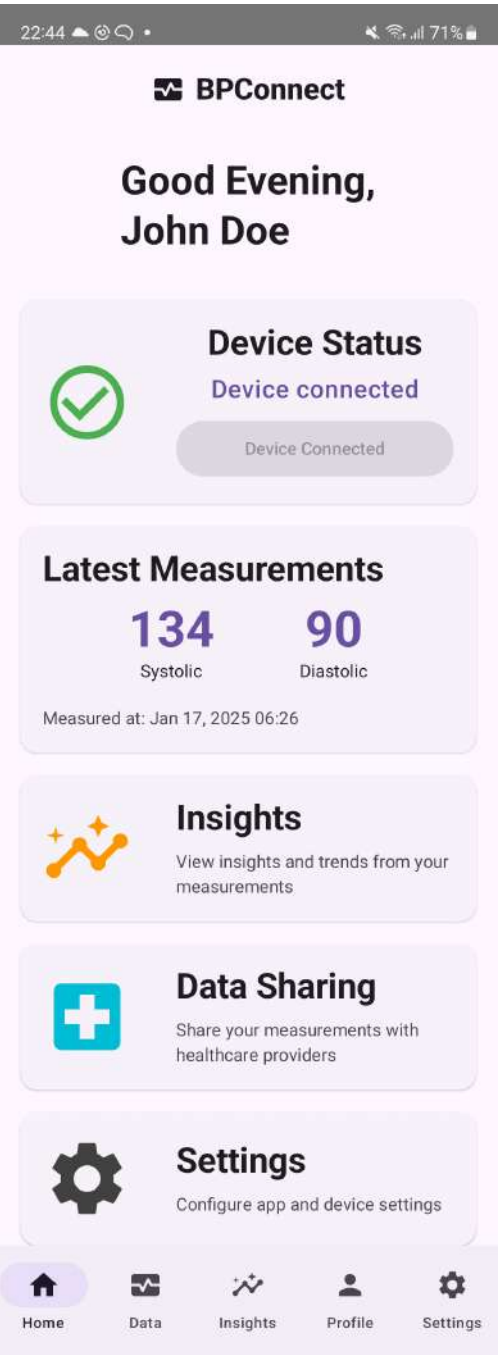


FIGURE 9.3: The application’s Home screen is the first page the user sees when the open the app. Therefore, it contains all of most important functions and information. Note that the image was taking using a "scrolling screenshot" feature, allowing for the whole UI to be visible even if it does not fit on one page.

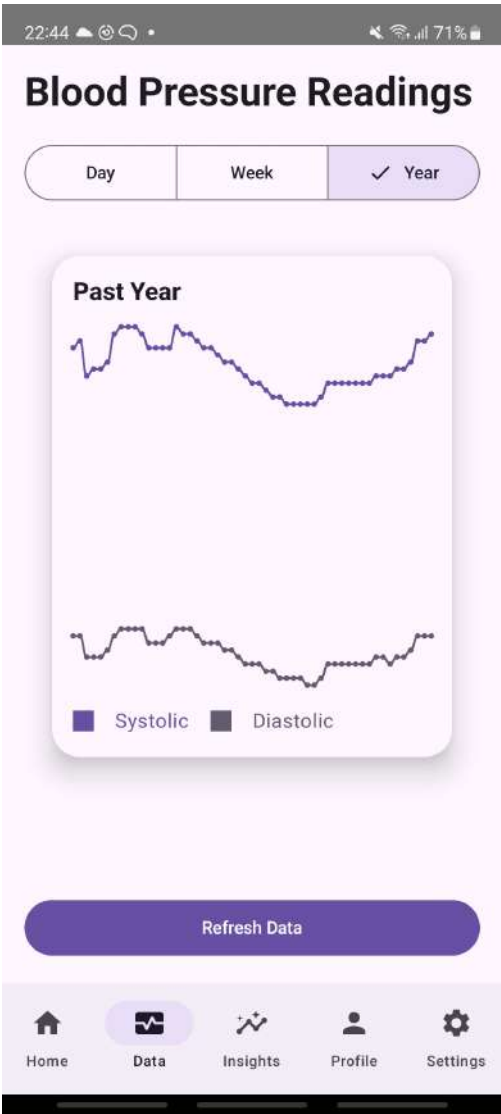


FIGURE 9.4: The Data screen of the app allows the user to view their historical blood pressure data interactively.

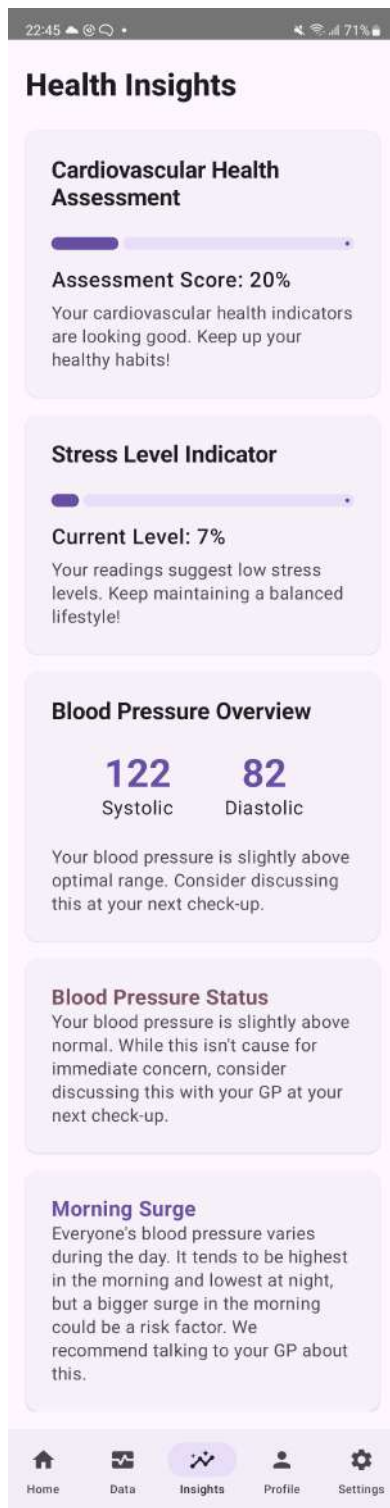


FIGURE 9.5: The insights screen of the application contains insights derived from the user. There are currently two types that can be displayed - scores, which are displayed at the top and give a numerical value, and alerts - which appear below and show information when certain conditions are met.

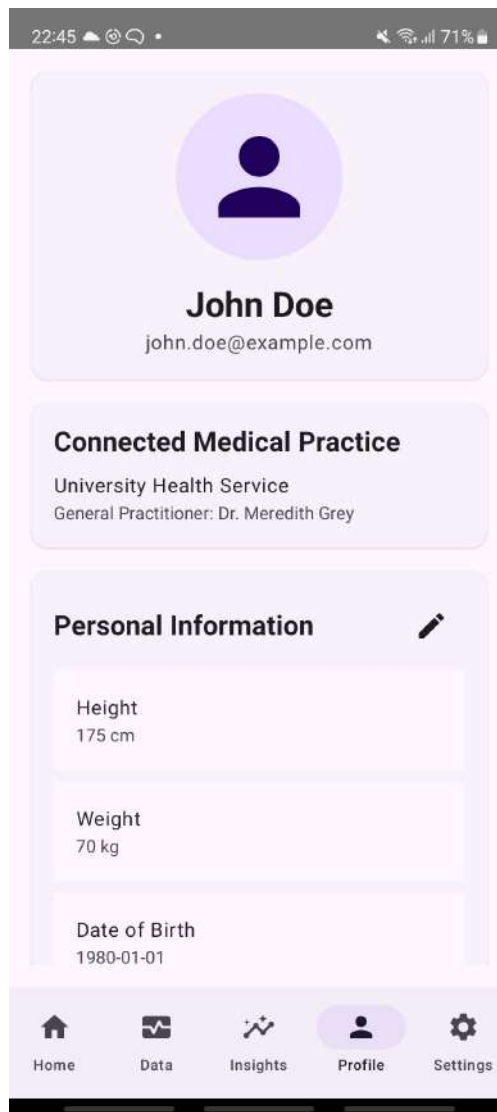


FIGURE 9.6: The profile screen allows the user to view and edit their personal information.

Full System Integration

Chapter

10

*“Talent wins games, but teamwork and intelligence win championships”
- Michael Jordan*

(OR)

To achieve the overall goal of the project of producing a continuous wireless blood pressure monitor, the five subsystems must be integrated successfully - including the fabricated sensor, interface circuitry, communications, data visualisation, and data processing. The final design process consisted of three iterations; a **Wired Prototype** (Section 10.1), a **Wireless Prototype** (Section 10.2), and a final **Wearable System** (Section 10.3). Each iteration of the Full System Integration included refinements in power requirement, form-factor, and usability, to bring the system closer to the final product addressing the Problem Statement in Section 1.1. A flowchart illustrating the achieved function is shown in Figure 10.1.

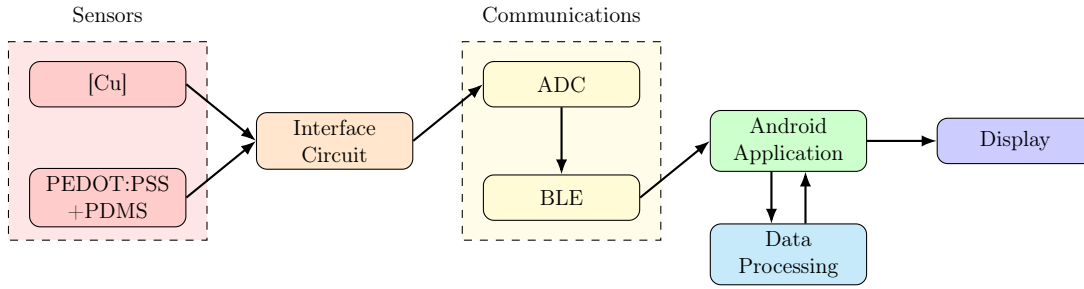


FIGURE 10.1: Flowchart representation of the Full System Integration

10.1 Wired Integration

The initial integration of the system was a wired prototype that aimed to validate the functionality of the sensor components and debug any issues that would arise from joining sub-systems for the first time. This integration also provided the first indication of whether the device was sensitive enough to detect blood pulse waveforms, due to a delay in Ethics Approval (Section 3.2).

The core component of this integration was the fabricated, soft, flexible piezoresistive sensor; PEDOT:PSS coated PDMS with Microdome microstructures. This sensor was connected in a Quarter Wheatstone Bridge configuration as in Section 6.3 to provide maximum sensitivity within the Sensitivity Region identified in Section 5. The MCP601 differential amplifier was selected for this initial integration, due to size constraints not being a concern yet.

To validate that the differential amplifier was functioning as expected, a test signal was applied to the inputs of the differential amplifier using a Rigol DG1062Z Function Generator. [67] This was configured as a $1[Hz]$ Sine wave, with Amplitude of $1.5[V_{p-p}]$, DC offset of $0.75[V]$, and a Phase Shift of 90° , to emulate the output of the Wheatstone Bridge when powered by a $3[V_{dc}]$ supply (Simulated in Figure 6.5). This output was validated using a Tektronix MDO4054B-3 Mixed Domain Oscilloscope, shown in Figure 10.2. [77] The input from the Function Generator was then passed into the differential amplifier, to ensure that the signal was amplified to the set gain of $A_v = 2$ (Figure 10.3).

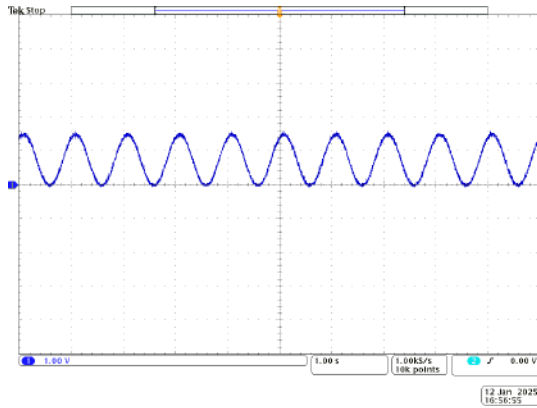


FIGURE 10.2: Oscilloscope capture illustrating the raw signal output from the Function Generator.

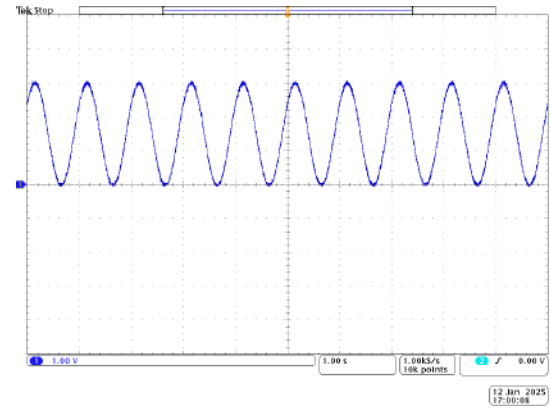


FIGURE 10.3: Amplified output from the Function Generator via the MCP601 Differential Amplifier.



FIGURE 10.4: Placement of the piezoresistive sensor on the skin, above the Radial Artery.

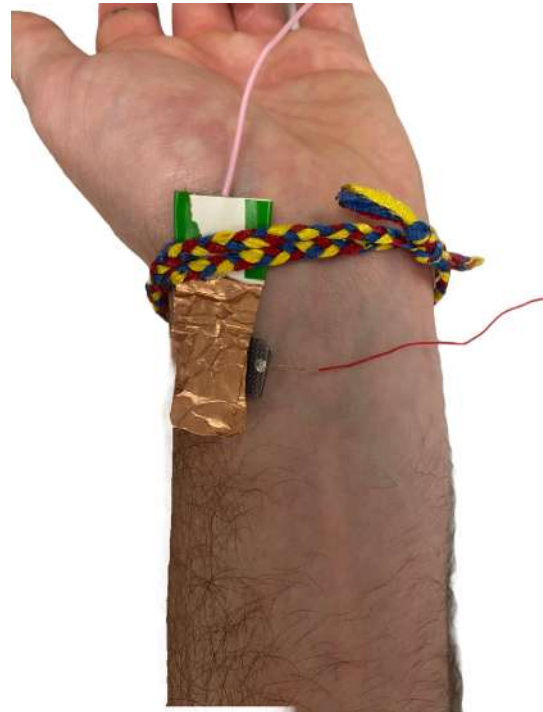


FIGURE 10.5: Placement of the [Cu] electrode on top of the piezoresistive sensor, completing the circuit through the conductive PEDOT:PSS layer.

With the Differential Amplifier setup performing as expected, the Piezoresistive PEDOT:PSS+PDMS sensor is placed on the wrist, aligning with the Radial Artery as shown in Figure 10.4. The solid copper layer is placed on top of the sensor, ensuring it doesn't overlap the [Ag] paste and short the circuit (Figure 10.5). Applying moderate pressure produced the waveform illustrated in Figure 10.6, which indicates that the sensor could correctly detect the pressure induced by the blood pulse. Figure 10.7 shows

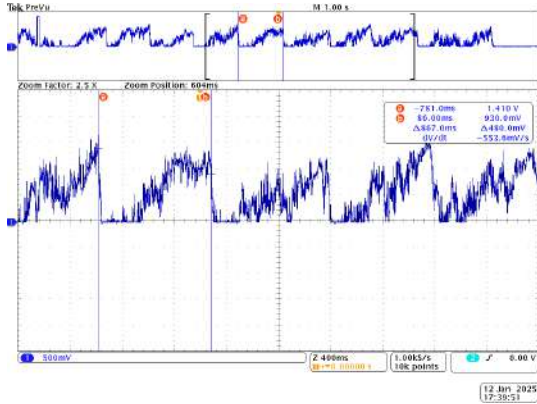


FIGURE 10.6: Oscilloscope capture of the waveform output by the piezoresistive sensor via the interface circuitry.

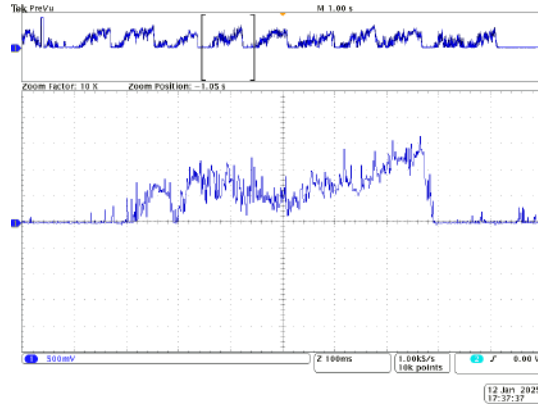


FIGURE 10.7: Zoomed-in blood pulse waveform from Figure 10.6, successfully showing that this method of blood pressure sensing can detect the micro-deflections caused by arterial blood pressure.

an enlarged and focussed view of one pulse wave. While the signal does contain high-frequency noise, it is clear evidence that this method of pressure sensing is capable of capturing pulse waveforms with distinguishable systolic and diastolic features. Further data processing could enhance the clarity of this waveform, making it more suitable for blood pressure estimation.

However, the output proved very sensitive to the amount of back-pressure applied to the sensor and this will remain a consistent issue faced throughout the Full System Integration, to be discussed in Section 12.1.

10.2 Wireless Integration

The second phase of integration marked a significant advancement in the project by incorporating all of the separate subsystems into a single holistic prototype shown in Figure 10.8. Instead of connecting the output of the differential amplifier to an oscilloscope, the signal is now passed into the communications module (Chapter 7). The nRF52840 DK could now power the system with its on-board 3[V] coin-cell battery and efficiently sample the sensor signal using an Analogue-to-Digital (ADC) converter. These signals are then transmitted over BLE to the mobile application. The app provides a real-time illustration of the captured pulse waveform, facilitating immediate assessment of the patient's cardiovascular health.

This full-scale integration demonstrates the system's functionality and that its components are compatible and operate cohesively. However, the design remains a bulky prototype unfriendly to the product's end-users, and requires miniaturisation.

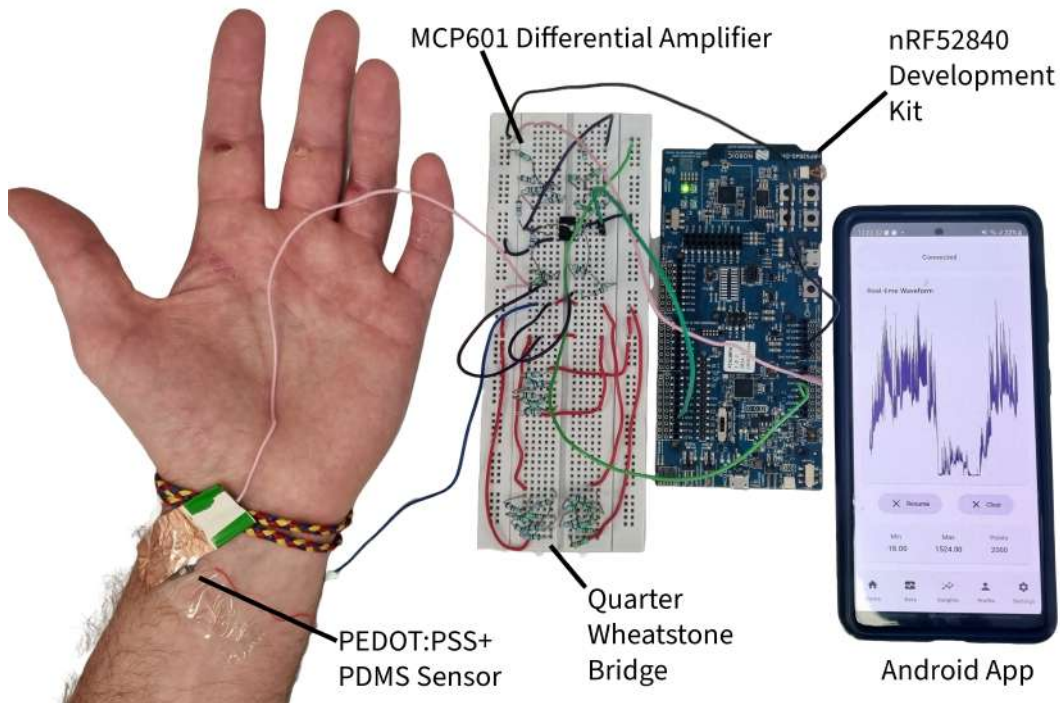


FIGURE 10.8: Wireless Integration of Sensors, Communications, and Android App subsystems, evidencing each part of the project interfacing successfully.

10.3 Wearable System

The third and final phase of integration successfully transitioned all subsystems into a more compact wearable system, achieving a significant down-sizing of both the sensor circuitry and the communications module used. This phase involved replacing the nRF52840 Development Kit with the smaller kit also developed by Nordic Semiconductor, the Thingy:52 (nRF6936), more suited for wearable applications and all-in-one sensor development. [57] Additionally, a custom CAD design for the device housing was designed to hold the Thingy52, sensor circuitry, and allowed an adjustable strap to hold down the sensors to the wrist and provide consistent back-pressure. These improvements made the system more user-friendly and enhanced its portability leading to the project's first real-world wearable prototype for application and testing.

10.3.1 Nordic Semiconductor Thingy:52

The embedded system was moved from the larger nrf52840 development kit to the smaller Nordic Thingy52 during integration. Given the highly decoupled source code from the nRF Connect SDK, the code was made to be platform-agnostic and capable of operating on both boards. The Thingy52 was programmed using the programmer option of the nRF Connect for Desktop app, which required the nRF52840 development kit to act as the intermediary and interface. A 10-pin J-link cable connected the development kit and

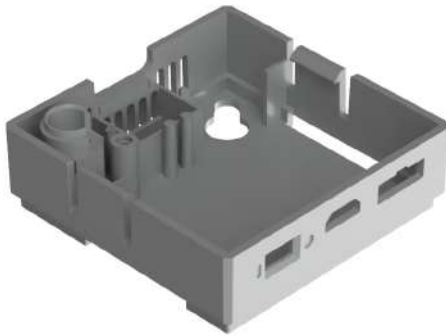


FIGURE 10.9: Autodesk Fusion360 model of the modified Thingy:52 device housing used for Communications.

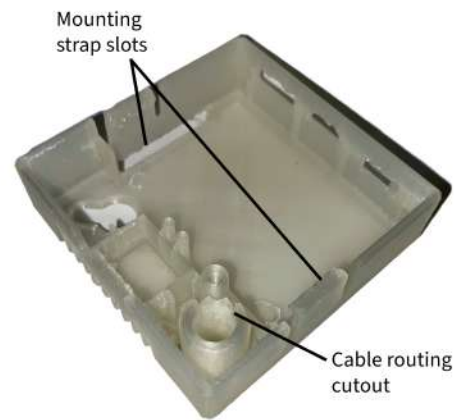


FIGURE 10.10: 3D printed model of the device housing, including wire-routing and mounting strap slots.

the Thingy 52, and a micro-USB connected the development kit to the desktop app. By selecting ‘Clear and Write’ on the programmer, the Thingy52 was flashed with the application.

10.3.2 Device Housing and Wrist Strap

To make the Thingy:52 wearable on a user’s wrist, some modifications were required to the device housing. A case for the device in .stp file format is publicly available on GrabCAD by user Steven Minichiello. [76] This was modified in Autodesk Fusion360 to include a routing-point for cables reaching the outside of the case (to be used in 10.3.3) and to include two slots for mounting the device to the wrist with a strap (Figure 10.9). [5] The case was 3D printed in translucent PLA polymer to ensure visibility of the status LEDs on the device, shown Figure 10.10.

To secure the housing to the wrist, a Velcro securing strap was run through the bottom of the case, upon which the two sensor electrodes (the [Cu] and the piezoresistive sensor itself) were mounted, with their wiring sewn inside. This was designed with accessibility in mind; one of the project goals was to design the device to be useable by individuals with reduced dexterity, and the Velcro strap aids this by providing a smooth and easy attachment mechanism (Figure 10.11).

10.3.3 Miniaturised Interface Circuit

The new, smaller form-factor necessitated a revision to the previous interface circuitry used. The new circuit, pictured in Figure 10.12, includes higher resistor values to fit the

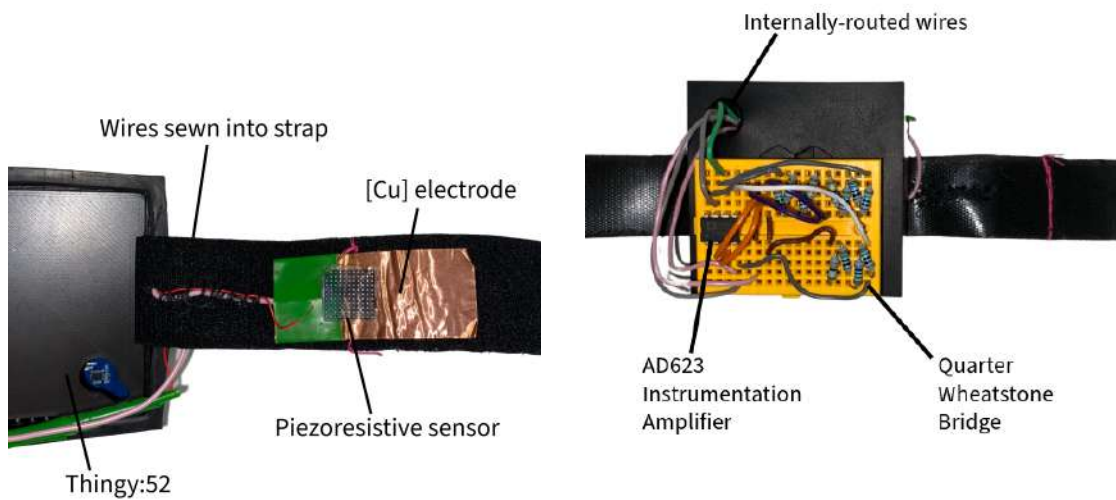


FIGURE 10.11: Sensor electrodes mounted on Velcro strap for the integrated wearable system.

FIGURE 10.12: Miniaturised interface circuit for the wearable device, utilising the AD623 Instrumentation Amplifier on a Development Board.



FIGURE 10.13: Inside view of the Thingy:52 case, showing the internally routed and soldered interface cables.

Wheatstone Bridge in a smaller area, and utilised the AD623 Instrumentation Amplifier in a unity-gain setup to extract the differential voltage from the bridge and (optionally) amplify it without external resistors. A PCB design was intended to be made for the interface circuitry, however, due to time restrictions this did not happen; instead the interface circuit is left on the development board attached via adhesive tape to the top of the Thingy:52. The wires for this circuit are routed internally through the housing



FIGURE 10.14: Final wearable demonstration of the wearable device, illustrating the new Thingy:52 Communications Module connected to the app and receiving data, in addition to the Data Processing Algorithm interpreting the received data and predicting the Blood Pressure based off this.

and soldered directly to the communications board (Figure 10.13).

10.4 Final Prototype

The final prototype for the project is pictured in Figure 10.14. This demonstrates the new, miniaturised wearable device connected over BLE to the app and illustrates significant improvements in portability and ease-of-use for the user. However, an issue arises with the system that can be seen by examining the waveform on the app; the Velcro mounting strap is insufficient for providing the correct amount of back-pressure required to achieve a suitable waveform, which was identified previously as a potential issue with the design.

Chapter

11

Conclusion

(OR, MC, LMA, GV, MR)

The development of the embedded system demonstrates significant advancements in enabling efficient real-time continuous wireless blood pressure monitoring utilising soft, flexible pressure sensors. Despite the initial challenges of integrating the different subsystems into a single device, this project has presented a proof-of-concept device that is a strong foundation for future innovations in wearable healthcare technologies. With continued research and development, this method of blood pressure monitoring has the potential to shift the current status-quo of cardiovascular disease treatment from a reactive to a proactive model, alleviating strain on hospitals, reducing the loss of productivity as a result of CVDs, and promoting fitter and healthier lifestyles.

The sensor system was a vital aspect of the project; ensuring the blood pulse waveform could be accurately extracted from the body using pressure sensors was foundational to the entire system's performance and proved to be the largest source of error for the project as a whole. Several sensor geometries and typologies were quantitatively compared to explore effects on sensitivity, with the Microdome PDMS + Solid [Cu] electrode sensor typology performing the best. Combining this sensor with highly effective interface circuitry was key for transducing a suitable waveform from the body's physiological response. While it was evidenced that the sensor was able to detect this response, it was clear that there were issues with extracting a consistent response due to the challenge of regulating back-pressure.

The successful setup of the BLE communications on both the nRF52840 and the Thingy:52 used NFC pairing and the notifications GATT protocol to ensure secure, low-energy, high-throughput and low-latency data transmission, which is crucial for the application of this health monitoring system. Similarly, the ADC configuration was optimised to capture pulse waveforms from the piezoresistive sensors at high fidelity and with continuous sampling through the double-buffering configuration. Through iterative testing and refinements, a reliable setup was built to interface between the sensors and the mobile application.

The data processing subsystem has demonstrated significant achievements in both blood pressure estimation and cardiovascular risk assessment. The implementation of advanced signal processing techniques combined with machine learning approaches has yielded promising results in both primary objectives. The blood pressure estimation component achieved clinical-grade accuracy with systolic MAE of 2.300 ± 0.076 mmHg and diastolic MAE of 1.391 ± 0.034 mmHg, exceeding current AAMI standards for non-invasive blood pressure measurement while maintaining real-time processing capabilities.

The CVD risk assessment system demonstrated robust performance metrics, achieving 78.66% overall accuracy with 87.00% precision in low-risk identification and a ROC

AUC of 0.6425. This performance provides a strong foundation for preventive healthcare applications, particularly in initial risk screening scenarios. The system maintains computational efficiency suitable for mobile platform requirements, with inference times below 100 ms, memory usage under 256 MB, and a compact model size of 18 MB.

These achievements in signal processing and machine learning contribute significantly to the project's goal of comprehensive health monitoring. The optimization of computational resources while maintaining clinical-grade accuracy positions the system well for integration with the project's hardware and mobile application components, enabling a complete solution for continuous cardiovascular health monitoring.

The mobile application, which bridges the void in between the user and their data, highlights the potential for connected healthcare technology to revolutionise the way preventative healthcare is approached. Instead of occasional measurements at check ups, continuous monitoring of blood pressure can enable patients to monitor their own health, and access intelligent, AI-driven, insights at their fingertips. Furthermore, it shows how key adaptations for accessibility could be taken to help increase uptake of novel health technology among previously under-represented demographics, maximising the net benefit.

Chapter

12

Future Work

(OR, MC, LMA, GV, MR)

The prototype produced at the end of this project is still in its early stages of development, allowing significant room for improvements for each of the subsystems built. For this device to truly evolve into a fully flexible and wearable continuous blood pressure monitoring system, it must ensure that it is suitable for both in-hospital and at-home monitoring of patients. The refinements and future developments that can realise this goal have been taken into consideration and are articulated in detail for prospective advancements of this product.

12.1 The Issue of Backpressure

Pressure sensors are sensitive to the amount of "back-pressure" applied to the sensor against the stimulus it is designed to measure. An issue was encountered with this project in regulating the amount of backpressure applied as the fabricated sensors were highly sensitive to applied stimuli. This often led to the signal saturating the output fully and not being able to record pressure data. This was not an issue with the wired and wireless implementations as the sensors were manually held against the skin, but for the wearable implementation this proved to be a significant issue as the Velcro strap was insufficient at supplying the correct amount of backpressure consistently. This could be addressed by implementing a one-way valve "airbag" design, similar to [37], which self-regulates the amount of applied pressure to the skin, producing a consistent pressure each time the sensor is used.

Potential improvements to be considered for the sensor fabrication is to use of electronic screen printing to fabricate the electrodes. The smaller IDE designs, with gap and rod widths of 200×200 and $100 \times 100 \mu\text{m}$, were not successful. Although the other successful IDEs were not used in the final product, the sensor characterisation demonstrated an obvious trend that decreasing the gap widths increased the sensor sensitivity. Therefore, investigating a more precise fabrication method, such as electronic screen printing, may lead to improved accuracy in the device. Additionally, fabricating a solid copper electrode instead of using copper tape, could enhance the durability of the electrode.

12.2 Communication Efficiency

The potential improvements and next steps for the communication system concern enhancing its efficiency and, thus, power consumption. The data handling can be improved by using differential coding of the waveform, where the samples are stored as the difference between each successive value which shortens the number of bits required to represent the waveform and thus improves the throughput, power consumption and overall efficiency of the BLE communication protocol. Similarly, the amount of data that is transmitted over BLE can be reduced if the blood pressure estimation model is

integrated into the board. Instead of transmitting 400 samples, only the systolic and diastolic blood pressure values would be sent at a rate of about 1 Hz, greatly reducing the power consumption.

The development and evaluation of cardiovascular monitoring systems have identified several key areas for future enhancement. These opportunities for improvement span across data acquisition, signal processing, and model development domains.

Future work should prioritize the acquisition of comprehensive cardiovascular datasets. While the current implementation demonstrates promising results with R^2 scores of 0.824 and 0.733 for systolic and diastolic pressure estimation respectively, access to additional clinical datasets would enable enhanced model validation across diverse patient populations. This expanded validation would support improved feature extraction methodologies and facilitate the development of more robust prediction algorithms. The integration of diverse datasets would particularly strengthen the system's generalization capabilities across different demographic groups and clinical conditions.

Current performance metrics indicate the need for enhanced signal processing capabilities, particularly in handling motion artifacts and environmental interference. Future development should focus on:

$$\begin{aligned} &\text{Adaptive Filtering : Real-time noise reduction} \\ &\text{Feature Extraction : Robust morphological analysis} \\ &\text{Signal Quality : Automated assessment and compensation} \end{aligned} \tag{12.1}$$

The implementation of advanced adaptive filtering techniques would significantly improve the system's resilience to motion artifacts and environmental noise, while enhanced feature extraction algorithms would ensure reliable morphological analysis under varying signal conditions.

The CVD risk assessment model, currently achieving 78.66% accuracy, presents several opportunities for advancement:

$$\begin{aligned} &\text{Risk Stratification : Continuous scoring system} \\ &\text{Feature Handling : Partial data accommodation} \\ &\text{Model Complexity : Optimized computational efficiency} \end{aligned} \tag{12.2}$$

The development of a continuous risk scoring system would enable more nuanced risk assessment, moving beyond the current binary classification approach. This enhancement would capture the progressive nature of cardiovascular risk while maintaining computational efficiency for mobile deployment. The architecture should

also be adapted to handle partially available patient data, increasing its practical utility in clinical settings.

Implementation of these enhancements would significantly improve the system's clinical utility while maintaining its current performance metrics. Optimising processing algorithms would enable robust real-time monitoring capabilities, while standardized data exchange protocols would facilitate seamless integration with existing healthcare information systems. This integration would support comprehensive patient monitoring and enable more effective clinical decision-making.

12.3 Mobile App Features

There are several areas where the app could be developed further. One particular area is the model integration. While, the model was integrated successfully into the application, it is able to produce outputs from given real-time data, which are then able to be stored and displayed in the user interface. However, this behaviour seems to be unstable in certain situations, often returning the blood pressure value as "0", indicating an error state and that the model was unable to calculate a value, which seems to happen in certain situations only. Further model refinement, improved data pre-processing, and data sample standardisation could remedy this.

Also, the Bluetooth functionality could be improved further, such as by implementing better support for NFC-initiated connections. Currently, the user must use the app's setup process, as additional features such as tap-to-connect that have been implemented on the sensor device aren't available on the app yet.

Considering the project brief, a key next step would be to create a web portal for medical professionals to access their patient's data. The app would periodically send recent measurements to a secure cloud service, which could then be used for more in-depth analysis and automatically updating patient's medical records.

Bibliography

- [1] J. Allen. Photoplethysmography and its application in clinical physiological measurement. *Physiological Measurement*, 28(3):R1, 2007.
- [2] American Medical Association. **Environmental Sustainability in Health Care: The Role of Biomedical Engineers**. *AMA Journal of Ethics*, 24(10):E986–993, 2022.
- [3] Analog Devices, Inc. **AD623: Low Cost, Low Power Instrumentation Amplifier**, 2016.
- [4] Apple Inc. **Health - Apple (UK)**, 2024. [Online].
- [5] Autodesk Inc. **Fusion 360, Version 2.0.20981**, 2024. [Online; Accessed: 18-Jan-2025].
- [6] Atheer Awad, Sarah J. Trenfield, Thomas D. Pollard, Jun Jie Ong, Moe Elbadawi, Laura E. McCoubrey, Alvaro Goyanes, Simon Gaisford, and Abdul W. Basit. **Connected healthcare: Improving patient care using digital health technologies**. *Advanced Drug Delivery Reviews*, 178:113958, 2021. ISSN 0169-409X.
- [7] Misbaou Barry, Fatoumata Barry, Mesut Gun, Paul Padurean, Jean Fortuné Ikoli, Eric Havet, Bessem Gara Ali, and Thierry Caus. **Influence of age and sex on the thickness of the radial artery wall**. *Current Problems in Cardiology*, 49(7):102523, 2024. ISSN 0146-2806.
- [8] A. Soni R. Yadav S. P. Singh Bijender, S. Kumar and A. Kumar. **Noninvasive blood pressure monitoring via a flexible and wearable piezoresistive sensor**. *ACS Omega*, 9(6):6355–6365, 2024.
- [9] William Bolton. **Chapter 2 - instrumentation system elements**. In William Bolton, editor, *Instrumentation and Control Systems (Third Edition)*, pages 17–70. Newnes, third edition edition, 2021. ISBN 978-0-12-823471-6.
- [10] Cadworks3D. H-Series Entry-Level 3D Printer. <https://cadworks3d.com/h-series-entry-level-3d-printer/>, . [Online; accessed 20-January-2025].
- [11] Cadworks3D. Master Mold Resin Product Page. <https://cadworks3d.com/product/master-mold-resin/>, . [Online; accessed 20-January-2025].

- [12] Jennifer K Carroll, Anne Moorhead, Raymond Bond, William G LeBlanc, Robert J Petrella, and Kevin Fiscella. **Who uses mobile phone health apps and does use matter? a secondary data analytics approach.** *J Med Internet Res*, 19(4):e125, Apr 2017. ISSN 1438-8871.
- [13] Bruce Carter and Ron Mancini. *Op Amps for Everyone*. Newnes, 4th edition, 2017. ISBN 978-0-12-811648-7.
- [14] B.M. Caulfield and S.C. Donnelly. **What is Connected Health and why will it change your practice?** *QJM: An International Journal of Medicine*, 106(8):703–707, August 2013. ISSN 1460-2725.
- [15] N. V. Chawla et al. SMOTE: Synthetic Minority Over-sampling Technique. *Journal of Artificial Intelligence Research*, 16:321–357, 2002. [Accessed: 20-Jan-2025].
- [16] et al. Chris T.D. Goodman. **Measuring arterial blood pressure**, 2023. Accessed: 2025-01-14.
- [17] R. B. D’Agostino et al. General Cardiovascular Risk Profile for Use in Primary Care. *Circulation*, 117(6):743–753, 2008. [Accessed: 20-Jan-2025].
- [18] Haris Dautović. Charts: A charting library for android with jetpack compose. <https://github.com/dautovicharis/Charts>, 2023. Accessed: 20 January 2025.
- [19] Andrew DeHennis and Junseok Chae. **Pressure sensors**. In Yogesh B. Gianchandani, Osamu Tabata, and Hans Zappe, editors, *Comprehensive Microsystems*, pages 101–133. Elsevier, 2008. ISBN 9780444521903. Accessed: 2025-01-15.
- [20] G. R. Dias. **A study on sphygmomanometers**, 2017. Accessed: 2025-01-14.
- [21] Yongmin Kim Donglok Kim, Ravi Managuli. **Data cache and direct memory access in programming mediaprocessors.** *IEEE Micro*, 21(4):34–42, Jul/Aug 2001.
- [22] Sinem Coleri Ergen. Zigbee/ieee 802.15. 4 summary. *UC Berkeley, September*, 10 (17):11, 2004.
- [23] European Society of Cardiology. **Late-Breaking Science: New data highlight the huge economic burden of CVD in Europe**, 2023. Accessed: 2025-01-10.
- [24] D. C. Goff et al. 2013 ACC/AHA Guideline on the Assessment of Cardiovascular Risk. *Journal of the American College of Cardiology*, 63(25):2935–2959, 2014. [Accessed: 20-Jan-2025].
- [25] Grand View Research. **Wearable medical devices market size, share trends analysis report by product (diagnostic devices, therapeutic devices), by site (handheld, shoe sensors), by grade type, by distribution channel, by application, by region, and segment forecasts, 2025 - 2030**, 2024. Accessed: 2025-01-10.

- [26] Guido Grassi, Cristina Giannattasio, Monica Failla, Antonio Pesenti, Giovanni Peretti, Edoardo Marinoni, Nicoletta Fraschini, Sabrina Vailati, and Giuseppe Mancia. **Sympathetic modulation of radial artery compliance in congestive heart failure**. *Hypertension*, 26(2):348–354, 1995.
- [27] Quinn Grundy. **A review of the quality and impact of mobile health apps**. *Annual Review of Public Health*, 43(Volume 43, 2022):117–134, 2022. ISSN 1545-2093.
- [28] Dinesh V Gunasekeran, Yih-Chung Tham, Daniel S W Ting, Gavin S W Tan, and Tien Y Wong. **Digital health during covid-19: lessons from operationalising new models of care in ophthalmology**. *The Lancet Digital Health*, 3(2):e124–e134, 2021. ISSN 2589-7500.
- [29] Jiang He, Yufei Zhang, Runhui Zhou, Lirong Meng, Tao Chen, Wenjie Mai, and Caofeng Pan. **Recent advances of wearable and flexible piezoresistivity pressure sensor devices and its future prospects**. *Journal of Materiomics*, 6(1):86–101, 2020.
- [30] HeartWest. **24-hour blood pressure monitoring**, 2025. Accessed: 2025-01-14.
- [31] Robin Heydon. *Bluetooth Low Energy: The Developer's Handbook*. Pearson Education, Upper Saddle River, NJ, 2013. ISBN 978-0-13-288836-3.
- [32] Jianguo Hu, Guanhua Dun, Xiangshun Geng, Jing Chen, Xiaoming Wu, and Tian-Ling Ren. **Recent progress in flexible micro-pressure sensors for wearable health monitoring**. *Nanoscale Advances*, 5:1718–1739, 2023.
- [33] Chuwei Zhong Cong Wang Ruijuan Chen Guang Zhang Jinhai Wang-Ran Wei Huiquan Wang, Mengting Han. **Non-invasive continuous blood pressure prediction based on ecg and ppg fusion map**. *Medical Engineering Physics*, 119, 2023. Accessed: 2025-01-14.
- [34] J. Zhou et al. J. Li, H. Jia. **Thin, soft, wearable system for continuous wireless monitoring of artery blood pressure**. *Nature Communications*, 14:5009, 2023. Accessed: 2025-01-15.
- [35] Garima Jain and Sanjeet Dahiya. Nfc: Advantages, limits and future scope. *International Journal on Cybernetics & Informatics (IJCI)*, 4(4):1–8, 2015.
- [36] Ho-Hyun Jang, Joon-Shik Park, and Bumkyoo Choi. **Flexible piezoresistive pulse sensor using biomimetic pdms mold replicated negatively from shark skin and pedot:pss thin film**. *Sensors and Actuators A: Physical*, 279:68–76, 2018. Accessed: 2025-01-15.
- [37] Jingkun Zhou Jian Li, Huiling Jia. **Thin, soft wearable system for continuous wireless monitoring of artery blood pressure**. *European Journal of Preventive Cardiology*, 14 (5009):1–12, 08 2023. ISSN 2041-1723.

- [38] Andrew Rucker Jones, Scott Conway, Glen Smith, J.C. Romanda, Kyle, Opal, and Sean Sullivan. Opencsv: Simple csv parsing and writing library for java. <https://opencsv.sourceforge.net>, 2025. Accessed: 20 January 2025.
- [39] Emil Jovanov, Aleksandar Milenkovic, Chris Otto, and Piet C. de Groen. **A wireless body area network of intelligent motion sensors for computer assisted physical rehabilitation**. *Journal of NeuroEngineering and Rehabilitation*, 2(1):6, March 2005. ISSN 1743-0003.
- [40] Sukriti Kc, Salina Tewolde, Anthony A. Lavery, Céire Costelloe, Chrysanthi Papoutsis, Claire Reidy, Bernard Gudgin, Craig Shenton, Azeem Majeed, John Powell, and Felix Greaves. **Uptake and adoption of the NHS App in England: an observational study**. *British Journal of General Practice*, 73(737):e932–e940, December 2023. ISSN 0960-1643, 1478-5242. Publisher: British Journal of General Practice Section: Research.
- [41] Maryam Khan, Muhammad Muqet Rehman, Shenawar Ali Khan, Muhammad Saqib, and Woo Young Kim. **Characterization and performance evaluation of fully biocompatible gelatin-based humidity sensor for health and environmental monitoring**. *Frontiers in Materials*, 10, 2023. ISSN 2296-8016.
- [42] J. Kim et al. Development and Validation of a Deep Learning-Based Cardiovascular Disease Risk Prediction Model Using a Large-Scale Health Screening Cohort. *JMIR Medical Informatics*, 9(3):e25321, 2021. [Accessed: 20-Jan-2025].
- [43] Arun Kumar and Pradeep Kumar Sharma. Bluetooth low energy for wearable sensor-based healthcare systems: A review. *Healthcare Technology Letters*, 4(4): 117–127, 2017.
- [44] Hao Lin, Wenyao Xu, Nan Guan, Dong Ji, Yangjie Wei, and Wang yi. **Noninvasive and continuous blood pressure monitoring using wearable body sensor networks**. *IEEE Intelligent Systems*, 30:1–1, 11 2015.
- [45] Jiun-Ren Lin, Timothy Talty, and Ozan K. Tonguz. **On the potential of bluetooth low energy technology in vehicular applications**. *IEEE Communications Magazine*, 53(1):267–274, 2015.
- [46] Matías A. Loewy. **New devices could change the way we measure blood pressure: Embedded in a cell phone or in accessories such as rings, bracelets or watches, the novel tools aim to make it easier to manage hypertension. but they must still pass several tests before hitting the clinic**. *Knowable Magazine*, Oct. 2023. Accessed: 17-Jan-2025.
- [47] Chaquopy Ltd. Chaquopy: Python for android. <https://chaquo.com/chaquopy/>, 2025. Accessed: 20 January 2025.

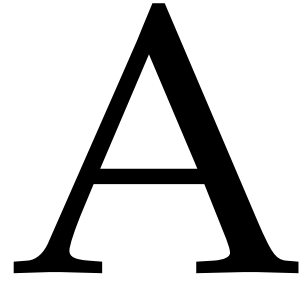
- [48] M. S. Islam M. R. A. Karim, S. K. Kabir and R. R. Kumar. **A study on verification of sphygmomanometers**, 2018. Accessed: 2025-01-14.
- [49] S. S. Mahmood et al. The Framingham Heart Study and the epidemiology of cardiovascular disease: a historical perspective. *The Lancet*, 383(9921):999–1008, 2014. [Accessed: 20-Jan-2025].
- [50] Nouhad Rizk Mahmoud Bassiouni, Islam Hegazy and El-Sayed A. El-Dahshan. **Combination of ecg and ppg signals for smart healthcare systems: Techniques, applications, and challenges**, 2021. Accessed: 2025-01-14.
- [51] Microchip Technology Inc. *MCP601/1R/2/3/4 2.7V to 6.0V Single-Supply CMOS Op Amps*, 2021. Accessed: 2025-01-17.
- [52] Richard Morton. **Colour contrast – why does it matter? – accessibility in government**, Jun 2016.
- [53] Paul Muntner, Daichi Shimbo, Robert M. Carey, Jamie B. Charleston, Trudy Gaillard, Shetal Misra, Martin G. Myers, Gbenga Ogedegbe, Joseph E. Schwartz, Raymond R. Townsend, Elaine M. Urbina, Anthony J. Viera, William B. White, and Jackson T. Jr. Wright. **Measurement of blood pressure in humans: A scientific statement from the american heart association**. *Hypertension*, 2019.
- [54] NASA. **Technology readiness levels (trl)**, 2023. Accessed: 2025-01-10.
- [55] National Health Service. **Blood pressure test**, 2023. Accessed: 2025-01-10.
- [56] National Instruments. Multisim. Version 14.3, National Instruments Corporation, Austin, TX, USA 2023. Available: <https://www.ni.com/en/support/downloads/software-products/download.multisim.html>.
- [57] Nordic Semiconductor. *Thingy:52 User Guide, Version 1.2*, December 2019. [Accessed: 18-Jan-2025].
- [58] Ofcom. **Smartphone ownership penetration in the United Kingdom (UK) in 2012-2024, by age**, 2024. [Online].
- [59] World Health Organization. **Global recommendations on physical activity for health**. *Nutrition Reviews*, 69(9):456–459, 2011.
- [60] C. P. O'Donnell. Zigbee technical analysis for iot applications. *International Journal of Computer Applications*, 124(16):1–7, 2015.
- [61] Leila Pfaeffli Dale, Rosie Dobson, Robyn Whittaker, and Ralph Maddison. **The effectiveness of mobile-health behaviour change interventions for cardiovascular disease self-management: A systematic review**. *European Journal of Preventive Cardiology*, 23(8):801–817, 08 2020. ISSN 2047-4873.

- [62] M. F. Piepoli et al. 2016 European guidelines on cardiovascular disease prevention in clinical practice. *European Heart Journal*, 37(29):2315–2381, 2016. [Accessed: 20-Jan-2025].
- [63] Barry M. Popkin, Linda S. Adair, and Shu Wen Ng. **Global nutrition transition and the pandemic of obesity in developing countries**. *Nutrition Reviews*, 70(1):3–21, 2012.
- [64] R. Ratliff. **77 of 2015’s most interesting digital health quotes**, December 2015. [Accessed: 20-Jan-2025].
- [65] Yusnita Rahayu, Tharek Abd. Rahman, and Razali Ngah. Ultra wideband technology and its applications. In *Proceedings of the IEEE Wireless Communications and Networking Conference (WCNC)*, pages 1–8. IEEE, 2008.
- [66] Yusnita Rahayu, Tharek Abd. Rahman, Razali Ngah, and P. S. Hall. Ultra wideband technology and its applications. In *2008 World of Wireless, Mobile and Multimedia Networks*, pages 1–6. IEEE, 2008.
- [67] Rigol Technologies, Inc. **DG1062Z 60MHz Function/Arbitrary Waveform Generator**, 2025. [Accessed: 18-Jan-2025].
- [68] Rohde Schwarz GmbH Co. KG. *RS HMC8012 Digital Multimeter User Manual*, 2025. [Online; Accessed: 18-Jan-2025].
- [69] Mohammad Shahadat Daniel M. Mulvihill Satyaranjan Bairagi, Shahid-ul-Islam and Wazed Ali. **Mechanical energy harvesting and self-powered electronic applications of textile-based piezoelectric nanogenerators: A systematic review**. *Nano Energy*, 111:108414, 2023. Accessed: 2025-01-15.
- [70] Nordic Semiconductor. Devzone. <https://devzone.nordicsemi.com/>, .
- [71] Nordic Semiconductor. Nordic developer academy. <https://academy.nordicsemi.com/courses/nrf-connect-sdk-intermediate/>, .
- [72] Nordic Semiconductor. Nordic developer academy. <https://academy.nordicsemi.com/courses/nrf-connect-sdk-fundamentals/>, .
- [73] Nordic Semiconductor. Techdocs. <https://docs.nordicsemi.com/>, .
- [74] Nordic Semiconductor. Nordic developer academy. <https://academy.nordicsemi.com/courses/bluetooth-low-energy-fundamentals/>, 2023.
- [75] Sigma-Aldrich. PEDOT:PSS (Catalog No. 655201) Specification Sheet. <https://www.sigmaaldrich.com/specification-sheets/293/258/655201-BULK.pdf>. [Online; accessed 20-January-2025].
- [76] Steven Minichiello. **Nordic Semiconductor Thingy:52 Multi-Sensor Bluetooth 5.0 to Cellular IoT Prototyping Platform (3D Model)**, April 2021. [Accessed: 18-Jan-2025].

- [77] Tektronix, Inc. [MDO4000 Mixed Domain Oscilloscope Datasheet](#), 2010. [Accessed: 18-Jan-2025].
- [78] Workineh Tesema, Bruno da Silva, Worku Jimma, and Johan Stiens. [Power saving techniques for wearable devices in medical applications](#). In *ECON 2022 – 48th Annual Conference of the IEEE Industrial Electronics Society*, pages 1–6, Brussels, Belgium, 2022. IEEE. ISBN 978-1-6654-8025-3. ©2022 IEEE.
- [79] R. Sheriff V. Andrew, N. Kumar and N. Kumar. [Comparison of white coat and masked hypertension](#), 2021. Accessed: 2025-01-14.
- [80] J. Welch, F. Guilak, and S.D. Baker. [A Wireless ECG Smart Sensor for Broad Application in Life Threatening Event Detection](#). In *The 26th Annual International Conference of the IEEE Engineering in Medicine and Biology Society*, volume 2, pages 3447–3449, September 2004.
- [81] World Health Organization. [Cardiovascular diseases \(cvds\) fact sheet](#), 2021. Accessed: 2025-01-11.
- [82] Jaime Zamora-Mejia, Alejandro Martinez-Castillo, Jose M. Rocha-Perez Diaz-Sanchez, Agustín L. Herrera-May, Uriel G. Zapata-Rodriguez, and Victor H. Carbajal-Gomez. [Advances in low-power electronics for wearable health monitoring devices](#). *Electronics*, 11(7):1108, 2022. This article belongs to the Special Issue Wireless Power/Data Transfer, Energy Harvesting System Design, Volume II.
- [83] Ting Zhang, Jiang Lu, Fei Hu, and Qi Hao. Bluetooth low energy for wearable sensor-based healthcare systems. In *2014 IEEE Healthcare Innovation Conference (HIC)*, pages 251–254, 2014.
- [84] X. Zhang et al. Machine Learning for Cardiovascular Disease Risk Prediction: A Systematic Review. *Journal of Medical Internet Research*, 22(8):e18716, 2020. [Accessed: 20-Jan-2025].
- [85] Ding Li Jin-Ming Jian Zhen Li Shou-Rui Ji Xin Li Jian-Dong Xu Hou-Fang Liu Yi Yang Zi-Bo Zhou, Tian-Rui Cui and Tian-Ling Ren. [Wearable continuous blood pressure monitoring devices based on pulse wave transit time and pulse arrival time: A review](#). *Materials*, 16(6):2133, Mar 2023. Accessed: 2025-01-14.
- [86] Xuanjie Zong, Nianqiang Zhang, Xiaopeng Ma, Jilai Wang, and Chengpeng Zhang. [Polymer-based flexible piezoresistive pressure sensors based on various micro/nanostructures array](#). *Composites Part A: Applied Science and Manufacturing*, 190:108648, 2025.

Primary Ethics Form

Appendix



Refer to the *Instructions* and to the *Guide* documents for a glossary of the key phrases in **bold** and for an explanation of the information required in each section. The *Templates* document provides some text that may be helpful in preparing some of the required appendices.

Replace the **highlighted text** with the appropriate information.

Note that the size of the text entry boxes provided on this form does **not** indicate the expected amount of information; instead, refer to the *Instructions* and to the *Guide* documents in providing the complete information required in each section. Do **not** duplicate information from one text box to another. Do not otherwise edit this form.

Reference number: ERGO/FEPS/99919	Submission version: 3	Date: 13.01.2025
Name of investigator(s) : Mikayla Colegrave (msc1n21), Oscar Robinson (or1g21), Luqmanul Mohd Awallizam (lhma1n20), Geethaarth Vagga (gv2g21), and Mukilan Rajapandian (mr1g20).		
Name of supervisor(s) (if student investigator(s)): Rujie Sun (Supervisor), Kai Yang (customer)		
Title of study: Soft, Wearable Pressure Sensors for Continuous Wireless Monitoring of Blood Pressure Enhanced by Artificial Intelligence		
<p>Note that failure to follow the University's policy on Ethics may lead to disciplinary action concerning Misconduct or a breach of Academic Integrity.</p> <p>By submitting this application, the investigator(s) undertake to:</p> <ul style="list-style-type: none"> Conduct the study in accordance with university policies governing: Ethics (http://www.southampton.ac.uk/ris/policies/ethics.html); Data management (http://www.southampton.ac.uk/library/research/researchdata/); Health and Safety (http://www.southampton.ac.uk/healthandsafety); Academic Integrity (http://www.calendar.soton.ac.uk/sectionIV/academic-integrity-statement.html). Ensure the study Reference number ERGO/FEPS/xxxx is prominently displayed on all advertising and study materials and is reported on all media and in all publications. Conduct the study in accordance with the information provided in the application, its appendices, and any other documents submitted; Submit the study for re-review (as an amendment through ERGO) or seek FEPS EC advice if any changes, circumstances, or outcomes materially affect the study or the information given. Promptly advise an appropriate authority (Research Integrity and Governance team) of any adverse study outcomes; Submit an end-of-study form if required to do so. 		

REFER TO THE INSTRUCTIONS AND GUIDE DOCUMENTS WHEN COMPLETING THIS FORM AND THE TEMPLATES DOCUMENT WHEN PREPARING THE REQUIRED APPENDICES.

STUDY DETAILS

What are the aims and objectives of this study?

The project aims to develop a soft, wearable pressure sensor system for continuous and wireless blood pressure (BP) monitoring, enhanced with artificial intelligence (AI). The main objectives consist of the following:

1. Design and fabrication of the pressure sensor array
2. Data processing to convert signals into blood pressure
3. Development of a deep learning model to analyse the sensor data
4. Integrating the wireless communication model
5. Test the accuracy of the device on participants

Background of the study (*a brief rationale for conducting the study*)

Cardiovascular diseases (CVDs), particularly diseases like hypertension, heart attacks and strokes, are a leading cause of death globally, with approximately 18 million each year. Traditional methods for measuring blood pressure (BP) only measure intermittent data therefore any fluctuations that occur throughout the day are missed. Continuous blood pressure monitoring can capture any variations diagnosing things like nocturnal hypertension or masked hypertension, which shows normal BP patterns in a clinical setting but is elevated during other daily activities, providing more information about cardiovascular health. Soft, wearable devices have made continuous BP monitoring easier, not only are they more comfortable than the traditional methods, but they also allow for improved healthcare systems as this technology can be used to design better treatment plans for patients as it provides real-time feedback.

Reference:

Li, Jian and Jia, Huiling and Zhou, Jingkun and Huang, Xingcan and Xu, Long and Jia, Shengxin and Gao, Zhan and Yao, Kuanming and Li, Dengfeng and Zhang, Binbin and Liu, Yiming and Huang, Ya and Hu, Yue and Zhao, Guangyao and Xu, Zitong and Li, Jiyu and Yiu, Chun Ki and Gao, Yuyu and Wu, Mengge and Jiao, Yanli and Zhang, Qiang and Tai, Xuecheng and Chan, Raymond H. and Zhang, Yuanting and Ma, Xiaohui and Yu, Xinge, Thin, soft, wearable system for continuous wireless monitoring of artery blood pressure, Nature Communications, 2023, URL <https://www.nature.com/articles/s41467-023-40763-3#citeas>

Key research question (*Specify hypothesis if applicable*)

RQ1. Can the piezoelectric/ piezoresistive sensors accurately and reliably measure blood pressure compared to standard clinical devices?

RQ2. Is the blood pressure data effectively communicated wirelessly and processed into a clear, interpretable format for end-users?

RQ3. Can AI algorithms effectively analyse blood pressure data from the wearable device to identify potential hypertension risks in participants?

Study design (*Give a brief outline of the study design and why it is being used*)

The study is designed to validate a wearable blood pressure monitoring device that is in

the very early stages of development. At present, only the sensor fabrication has been completed, and the prototype is not yet a fully wearable device. Consequently, this study will not involve testing the device on other participants or patients; testing will be conducted solely by the investigators.

The device integrates piezoelectric/piezoresistive sensors on a flexible PCB embedded within a sleeve, engineered for comfort and wearability by the user. The goal of the device is to accurately capture blood pressure changes through continuous monitoring and wirelessly transmit data to a smartphone application for real-time monitoring and AI-based hypertension risk assessment.

To assess the functionality of the sensor in its current form, the investigators will perform a controlled sequence task, the hand grip and cold pressor task, designed to induce a gradual increase in blood pressure. This structured protocol allows for repeated, dynamic measurements, enabling an evaluation of the sensor's accuracy and the reliability of wireless communication. By comparing the data collected from the device to standard clinical data, an initial evaluation of the sensor's performance will be formed.

This preliminary study aims to validate the sensor's capabilities and inform further development of the wearable device. If the results demonstrate a positive correlation between the sensor data and standard clinical data, this will provide a foundation for future work towards a wearable prototype that could eventually be applied in real healthcare settings.

As noted in the submission questionnaire, section H10.2 indicates that the device is categorised as a medical device, and it is not CE marked. This preliminary study aims to validate the sensor's capabilities and inform further development of the wearable device. If the results demonstrate a positive correlation between the sensor data and standard clinical data, this will provide a foundation for future work towards a wearable prototype that could eventually be applied in real healthcare settings.

PRE-STUDY

Characterise the proposed **participants**

The participants for this research project consist solely of the investigators involved in the study. Since this project is only a 4th year student group design project that takes place only in the first semester of the academic year, it will not be tested with patients during this study.

Describe how **participants** will be approached

As the participants in this study are the investigators themselves, the approach involves team agreement and consent.

Describe how inclusion/exclusion criteria will be applied (if any)

For this experiment, while the investigators themselves are serving as participants, the following inclusion and exclusion criteria are applied to ensure the safety and reliability of the data collected. These criteria reflect those that would be expected of external

participants in future studies and are followed by the investigators as well

Inclusion criteria

1. Patients who are currently using conventional BP monitoring methods or have known BP issues
2. Participants who generally have stable health
3. Participants who have given consent

Exclusion criteria

1. Severe cardiovascular conditions such as recent heart attack or stroke
2. Pregnancy
3. Participants taking any BP altering medications
4. Participants with electrical implants such as pacemakers
5. Participants with chronic skin conditions that may interfere with the effectiveness of the device
6. Substance abuse

The investigators will self-assess against these criteria and confirm their eligibility before participating in data collection. Any investigator who does not meet the inclusion criteria or falls under the exclusion criteria will abstain from participating in the experiment. This ensures that even with internal participants, the study maintains safety, integrity, and adherence to ethical standards.

Describe how **participants** will decide whether or not to take part

As the participants in this study are the investigators themselves, they already have a comprehensive understanding of the project, its objectives, and the procedures involved. However, their decision to take part in data collection remains entirely voluntary. The participants will be given a participant information sheet before taking part in the experiment as an extra precaution to make sure the purpose of the experiment is fully understood. The participants will be asked to sign a consent form if they decide they are happy to participate in the experiment.

Participant Information (Appendix (i))

Provide the **Participant Information** in the form that it will be given to **participants** as Appendix (i). All studies must provide **participant information**.

Consent Form/Information (Appendix (iii))

Provide the **Consent Form** (or the request for consent) in the form that it will be given to **participants** as Appendix (iii). All studies must obtain **participant** consent. Some studies may obtain verbal consent (and only present consent information), other studies will require written consent, as explained in the *Instructions*, *Guide*, and *Templates* documents.

DURING THE STUDY

Describe the study procedures as they will be experienced by the **participants**

Upon beginning the experiment, the investigators will meet to review the study objectives, tasks, and timeline. Although they are familiar with the project, a detailed explanation of the purpose of the wearable blood pressure sensor sleeve, the steps involved, and the

expected outcomes will be reiterated to align the team. This ensures that all participants approach the task with a clear understanding and consistency.

Investigators will have the opportunity to clarify any remaining questions or address concerns. They will provide verbal confirmation of their willingness to participate, which will be documented to reflect informed consent.

Each investigator will fit the wearable blood pressure sensor sleeve to themselves or with assistance from another team member to ensure proper placement and comfort. The device will be checked for:

1. **Correct Initial Pressure:** Ensuring accurate sensor calibration.
2. **Comfort:** Adjustments will be made to avoid discomfort or undue pressure during the experiment.

If at any point during the experiment an investigator feels discomfort or wishes to stop, they can do so without penalty, and their data will be excluded from further analysis.

Baseline Measurement

Once the wearable sleeve is fitted correctly, the investigator will sit comfortably and rest for 5 minutes to establish a baseline blood pressure measurement.

Task Sequence (3 Repetitions)

Each investigator will perform the following sequence three times:

1. **Hand Grip Exercise:**
 - The investigator will tightly grip their hand into a fist for 2 minutes to gradually elevate blood pressure.
2. **Cold Pressor Challenge:**
 - Immediately after the hand grip exercise, the investigator will immerse their hand into a bucket of ice-cold water for 1 minute to further increase blood pressure.
3. **Rest Period:**
 - The investigator will remove their hand from the water and rest for 5 minutes, allowing blood pressure to return to baseline.

This sequence will be repeated three times to obtain sufficient data for analysis.

Data Monitoring and Analysis

During the experiment, the wearable device will continuously collect blood pressure measurements. These will be displayed in real-time on a smartphone GUI for monitoring. The collected data will be processed, and the AI model will analyse blood pressure patterns to assess its performance in predicting potential conditions like hypertension.

End of Experiment

After completing the task sequence, the investigator-participants will debrief and provide feedback on the device's functionality and comfort. Any observations regarding the data collection process will be documented to guide future refinements of the prototype.

By following these procedures, the investigators ensure a systematic approach to testing the prototype while adhering to ethical standards and maintaining participant safety and comfort.

Identify how, when, where, and what kind of data will be recorded (not just the formal research data, but including all other study data such as e-mail addresses and signed consent forms)

Blood pressure data

Signed Consent form

Participant questionnaire/data gathering methods (Appendix (ii))

As Appendix (ii), reproduce any and all **participant** questionnaires or data gathering instruments in the exact forms that they will be given to or experienced by **participants**. If conducting less formal data collection, or data collection that does not involve direct questioning or observation of participants (eg secondary data or "big data"), provide specific information concerning the methods that will be used to obtain the data of the study.

POST-STUDY

Identify how, when, and where data will be stored, processed, and destroyed

The data will be anonymised and stored in the university of Southampton one drive, which will be password protected and only accessible by the investigators. Since this is only a student project, the data will be destroyed once the investigators graduate in July 2025.

STUDY CHARACTERISTICS

(L.1) The study is funded by a commercial organisation: **No**

If 'Yes', provide details of the funder or funding agency *here*.

N/A

(L.2) There are **restrictions** upon the study: **No**

If 'Yes', explain the nature and necessity of the **restrictions** *here*.

N/A

(L.3) Access to **participants** is through a third party: **No**

If 'Yes', provide evidence of your permission to contact them as (v) in the *Checklist* below. Do *not* provide explanation or information on this matter *here*.

(M.1) **Personal data** is or *may be collected or processed: **yes**

Data will be processed outside the UK: **No**

If 'Yes' to either question, provide the **DPA Plan** as (iv) in the *Checklist* below. Do *not* provide information or explanation on this matter here. Note that using or recording e-mail addresses, telephone numbers, signed consent forms, or similar study-related **personal data** requires M.1 to be "Yes".

(* Secondary data / "big data" may be *de-anonymised*, or may contain **personal data**. If so, answer 'Yes'.)

(M.2) There is **inducement** to **participants**: **No**

If 'Yes', explain the nature and necessity of the inducement *here*.

N/A

(M.3) The study is **intrusive**: **No**

If 'Yes', provide the **Risk Management Plan**, the **Debrief Plan**, and Technical Details as (vi), (vii), and (ix) in the *Checklist* below, and explain *here* the nature and necessity of the intrusion(s).

N/A

(M.4) There is **risk of harm** during the study: **No**

If 'Yes', provide the **Risk Management Plan**, the **Contact Information**, the **Debrief Plan**, and Technical Details as (vi), (vii), (viii), and (ix) in the *Checklist* below, and explain *here* the necessity of the risks.

N/A

(M.5) The true purpose of the study will be hidden from **participants**: **No**

The study involves **deception** of **participants**: **No**

If 'Yes' to either question, provide the **Debrief Plan** and Technical Details as (vii) and (ix) in the *Checklist* below, and explain *here* the necessity of the deception.

N/A

(M.6) **Participants** may be minors or otherwise have **diminished capacity**: **No**

If 'Yes', AND if one or more Study Characteristics in categories M or H applies, provide the **Risk Management Plan**, the **Contact Information**, and Technical Details as (vi), (vii), & (ix) in the *Checklist* below, and explain *here* the special arrangements that will ensure informed consent.

N/A

(M.7) **Special category personal data** is collected or processed: **Yes**

If 'Yes', provide the **DPA Plan** and Technical Details as (iv) and (ix) in the *Checklist* below. Do *not* provide explanation or information on this matter here.

(H.1) The study involves: **invasive** equipment, material(s), or process(es); or **participants** who are not able to withdraw at any time and for any reason; or animals; or human tissue; or biological samples: **No**

If 'Yes', provide Technical Details and further justifications as (ix) and (x) in the *Checklist* below. Do *not* provide explanation or information on these matters here. Note that the study will require separate approval by the Research Governance Office.

Technical details

If one or more Study Characteristics in categories M.3 to M.7 or H applies, provide the description of the technical details of the experimental or study design, the power calculation(s) which yield the required sample size(s), and how the data will be analysed, as separate appendices.

CHECKLIST OF DOCUMENTS TO UPLOAD

Please provide the following forms, *naming the files as explicitly* as possible, e.g., "Participant Information", "Questionnaire", "Consent Form", "DPA Plan", "Permission to contact", "Risk Management Plan", "Debrief Plan", "Contact Information", and/or "Technical details" as appropriate. Each document must specify the reference number in the form ERGO/FPSE/xxxx, the document version number, and its date of last edit.

- (i): **Participant Information** in the form that it will be given to **participants**.
- (ii): Data collection method (eg for secondary data or "big data") / **Participant Questionnaire** in the form that it will be given to **participants**.
- (iii): **Consent Form** (or consent information if no **personal data** is collected) in the form that it will be given to **participants**.
- (iv): **DPA Plan**.
- (v): Evidence of permission to contact (prospective) **participants** through any third party.
- (vi): **Risk Management Plan**.
- (vii): **Debrief Plan**.
- (viii): **Contact Information**.
- (ix): Technical details of the experimental or study design, the power calculation(s) for the required sample size(s), and how the data will be analysed.
- (x): Further details and justifications in the case of: **invasive** equipment, material(s), or process(es); **participants** who are not able to withdraw at any time and for any reason; animals; human tissue; or biological samples.

Appendix

B

Consent Form

CONSENT FORM

Study Title: Soft, Wearable Pressure Sensors for Continuous Wireless Monitoring of Blood Pressure Enhanced by Artificial Intelligence

Ethics/ERGO number: 99919

Version and date: 2 and 13.01.2025

Thank you for your interest in this study. It is very important to us to conduct our studies in line with ethics principles, and this Consent Form asks you to confirm if you agree to take part in the above study. Please carefully consider the statements below and add your initials and signature only if you agree to participate in this research and understand what this will mean for you.

Please add your initials to the boxes below if you agree with the statements:

Mandatory Consent Statements	Participant Initials
I confirm that I read the Participant Information Sheet version 2 dated 13.01.2025 explaining the study above and I understand what is expected of me.	
I was given the opportunity to consider the information, ask questions about the study, and all my questions have been answered to my satisfaction.	
I agree to take part in this study and understand that data collected during this research project will be used for the purpose of this study.	
I understand that my participation is voluntary and that I am free to withdraw from this study at any time without giving a reason.	

Participant Eligibility Checklist

Please complete the following checklist to confirm your eligibility to participate in this study. Tick the box if the statement applies to you.

Exclusion Criteria	Yes	No
I have a severe cardiovascular condition, such as a recent heart attack or stroke.	<input type="checkbox"/>	<input type="checkbox"/>
I am pregnant.	<input type="checkbox"/>	<input type="checkbox"/>
I am taking BP-altering medications.	<input type="checkbox"/>	<input type="checkbox"/>
have an electrical implant, such as a pacemaker.	<input type="checkbox"/>	<input type="checkbox"/>
I have a chronic skin condition that may interfere with the effectiveness of the device	<input type="checkbox"/>	<input type="checkbox"/>
I have a history of substance abuse.	<input type="checkbox"/>	<input type="checkbox"/>

Name of participant

Signature

Date

Name of person taking consent

Signature

Date

*Once this Consent Form has been signed by all parties, a copy of the signed and dated form should be provided to the study participant. Original signed copy should be stored in the study site file (If applicable).

Participant Information Sheet

Appendix

C

Participant Information Sheet

Study Title: Title: Soft, Wearable Pressure Sensors for Continuous Wireless Monitoring of Blood Pressure Enhanced by Artificial Intelligence

Researcher: (msc1n21), Oscar Robinson (or1g21), Luqmanul Mohd Awallizam (lhma1n20), Geethaarth Vagga (gv2g21), and Mukilan Rajapandian (mr1g20) **ERGO number:** 99919

You are being invited to take part in the above research study. To help you decide whether you would like to take part or not, it is important that you understand why the research is being done and what it will involve. Please read the information below carefully and ask questions if anything is not clear or you would like more information before you decide to take part in this research. You may like to discuss it with others, but it is up to you to decide whether to take part. If you are happy to participate you will be asked to sign a consent form.

What is the research about?

This research aims to evaluate the functionality of a wearable blood pressure sensor that uses advanced piezoresistive materials. The device is designed to continuously measure blood pressure and transmit data wirelessly to a smartphone application for real-time monitoring. The sensor data is securely transferred to the app, where it is analysed, and artificial intelligence is used to predict potential cardiovascular diseases. By analysing data collected during controlled tasks, the study seeks to validate the sensor's accuracy and its potential for future applications in healthcare.

Why have I been asked to participate?

You have been asked to participate because you are a university student over the age of 18 who has a generally stable health and may be currently using conventional BP monitoring methods or have known BP issues (although not essential). Please DO NOT participate in this study if either of these apply to you:

1. Severe cardiovascular conditions such as recent heart attack or stroke
2. Pregnancy
3. Participants taking any BP altering medications
4. Participants with electrical implants such as pacemakers
5. Participants with chronic skin conditions that may interfere with the effectiveness of the device
6. Substance abuse

What will happen to me if I take part?

If you decide to take part in this study, you will be asked to wear a blood pressure sensor sleeve. The process will proceed as follows:

1. **Preparation:** The investigators will provide a detailed explanation of the purpose of the wearable blood pressure sensor sleeve, the steps involved, and the expected outcomes. You will have the opportunity to ask questions or raise concerns before starting the experiment. Verbal confirmation of your willingness to participate will be documented as informed consent.
2. **Fitting the Device:** The wearable blood pressure sensor sleeve will be fitted to your arm, either by yourself or with assistance from a team member, to ensure proper placement and comfort. The device will be checked to ensure:
 - o Correct initial pressure for accurate sensor calibration.
 - o Comfort, with adjustments made as needed to avoid discomfort or undue pressure.

3. **Baseline Measurement:** After the sleeve is properly fitted, you will sit comfortably and rest for 5 minutes to establish a baseline blood pressure measurement.
4. **Task Sequence:** You will perform the following sequence three times:
 - **Hand Grip Exercise:** You will tightly grip your hand into a fist for 2 minutes to gradually elevate blood pressure.
 - **Cold Pressor Challenge:** Immediately after the hand grip exercise, you will immerse your hand into a bucket of ice-cold water for 1 minute to further increase blood pressure.
 - **Rest Period:** After removing your hand from the water, you will rest for 5 minutes, allowing your blood pressure to return to baseline.

NOTE:

1. All blood pressure signals collected will remain anonymous when the results are analysed.

Are there any risks involved?

The experiment is low risk and only requires you to do a few simple hand exercises.

What data will be collected?

During the experiment you will be connected to a pressure sensor where your continuous blood pressure will be recorded.

Will my participation be confidential?

Your participation and the information we collect about you during the research will be kept strictly confidential.

Only members of the research team and responsible members of the University of Southampton may be given access to data about you for monitoring purposes and/or to carry out an audit of the study to ensure that the research is complying with applicable regulations. Individuals from regulatory authorities (people who check that we are carrying out the study correctly) may require access to your data. All of these people have a duty to keep your information, as a research participant, strictly confidential.

Data files will be protected by passwords accessible folders; laptops will be protected by user-specific passwords; desktops will be protected by university login credentials; physical data will be kept in filing cabinets and protected by the locker in the project supervisor's office. The data will be destroyed by the investigators once the project is done and they have graduated in July 2024.

Do I have to take part?

No, it is entirely up to you to decide whether or not to take part. If you decide you want to take part, you will need to sign a consent form to show you have agreed to take part. However, if you would like to take part, please email the researchers using msc1n21@soton.ac.uk, orlg21@soton.ac.uk, lhmaln20@soton.ac.uk, gv2g21@soton.ac.uk, mrlg20@soton.ac.uk to schedule a time when you are available.

What happens if I change my mind?

You have the right to change your mind and withdraw at any time without giving a reason and without your participant rights being affected.

What will happen to the results of the research?

Your personal details will remain strictly confidential. Research findings made available in any reports or publications will not include information that can directly identify you without your specific consent. All data collected will be destroyed by the project supervisor in 2 years.

Where can I get more information?

If you would like more information of the study, please contact the researchers via :
msc1n21@soton.ac.uk, orlg21@soton.ac.uk, lhmaln20@soton.ac.uk , gv2g21@soton.ac.uk,
mr1g20@soton.ac.uk

What happens if there is a problem?

If you have a concern about any aspect of this study, you should speak to the researchers who will do their best to answer your questions.

If you remain unhappy or have a complaint about any aspect of this study, please contact the University of Southampton Head of Research Ethics and Clinical Governance (023 8059 5058, rgoinfo@soton.ac.uk) or contact the project supervisor, Rujie Sun (Rujie.Sun@soton.ac.uk).

Data Protection Privacy Notice

The University of Southampton conducts research to the highest standards of research integrity. As a publicly-funded organisation, the University has to ensure that it is in the public interest when we use personally-identifiable information about people who have agreed to take part in research. This means that when you agree to take part in a research study, we will use information about you in the ways needed, and for the purposes specified, to conduct and complete the research project. Under data protection law, 'Personal data' means any information that relates to and is capable of identifying a living individual. The University's data protection policy governing the use of personal data by the University can be found on its website (<https://www.southampton.ac.uk/legalservices/what-we-do/data-protection-and-foi.page>).

This Participant Information Sheet tells you what data will be collected for this project and whether this includes any personal data. Please ask the research team if you have any questions or are unclear what data is being collected about you.

Our privacy notice for research participants provides more information on how the University of Southampton collects and uses your personal data when you take part in one of our research projects and can be found at <http://www.southampton.ac.uk/assets/sharepoint/intranet/Is/Public/Research%20and%20Integrity%20Privacy%20Notice/Privacy%20Notice%20for%20Research%20Participants.pdf>

Any personal data we collect in this study will be used only for the purposes of carrying out our research and will be handled according to the University's policies in line with data protection law. If any personal data is used from which you can be identified directly, it will not be disclosed to anyone else without your consent unless the University of Southampton is required by law to disclose it.

Data protection law requires us to have a valid legal reason ('lawful basis') to process and use your Personal data. The lawful basis for processing personal information in this research study is for the performance of a task carried out in the public interest. Personal data collected for research will not be used for any other purpose.

For the purposes of data protection law, the University of Southampton is the 'Data Controller' for this study, which means that we are responsible for looking after your information and using it properly. The University of Southampton will keep identifiable information about you for 2 years after the study has finished after which time any link between you and your information will be removed.

To safeguard your rights, we will use the minimum personal data necessary to achieve our research study objectives. Your data protection rights – such as to access, change, or transfer such information - may be limited, however, in order for the research output to be reliable and accurate. The University will not do anything with your personal data that you would not reasonably expect.

If you have any questions about how your personal data is used, or wish to exercise any of your rights, please consult the University's data protection webpage (<https://www.southampton.ac.uk/legalservices/what-we-do/data-protection-and-foi.page>) where you can make a request using our online form. If you need further assistance, please contact the University's Data Protection Officer (data.protection@soton.ac.uk).

Thank you for taking the time to read the information sheet and considering taking part in the research.

Data Protection Agreement

Appendix

D

DPA Plan

Ethics reference number: ERGO/FEPS/99919	Version: 1	Date: 2024.12.10
Study Title: Soft, Wearable Pressure Sensors for Continuous Wireless Monitoring of Blood Pressure Enhanced by Artificial Intelligence		
Investigator: Mikayla Colegrave (msc1n21), Oscar Robinson (or1g21), Luqmanul Mohd Awallizam (lhma1n20), Geethaarthha Vagga (gv2g21), and Mukilan Rajapandian (mr1g20).		

The following is an exhaustive and complete list of all the data that will be collected (through questionnaires, interviews, extraction from records, etc) consent forms and the blood pressure data collected by the piezoresistive sensors in the experiment.

The data is relevant to the study purposes because they are important in answering the research questions outlined in the ethics application form. The data collected to answer both the research questions will come from the continuous blood pressure signals.

The data will be processed fairly because the participants will have given explicit consent

The data's accuracy is ensured because the experimental protocol is carefully designed and will be followed. The recording equipment is all reliable and well-maintained. Further, the data will be appropriately stored with suitable IDs to link the multimodal data sources.

Data will be stored on The University Server. The data will be held in accordance with university policy on data retention.

Data files will be protected by encryption and secure access controls; laptops will be protected by strong passwords and encryption; desktops will be protected by firewalls and antivirus software. No physical data will be created.

The data will be destroyed by investigator at all online and laptop location after finishing this project, by graduation in July 2025.

The data will be processed in accordance with the rights of the participants because they will have the right to access, correct, and/or withdraw their data at any time and for any reason. Participants will be able to exercise their rights by contacting the investigator (e-mail: msc1n21@soton.ac.uk, or1g21@soton.ac.uk, lhma1n20@soton.ac.uk, gv2g21@soton.ac.uk, mr1g20@soton.ac.uk) or the project supervisor (e-mail: Rujie.Sun@soton.ac.uk).

The data will be anonymised by extracting features from blood pressure signals recorded during the study. Consent forms will be linked to the data by ids given to the participant.

The data will NOT be transferred outside the European Economic Area (EEA).

Data Protection Act 2018 (DPA) best practice

If the study involves personal or sensitive data, explicitly explain how data will be collected, stored, analysed, held securely, and in turn destroyed. The DPA does not apply to anonymous data and a DPA Plan is not required in the case of such data.

The principles of the DPA are that personal data must be:

1. Processed fairly and lawfully.
2. Processed for specified purposes and in an appropriate way.
3. Adequate, relevant and not excessive for the purposes.
4. Accurate and up-to-date.
5. Not kept for longer than necessary.
6. Processed in accordance with the rights of data subjects (participants).
7. Protected by appropriate security, both practical and organisational.
8. Not transferred outside the European Economic Area (EEA) without adequate data protection controls.

Data is recorded information, whether stored electronically on computer or in paper-based filing systems. Personal data is information about an identifiable living individual. It can be factual, such as the date of a person's interview, or an opinion, such someone's view on how the person has performed on a task. It obviously includes individuals' contact addresses or telephone numbers. (Less obviously, note that personal data is being processed where information is collected and analysed with the intention of distinguishing one individual from another and to take a particular action in respect of an individual. This can take place even if no obvious identifiers, such as names or addresses, are held.) Processing is any activity that involves data, including collecting, recording or retrieving, using, disclosing, organising, adapting, changing, updating, or destroying it.

The DPA identifies Sensitive Personal Data as:

- a) the racial or ethnic origin of the data subject (participant);
- b) his political opinions;
- c) his religious beliefs or other beliefs of a similar nature;
- d) whether he is a member of a trade union;
- e) his physical or mental health or condition;
- f) his sexual life;
- g) the commission or alleged commission by him of any offence or
- h) any proceedings for any offence committed or alleged to have been committed by him, the disposal of such proceedings and the sentence of court in such proceedings.

The processing of sensitive data must meet at least one of the 10 stricter conditions laid down in Schedule 3 of the DPA. It may be useful to know that condition 1 of this schedule permits processing of such data if the data subject has given his explicit consent, and condition 5 if the information has been made public as a result of steps deliberately taken by the data subject.

Keep in mind that the Police have a right of access to personal data held by the study for the purpose of safeguarding national security; preventing or detecting crime; prosecuting or apprehending offenders; assessing or collecting tax; or protecting the vital interests of the data subject or another.

Researchers are exempted: from the second data protection principle, meaning that personal data can be processed for purposes other than for which they were originally obtained; from the fifth data protection principle, meaning that personal data can be held indefinitely; and from the data subject's right of access to his personal data provided the data is processed for research purposes

and the results do not identify data subjects. In addition, the Data Protection (Processing of Sensitive Personal Data) Order 2000 para.9 provides that processing in the course of maintaining archives for research purposes is permissible where the sensitive personal data are not used to take decisions about any person without their consent and no substantial damage or distress is caused to any person by the keeping of those data. These exemptions do NOT give a blanket exemption from all the Data Protection Principles to data provided and/or used for research purposes. Researchers wishing to use personal data should be aware that the Data Protection Principles still generally apply, notably the requirement to keep data secure¹.

A study may seek to anonymise the data it keeps. Anonymisation involves the removal of participants' personal information (names; e-mail address; whatever data it is that might permit identification; etc) from the data such that what remains cannot be used to identify them. Note that audio and video recordings (and often transcriptions too) cannot easily be anonymised, so they should normally be treated as non-anonymous data. Anonymised data can usually be kept without security and can easily be passed to other investigators for specialist analysis.

The DPA requires access to be granted to participants to all of their data, if any part of that data allows their identification. If the data has been anonymised, two issues arise.

1. If the personal information has been removed from the data AND DESTROYED, then the DPA is no longer applicable, and the data can be kept without security. However, investigators should note that they will be unable to follow up or subsequently contact participants in any way, or associate individuals with particular data, and should not attempt to suggest they might do so.
2. If the personal information has been removed from the bulk of the data, but NOT destroyed (ie, is kept separately), then the DPA remains applicable. In this situation, the personal information needs to be (a) kept both separately and securely from the anonymised data, and (b) to be linked or 'keyed' to the anonymised data, such keys to be similarly kept securely (and often kept with the personal information).

If personal data is collected, in the 'Participant Information', inform the participant of:

- the processes the study will take to ensure data security;
- their right to access and correct their data and their right to request removal of their data;
- the authority which will give them access to their data (provide the contact information).

If sensitive data is collected, or the study involves clinical studies, human tissue samples, invasive procedures, or young or vulnerable people, provide additional detail. In the 'Participant Information', inform the participant of:

- the separation of identifying data and the anonymisation process;
- the method of linking the consent form (if any) to the participant's data;
- the processes for the destruction of all study data (if appropriate).

The study should conform to the University policy on data management applicable:

<http://www.southampton.ac.uk/library/research/researchdata/>

Investigators may find the University's survey platform useful:

<https://www.isurvey.soton.ac.uk/>

¹ http://www.jisc.ac.uk/publications/generalpublications/2001/pub_dpacop_0101.aspx

Contacts

risethic@soton.ac.uk.

Appendix

E

Risk Assessment

Title of the risk assessment	Soft, Wearable Pressure Sensors for Continuous Wireless Monitoring of Blood Pressure Enhanced by Artificial Intelligence	
Date risk assessment carried out	10.12.2024	
Describe the work being assessed	Conducting an experiment to collect data using self-designed piezoresistive sensors strapped to the wrist to measure blood pressure in real time. The sensors have been fabricated using PDMS coated with PEDOT to form the piezoresistive material, with a copper electrode placed on top to facilitate signal measurement. The sensors are securely fastened to the wrist to ensure proper placement and comfort for the investigators participating in the study. Investigators will perform controlled tasks designed to induce changes in blood pressure, such as handgrip exercises and cold pressor challenges, while the sensors record data. The device is powered by a low-voltage power source, well within safe levels for human use, and no exposed wires are present to ensure safety during the experiment.	
Describe the location at which the work is being carried out	building 16 lab	
Where appropriate list the individuals doing the work and the dates/times when the work will be carried out	Mikayla Colegrave, Oscar Robinson, Luqmanul Mohd Awalizam, Geethaarthha Vagga, Mukilan Rajapandian 10.12.24 to 24.01.25	
List any other generic or specific risk assessments or other documents that relate to this assessment-use hyperlinks if possible	none	
Name and post of risk assessor	no	
List the names and posts of those assisting in compiling this risk assessment	no	
Name, post and where required, signature of the responsible manager/supervisor approving the risk assessment	project supervisor: Rujie Sun HS/UOS/FR/038/02	

Reference number and version number of risk assessment	version 1
--	-----------

Title of the risk assessment	Soft, Wearable Pressure Sensors for Continuous Wireless Monitoring of Blood Pressure Enhanced by Artificial Intelligence
Date risk assessment carried out	10.12.2024
Describe the work being assessed	Conducting an experiment to collect data using self-designed piezoresistive sensors strapped to the wrist to measure blood pressure in real time. The sensors have been fabricated using PDMS coated with PEDOT to form the piezoresistive material, with a copper electrode placed on top to facilitate signal measurement. The sensors are securely fastened to the wrist to ensure proper placement and comfort for the investigators participating in the study. Investigators will perform controlled tasks designed to induce changes in blood pressure, such as handgrip exercises and cold pressor challenges, while the sensors record data. The device is powered by a low-voltage power source, well within safe levels for human use, and no exposed wires are present to ensure safety during the experiment.
Describe the location at which the work is being carried out	building 16 lab
Where appropriate list the individuals doing the work and the dates/times when the work will be carried out	Mikayla Colegrave, Oscar Robinson, Luqmanul Mohd Awallizam, Geethaantha Vagga, Mukilian Rajapandian 10.12.24 to 24.01.25
List any other generic or specific risk assessments or other documents that relate to this assessment- use hyperlinks if possible	none
Name and post of risk assessor	no
List the names and posts of those assisting in compiling this risk assessment	no
Name, post and where required, signature of the responsible manager/supervisor approving the risk assessment	project supervisor: Rujie Sun <i>Rujie Sun</i>
Reference number and version number of risk assessment	version 1

note that fields/cells will expand to accommodate multiple lines of text - use ALT-ENTER to force a new line in a cell - note that additional lines may cause the form to run over to a new page

Post Risk Assessment Actions		
Title of risk assessment Soft, Wearable Pressure Sensors for Continuous Wireless Monitoring of Blood Pressure Enhanced by Artificial Intelligence		
Have any of the specialist control measures listed below been identified as required during this risk assessment? - indicate yes or no - if yes then include details on the post assessment action list below.		
Is any exposure monitoring required?		yes/no no
Is any occupational health monitoring required?		no
Are there any hazards or other factors that could affect pregnant or nursing mothers?		no
Is any specific training required before people can carry out this work?		
Site local safety induction		no
Are any additional procedures or risk assessments required as a result of this assessment?		
Post Assessment actions		
ref action	by whom	by when

Document Revision History

History Revision	Revision Date	Revised parts	What has been changed	Originator
HS/UOS/FR/038/00	17/02/2011		Initial Issue for training ans consultation	Tony Harmsworth
HS/UOS/FR/038/01		Front sheet	Activity and Task Tools combined after consultation within the CHSG	MSJ, RB, SC, GGJ
			Tabs removed from bottom of sheets to make the form simpler	
			Bug fixes	
	08/06/2011		Sign off	GGJ
2	25/08/2011		Matrix redesigned, signature field added, blank print button added	RB
			Sign off	GGJ

Gantt Chart (Revision A)

Appendix

F

Wearable Blood Pressure Monitor - Project Planning

Select a column to highlight at right (current day). A legend describing the charting follows.

Current Day:	10
--------------	----

Plan Duration

	Actual Start	% Complete
1.00	100%	100%
2.00	100%	100%
3.00	100%	100%
4.00	100%	100%
5.00	100%	100%
6.00	100%	100%
7.00	100%	100%
8.00	100%	100%
9.00	100%	100%
10.00	100%	100%
11.00	100%	100%
12.00	100%	100%
13.00	100%	100%
14.00	100%	100%
15.00	100%	100%
16.00	100%	100%
17.00	100%	100%
18.00	100%	100%
19.00	100%	100%
20.00	100%	100%
21.00	100%	100%
22.00	100%	100%
23.00	100%	100%
24.00	100%	100%
25.00	100%	100%
26.00	100%	100%
27.00	100%	100%
28.00	100%	100%
29.00	100%	100%
30.00	100%	100%
31.00	100%	100%
32.00	100%	100%
33.00	100%	100%
34.00	100%	100%
35.00	100%	100%
36.00	100%	100%
37.00	100%	100%
38.00	100%	100%
39.00	100%	100%
40.00	100%	100%
41.00	100%	100%
42.00	100%	100%
43.00	100%	100%
44.00	100%	100%
45.00	100%	100%
46.00	100%	100%
47.00	100%	100%
48.00	100%	100%
49.00	100%	100%
50.00	100%	100%
51.00	100%	100%
52.00	100%	100%
53.00	100%	100%
54.00	100%	100%
55.00	100%	100%
56.00	100%	100%
57.00	100%	100%
58.00	100%	100%
59.00	100%	100%
60.00	100%	100%
61.00	100%	100%
62.00	100%	100%
63.00	100%	100%
64.00	100%	100%
65.00	100%	100%
66.00	100%	100%
67.00	100%	100%
68.00	100%	100%
69.00	100%	100%
70.00	100%	100%
71.00	100%	100%
72.00	100%	100%
73.00	100%	100%
74.00	100%	100%
75.00	100%	100%
76.00	100%	100%
77.00	100%	100%
78.00	100%	100%
79.00	100%	100%
80.00	100%	100%
81.00	100%	100%
82.00	100%	100%
83.00	100%	100%
84.00	100%	100%
85.00	100%	100%
86.00	100%	100%
87.00	100%	100%
88.00	100%	100%
89.00	100%	100%
90.00	100%	100%
91.00	100%	100%
92.00	100%	100%
93.00	100%	100%
94.00	100%	100%
95.00	100%	100%
96.00	100%	100%
97.00	100%	100%
98.00	100%	100%
99.00	100%	100%
100.00	100%	100%

Actual (beyond plan)

% Complete (beyond)

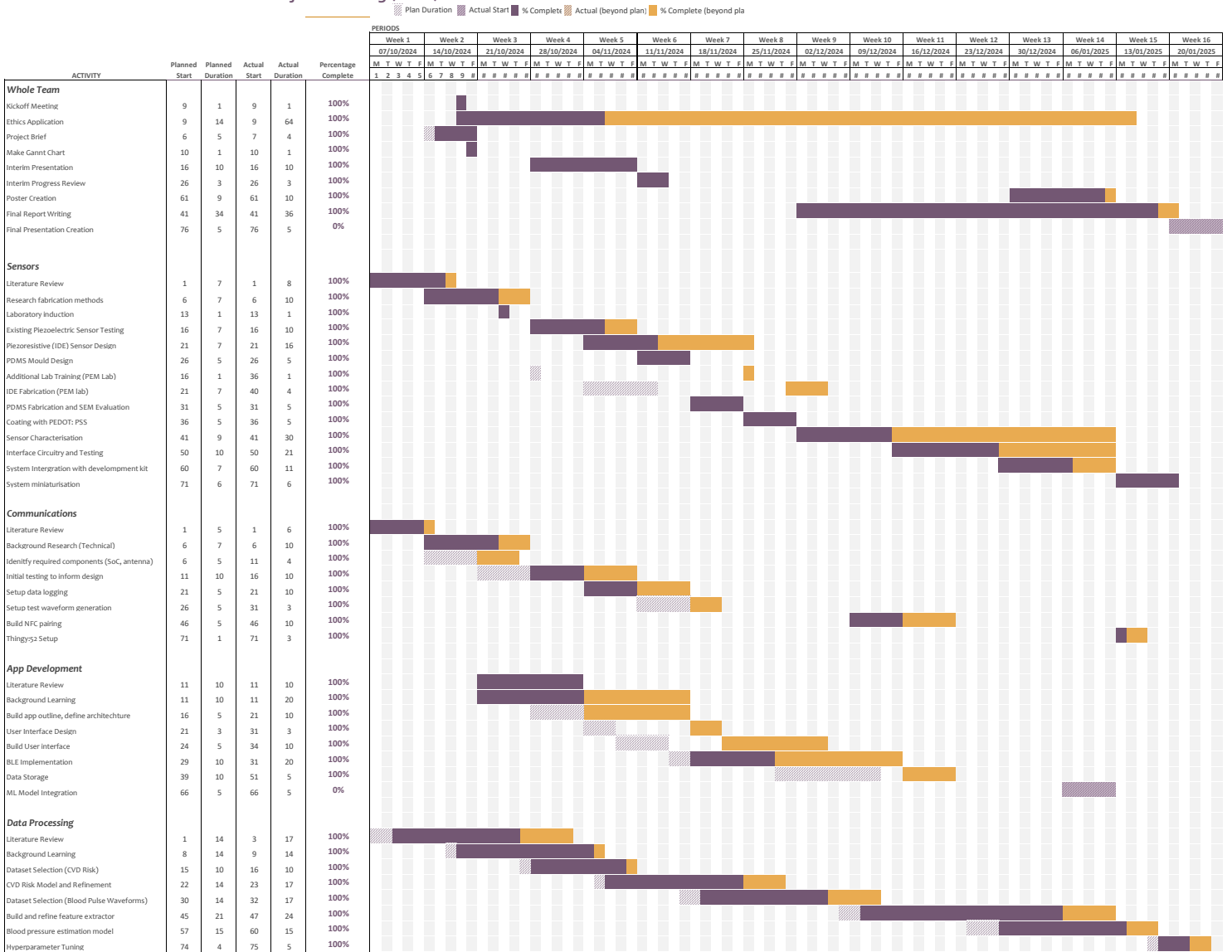
[illegible]

Gantt Chart (Revision B)

Appendix

G

Wearable Blood Pressure Monitor - Project Planning (RevB)



Financial Expenditure

Appendix

H

Item Name	Cost (GBP)	Quantity	Link
NORDIC SEMICONDUCTOR NRF52840-DK	£45.58	1	Onecall
NORDIC SEMICONDUCTOR NRF52840-DONGLE	£12.82	1	Onecall
Samtec Flat Ribbon Cable, 10-Way, 1.27mm Pitch	£11.17	1	RS

TABLE H.1: Financial Expenditure Table - GDP Group 12